

**COMENIUS UNIVERSITY IN BRATISLAVA  
FACULTY OF MATHEMATICS, PHYSICS AND  
INFORMATICS**

**NUCLEI AS A LABORATORY TO STUDY THE  
ABSOLUTE MASS AND STATISTICS OF  
NEUTRINOS**

Dissertation Thesis

Study program: Nuclear and Subnuclear Physics  
Study field: 4.1.5 Nuclear and Subnuclear Physics  
Department: Department of Nuclear Physics and Biophysics  
Supervisor: prof. RNDr. Fedor Šimkovic, CSc.  
Evidence no.: ab08b75f-101b-4fd5-b442-7ad2ead57da7

**Bratislava 2012**

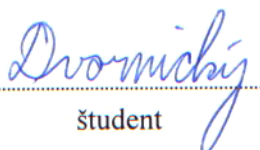
**Mgr. Rastislav Dvornický**

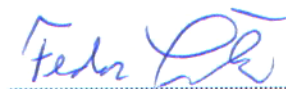


Univerzita Komenského v Bratislave  
Fakulta matematiky, fyziky a informatiky

## ZADANIE ZÁVEREČNEJ PRÁCE

- Meno a priezvisko študenta:** Mgr. Rastislav Dvornický  
**Študijný program:** jadrová a subjadrová fyzika (Jednoodborové štúdium, doktorandské III. st., denná forma)  
**Študijný odbor:** 4.1.5. jadrová a subjadrová fyzika  
**Typ záverečnej práce:** dizertačná  
**Jazyk záverečnej práce:** anglický  
**Sekundárny jazyk:** slovenský
- Názov:** Nuclei as a laboratory to study the absolute mass and statistics of neutrinos  
**Literatúra:** Nuclear and particle physics textbooks and articles of periodical journals and of arXiv.  
**Cieľ:** The study of fundamental properties of neutrinos, namely the absolute neutrino mass scale and statistical properties of neutrinos, with help of weak nuclear processes.  
**Anotácia:** The aim of this thesis is to investigate the absolute scale of neutrino masses and the statistics of neutrinos. The attention will be paid to the determination of neutrino mass from single beta-decays of tritium, rhenium and indium, i.e. beta-emitters with low Q-values. The effect of neutrino mass on the shape of the electron energy spectrum near the kinematical endpoint will be analyzed via the Kurie function. Further, the statistics of neutrinos will be discussed in the context of the two-neutrino double beta-decay. A possibility of neutrinos obeying at least partly Bose-Einstein statistics will be addressed. The associated nuclear matrix elements will be determined within the Single State Dominance (SSD) and Higher States Dominance (HSD) hypotheses. A possibility of realization of the SSD hypothesis for the two-neutrino double-beta decay of  $^{150}\text{Nd}$  will be studied as well.  
**Kľúčové slová:** neutrino mass, mixing of neutrinos, tritium beta decay, forbidden beta decays, Kurie plot, double beta decay, statistics of neutrinos, beyond standard model weak interactions
- Školiteľ:** prof. RNDr. Fedor Šimkovic, CSc.  
**Katedra:** FMFI.KJFB - Katedra jadrovej fyziky a biofyziky  
**Dátum zadania:** 10.09.2006  
**Dátum schválenia:** 08.03.2012
- prof. RNDr. Jozef Masarik, DrSc.  
garant študijného programu

  
študent

  
školiteľ práce

# Declaration

I hereby declare that this submitted thesis is my own work and that, to the best of my knowledge and belief, it contains no material previously published or written by another person nor material which to a substantial extent has been accepted for the award of any degree or diploma of the university or other institute of higher education, except where due to acknowledgement has been made in the text.

Bratislava, March 2012

Rastislav Dvornický

# Acknowledgements

Hereby, I would like to thank to people that gave me support during my PhD studies in form of knowledge or useful advices. The first and definitely one of the most important persons to thank is my supervisor Fedor Šimkovic to whom I am grateful that I had so many opportunities to attend several summer schools, conferences and also for many useful discussions, which we had together. I am also grateful to prof. Amand Fässler for his kind hospitality during my stays at Institute for Theoretical Physics, University of Tübingen. I would like to thank to prof. Kazuo Muto for his kind hospitality during my stay at Tokyo Institute of Technology. I would like to thank to people who helped me with many technical details during all those years of my PhD studies. Namely, I am grateful to Vladimír Fekete, Pavel Šťavina, Tibor Ženiš and at last, but not at least, to Rastík Hodák. I am thankful also to my family for the support during all those years. Finally, I want to especially thank to Zdenka Kalaninová for supporting me in every possible way during my PhD studies and for being so patient with me.

Thank you very much!

# Abstract

In this thesis the absolute mass scale and statistical properties of neutrinos are investigated in the context of the single and double  $\beta$ -decay processes. To our knowledge the first relativistic calculation of the  $\beta$ -decay of tritium is presented. By taking the advantage of the elementary particle treatment of  ${}^3H$  and  ${}^3He$  the form for the  $\beta$ -decay endpoint spectrum of tritium is obtained, considering the effects of higher order terms of hadron current and nuclear recoil. This approach is used also to study the role of interactions beyond the Standard Model (effective scalar and tensor interactions) in the  $\beta$ -decay of tritium. Till now the unknown energy distribution of emitted electrons for the first unique forbidden  $\beta$ -decay of  ${}^{187}Re$  is calculated. It is found that the p-wave emission of electron dominates over the s-wave in this process. It is shown that the Kurie plot near the endpoint of the first unique forbidden  $\beta$ -decay of  ${}^{187}Re$  and of the second unique forbidden  $\beta$ -decay of  ${}^{115}In$  is within a good accuracy linear in the limit of massless neutrinos like the Kurie plot of the super-allowed  $\beta$ -decay of  ${}^3H$ . Next, it is assumed that the Pauli exclusion principle is violated for neutrinos, and thus, neutrinos obey at least partly the Bose-Einstein statistics. It is shown that this violation strongly changes the two-neutrino double  $\beta$ -decay rates and modifies the energy distributions of the emitted electrons. The case of pure bosonic neutrinos is excluded by the present data. Further, a discussion is given on possible realization of the Single State Dominance hypothesis in the case of the two-neutrino double  $\beta$ -decay of  ${}^{150}Nd$ . The obtained theoretical results within this thesis are important for the tritium experiment KATRIN, which is under construction, and for the planned rhenium experiment MARE as well as for the next generation of double  $\beta$ -decay experiments like SuperNEMO, EXO, SNO+, etc.

**keywords:** neutrino mass, double  $\beta$ -decay, tritium  $\beta$ -decay, forbidden  $\beta$ -decays, Kurie plot, bosonic neutrinos, weak interactions

# Abstrakt

V danej práci sú skúmané absolútna škála hmotností a štatistické vlastnosti neutrín v kontexte obyčajného a dvojitého  $\beta$  rozpadu. Pokiaľ vieme po prvý krát je prezentovaný relativistický výpočet  $\beta$  rozpadu trícia. Využitím prístupu popisu jadra  ${}^3H$  a  ${}^3He$  ako elementárnej častice je získaný tvar konca spektra v  $\beta$  rozpade trícia berúc do úvahy efekty členov vyšších rádov hadrónových prúdov a jadrá so spätným rázom. Tento prístup je použitý k štúdiu úlohy interakcií za Štandardným Modelom (efektívne skalárne a tenzorové interakcie) v tríciovom  $\beta$  rozpade. Až doposiaľ neznáme energetické rozdelenie elektrónov emitovaných v prvom zakázanom  $\beta$  rozpade  ${}^{187}Re$  je vypočítané. Zistilo sa, že emisia elektrónu v  $p$  vlne dominuje nad  $s$  vlnami v danom procese. Je ukázané, že Kurieho graf v blízkosti konca spektra prvého zakázaného  $\beta$  rozpadu  ${}^{187}Re$  a druhého zakázaného rozpadu  ${}^{115}In$  je s dobrou presnosťou priamka v prípade bezhmotných neutrín, rovnako ako Kurieho graf pre povolený  $\beta$  rozpad  ${}^3H$ . Ďalej je predpokladané narušenie Pauliho vylučovacieho princípu pre neutrína, čím by sa aspoň čiastočne riadili Bose-Einsteinovou štatistikou. Je ukázané, že toto narušenie silne mení rozpadové šírky dvojneutrínového dvojitého  $\beta$  rozpadu a modifikuje energetické rozdelenie emitovaných elektrónov. Súčasné dáta vylučujú prípad čisto bozónových neutrín. Možná realizácia hypotézy dominancie jedného stavu v dvojneutrínovom dvojitom  $\beta$  rozpade jadra  ${}^{150}Nd$  je diskutovaná. Získané teoretické výsledky v rámci tejto práce sú dôležité pre tríciový experiment KATRIN, ktorý je vo fáze konštrukcie a pre plánovaný experiment MARE, ako aj pre experimenty budúcich generácií dvojitého  $\beta$  rozpadu ako SuperNEMO, EXO, SNO+, atď.

**klúčové slová:** hmotnosť neutrína, dvojitý  $\beta$  rozpad, tríciový  $\beta$  rozpad, zakázané  $\beta$  rozpady, Kurieho graf, bozónové neutrína, slabé interakcie

# Contents

<b>1</b>	<b>Introduction</b>	<b>3</b>
<b>2</b>	<b>Aims of the thesis</b>	<b>15</b>
<b>3</b>	<b>Neutrino mass and <math>\beta</math>-decay of tritium</b>	<b>17</b>
3.1	A conventional description of the $\beta$ -decay of tritium . . . . .	17
3.2	A relativistic treatment of tritium $\beta$ -decay . . . . .	23
3.3	Weak interactions beyond the Standard Model . . . . .	29
<b>4</b>	<b>Neutrino mass and forbidden unique <math>\beta</math>-decays of rhenium and indium</b>	<b>34</b>
4.1	Theoretical treatment of the first unique forbidden $\beta$ -decay of rhenium	34
4.2	The dominance of electron $p$ -wave in the first unique forbidden $\beta$ -decay of rhenium . . . . .	37
4.3	The Kurie function . . . . .	42
4.4	Second unique forbidden $\beta$ -decay of indium . . . . .	45
<b>5</b>	<b>Double <math>\beta</math>-decay within Single State Dominance hypothesis</b>	<b>49</b>
5.1	Theoretical description of the double $\beta$ -decay . . . . .	49
5.2	Double $\beta$ -decay to the $0^+$ ground state . . . . .	56
5.3	Double $\beta$ -decay to the $2_1^+$ excited state . . . . .	58
5.4	Nuclear electron capture and $\beta$ -decay . . . . .	60
5.5	Double $\beta$ -decay within the Single State Dominance hypothesis . . . . .	63
<b>6</b>	<b>Statistics of neutrinos and two-neutrino double <math>\beta</math>-decay</b>	<b>70</b>
6.1	Bosonic neutrinos in two-neutrino double $\beta$ -decay . . . . .	72
6.2	Single State Dominance hypothesis . . . . .	76
6.3	Higher States Dominance hypothesis . . . . .	77
6.4	The two-neutrino double $\beta$ -decay with partly bosonic neutrinos . . . . .	79
6.5	Effect of bosonic neutrinos in two-neutrino double $\beta$ -decay of $^{100}\text{Mo}$ . . . . .	81
6.6	Restriction bounds on bosonic component of neutrinos . . . . .	86
6.6.1	The half-life . . . . .	87

6.6.2	The energy distributions . . . . .	89
6.6.3	Ratios of half-lives to excited and ground state . . . . .	89
	<b>Summary</b>	<b>92</b>
	<b>Résumé</b>	<b>95</b>
<b>A</b>	<b>Phase space integrals evaluation within the relativistic treatment of tritium <math>\beta</math>-decay</b>	<b>106</b>
<b>B</b>	<b>Distorted relativistic electron wave function with Coulomb field</b>	<b>112</b>
<b>C</b>	<b>Fierz transformation</b>	<b>117</b>
	<b>List of publications</b>	<b>119</b>
	<b>Bibliography</b>	<b>120</b>



# Chapter 1

## Introduction

Recently, it has been established that neutrinos played an important role in the early Universe in several ways. First, the number of neutrino species does influence the primordial nucleosynthesis that eventually affects the composition of elements in the Universe [1, 2]. Second, during the evolution of the Universe, massive neutrinos affect the formation of large-scale structures in the form of hot dark matter. It appears that only about 4% of the energy/matter in the Universe consists of ordinary matter (baryons). The remaining 95% is composed of invisible "dark matter" ( $\sim 25\%$ ) and unknown "dark energy" ( $\sim 70\%$ ). The neutrinos that decoupled from the primordial plasma, known also as relic neutrinos, are still the second most abundant particles in the Universe right next to the photons. The aim of this thesis is to investigate fundamental properties of neutrinos, one of the most intriguing particles in the Universe.

### The early period of neutrino history

The history of neutrinos dates back to the 4-th December 1930 with a proposal of Wolfgang Pauli in an open letter to participants of physics conference held at Tübingen. In order to resolve the problem of energy conservation as well as of spin statistics in nuclear  $\beta$ -decay, he suggested the existence of weakly interacting light neutral fermion. It was Enrico Fermi who proposed the name "neutrino".

Another crucial step was the theory of  $\beta$ -decay formulated by Enrico Fermi, in 1934, in analogy with quantum electrodynamics. Also he pointed out in 1934 that the shape of the electron energy spectrum of the  $\beta$ -decay, near the endpoint, is sensitive to the neutrino mass [3]. Namely, the endpoint is shifted to lower energies and the shape is tilted. The first measurement was performed by Hanna and Pontecorvo [4] with tritium filled proportional chamber. Their bound  $\sim 1\text{ keV}$  was limited by the detector resolution.

It was Eugene Wigner who suggested to Maria Goeppert-Mayer in 1935 [5], only one year after Fermi published his theory describing the  $\beta$ -decay, a rare process - the two-neutrino double  $\beta$ -decay, which involves the emission of two electrons and two antineutrinos.

In 1987 the first actual laboratory observation of the two-neutrino double  $\beta$ -decay was done for  $^{82}\text{Se}$  by M. Moe and collaborators [6], who used a time projection chamber. So far the  $2\nu\beta\beta$ -decay has been recorded for nuclei:  $^{48}\text{Ca}$ ,  $^{76}\text{Ge}$ ,  $^{82}\text{Se}$ ,  $^{96}\text{Zr}$ ,  $^{100}\text{Mo}$ ,  $^{116}\text{Cd}$ ,  $^{128}\text{Te}$ ,  $^{130}\text{Te}$ ,  $^{136}\text{Xe}$ ,  $^{150}\text{Nd}$ ,  $^{238}\text{U}$  [7, 8]. In addition, the  $2\nu\beta\beta$ -decay of  $^{100}\text{Mo}$  and  $^{150}\text{Nd}$  to the  $0^+$  excited state of the daughter nucleus has been observed.

In 1937, Majorana published the symmetry theory between the electrons and positrons [9]. In this theory, he proposed a possible existence of completely neutral particles that are their own antiparticles. They are known as the Majorana particles.

In 1939, Wolfgang Furry [10] discussed the possibility of Majorana neutrinos in neutrinoless double  $\beta$ -decay, a process which involves the emission of two electrons and no antineutrinos. It was proved by Schechter and Valle that, if  $0\nu\beta\beta$ -decay takes place, regardless of the mechanism causing it, the neutrinos are Majorana particles with non-zero mass [11].

The neutrinoless double  $\beta$ -decay has not yet been confirmed.

After the Fermi formulated the theory of  $\beta$ -decay, George Gamow and Edward Teller extended the theory by introducing the axial-vector currents in order to explain the change of one unit of the nuclear spin in some nuclear  $\beta$ -decays. However, the extension was made in such a way that the parity was still conserved.

It was then realized that other couplings, e.g. scalar, pseudoscalar and tensor, could participate in weak interactions. The ultimate combination of couplings remained an unsolved question for about two decades, mostly due to misleading interpretation of impressive experiments.

After the discovery of parity violation in kaon decays by Lee and Yang in 1956 [12], the combination of Lorentz invariant interactions in the Lagrangian of the weak interactions had become even more complicated. This apparently confusing situation was simplified with the form of the  $V - A$  theory formulated in 1958 by Feynman and Gell-Mann [13], Sudarshan and Marshak [14]. The  $V - A$  structure of the weak interactions can be realized by using the two-component theory of massless neutrinos. This theory incorporates the left-handed neutrinos and right-handed antineutrinos.

The observations of the muon decay led Bruno Pontecorvo to propose the universality of the Fermi theory of weak interactions of electrons and of muons. The concept of lepton number was introduced by Konopinski. The lepton number  $L = 1$  for the following particles:  $e^-$ ,  $\mu^-$ ,  $\tau^-$ ,  $\nu_e$ ,  $\nu_\mu$ ,  $\nu_\tau$ , while  $L = -1$  for their antiparticles. The lep-

Table 1.1: Flavor lepton numbers given for three generations of leptons.

Lepton number	$e^-$	$\nu_e$	$\mu^-$	$\nu_\mu$	$\tau^-$	$\nu_\tau$
$L_e$	1	1	0	0	0	0
$L_\mu$	0	0	1	1	0	0
$L_\tau$	0	0	0	0	1	1

ton number  $L$  is conserved in the  $V - A$  theory as well as in a Standard Model theory of weak interactions.

## Neutrinos in the concept of Standard Model

An important milestone in the theory of weak interactions is the formulation of the Standard Model by Glashow, Weinberg and Salam [15] in 1967. The theory is based on a  $SU(2) \otimes U(1)$  gauge model. The unique theoretical predictions of the neutral currents and  $Z$  boson were confirmed at CERN [16] in 1973. The model involves also the Higgs mechanism, i.e. particles get their masses via the spontaneous symmetry breaking mechanism. After experimental discoveries of several particles it is found that the building blocks of SM are arranged in three generations, e.g. for neutrinos particularly

$$\begin{pmatrix} \bar{\nu}_e \\ e^- \end{pmatrix}_L, \quad \begin{pmatrix} \bar{\nu}_\mu \\ \mu^- \end{pmatrix}_L, \quad \begin{pmatrix} \bar{\nu}_\tau \\ \tau^- \end{pmatrix}_L.$$

The number of these generations was fixed by LEP experiments at CERN within the  $Z$  boson invisible decay width [17]. The concept of the flavor lepton number, shown in Table 1.1, was established. The subscript  $L$  denotes the left-handed components of these leptons  $l$  ( $= e, \mu, \tau$ ) and corresponding antineutrinos  $\bar{\nu}_l$ . They form doublets, which enter to the weak interactions within the Lagrangian of SM. On the other hand, the right-handed components form singlets ( $e_R, \mu_R, \tau_R$ ) and do not participate in the weak interactions.

It is worth mentioning that there is no symmetry incorporated in the SM that would imply the flavor lepton number conservation.

No experiments performed so far have shown deviation from the predictions of the SM, except the neutrino oscillation experiments.

# Neutrino mixing and oscillations

The idea of neutrino oscillations was first proposed by Bruno Pontecorvo [18] in 1957 in analogy with the  $K$  oscillations phenomenon. At that time, the possible oscillation was  $\nu \leftrightarrow \bar{\nu}$  for Majorana neutrinos. Later on, neutrino mixing was proposed by Maki, Nakagawa and Sakata [19] in 1962 with the assumption of two generations of neutrinos,  $\nu_e$  and  $\nu_\mu$  that are mixed states of two mass eigenstates  $\nu_1$  and  $\nu_2$ . In 1967 in paper [20] Pontecorvo considered all possible transitions between  $\nu_e$  and  $\nu_\mu$  and applied the idea of neutrino oscillations to the solar neutrinos. In 1969 Gribov and Pontecorvo [21] considered the two-neutrino oscillations in case of two massive Majorana neutrinos. Starting from 1975 many papers were published by Bilenky and Pontecorvo (see [22]) who developed phenomenological theory of the neutrino oscillations, considering all possible neutrino mass terms (Dirac, Majorana, Dirac and Majorana).

The atmospheric, solar and accelerator neutrino oscillation experiments (KamLAND, K2K, SNO, etc.) are explained in a framework of three neutrino mixing model. In more detail,

$$\begin{pmatrix} \nu_e \\ \nu_\mu \\ \nu_\tau \end{pmatrix} = \begin{pmatrix} c_{12}c_{13} & s_{12}c_{13} & s_{13}e^{-i\delta} \\ -s_{12}c_{23} - c_{12}s_{23}s_{13}e^{i\delta} & c_{12}c_{23} - s_{12}s_{23}s_{13}e^{i\delta} & s_{23}c_{13} \\ s_{12}s_{23} - c_{12}c_{23}s_{13}e^{i\delta} & -c_{12}s_{23} - s_{12}c_{23}s_{13}e^{i\delta} & c_{23}c_{13} \end{pmatrix} \begin{pmatrix} \nu_1 \\ \nu_2 \\ \nu_3 \end{pmatrix},$$

the three flavor states  $(\nu_e, \nu_\mu, \nu_\tau)$  are linear combination of the three mass eigenstates  $(\nu_1, \nu_2, \nu_3)$ . The Pontecorvo-Maki-Nakagawa-Sakata mixing matrix  $U_{PMNS}$  ( $U_{li}$ ;  $l = e, \mu, \tau$ ;  $i = 1, 2, 3$ ) is given here in the standard notation for Dirac neutrinos.  $s_{ij} = \sin \theta_{ij}$  and  $c_{ij} = \cos \theta_{ij}$ .  $\theta_{ij}$  is the mixing angle and  $\delta$  is the CP-violating phase. If neutrinos are Majorana particles the mixing matrix is multiplied by a diagonal phase matrix  $P = \text{diag}(e^{i\alpha_1}, e^{i\alpha_2}, e^{i\delta})$ , which contains two additional CP-violating Majorana phases  $\alpha_1$  and  $\alpha_2$ .

The results from the neutrino oscillation experiments can provide information only on the differences in the square masses  $\Delta m_{ij}^2 = m_i^2 - m_j^2$  of neutrinos, not on their masses, and on the values of mixing angles  $\theta_{ij}$ . The neutrino oscillation parameters, which will be used to discuss the absolute scale of neutrino masses are listed below:

- $\theta_{12}$ : The reactor neutrino oscillation experiment KamLAND [23] has determined  $\tan^2 \theta_{12} = 0.452_{-0.033}^{+0.035}$ .
- $\theta_{13}$ : The accelerator neutrino oscillation experiment T2K has obtained the bound  $0.04 < \sin^2 2\theta_{13} < 0.34$  [24] and reactor neutrino oscillation experiment DOUBLE CHOOZ has determined  $\sin^2(2\theta_{13}) = 0.085 \pm 0.029$  (*stat*)  $\pm 0.042$  (*syst*) (68% CL) [25].

- $\Delta m_{12}^2$ : The global fit value of the mass squared difference entering the solar neutrino oscillation experiments  $\Delta m_{SUN}^2 = \Delta m_{12}^2 = m_2^2 - m_1^2$  is  $\Delta m_{SUN}^2 = (7.65_{-0.20}^{+0.13}) \times 10^{-5} eV^2$  [26].
- $\Delta m_{31}^2$  ( $\Delta m_{32}^2$ ): The mass squared difference entering the atmospheric neutrino oscillation experiments  $\Delta m_{ATM}^2 = |\Delta m_{31}^2| = |m_3^2 - m_1^2|$  (in case of normal hierarchy and  $\Delta m_{ATM}^2 = |\Delta m_{32}^2| = |m_3^2 - m_2^2|$  in case of inverted hierarchy). The long baseline accelerator neutrino oscillation experiment MINOS has determined  $\Delta m_{ATM}^2 = (2.43 \pm 0.13) \times 10^{-3} eV^2$  [27].

We note that the absolute scale of neutrino masses is not known until now. Based on the above for the neutrino masses we have following scenarios:

- **Normal spectrum:**  $m_1 < m_2 < m_3$ , then the mass squared differences are given as

$$\Delta m_{SUN}^2 = m_2^2 - m_1^2, \quad \Delta m_{ATM}^2 = m_3^2 - m_2^2. \quad (1.1)$$

The absolute scale of the neutrino masses is determined by the mass of the lightest neutrino  $m_0$ ,

$$m_1 = m_0, \quad m_2 = \sqrt{\Delta m_{SUN}^2 + m_0^2}, \quad m_3 = \sqrt{\Delta m_{ATM}^2 + \Delta m_{SUN}^2 + m_0^2} \quad (1.2)$$

- **Inverted spectrum:**  $m_3 < m_1 < m_2$ , then the mass squared differences are given as

$$\Delta m_{SUN}^2 = m_2^2 - m_1^2, \quad \Delta m_{ATM}^2 = m_1^2 - m_3^2. \quad (1.3)$$

The absolute scale of the neutrino masses is determined by the mass of the lightest neutrino  $m_0$ ,

$$m_1 = \sqrt{\Delta m_{ATM}^2 + m_0^2}, \quad m_2 = \sqrt{\Delta m_{ATM}^2 + \Delta m_{SUN}^2 + m_0^2}, \quad m_3 = m_0 \quad (1.4)$$

# Determination of the absolute scale of neutrino masses

Information on absolute scale of neutrino masses can be obtained by three different methods:

1. The limit on the sum of neutrino masses,

$$m_{cosmo} = \sum_{i=1}^3 m_i, \quad (1.5)$$

is obtained from the astrophysical and cosmological observations [28]. For the purpose of illustration we present a global average  $m_{cosmo} = 0.71 \text{ eV}$ .

2. Search for neutrinoless double  $\beta$ -decay, where the effective Majorana neutrino mass,

$$m_{\beta\beta} = \sum_{i=1}^3 (U_{PMNS})_{ei}^2 m_i = c_{12}^2 c_{13}^2 e^{2i\alpha_1} m_1 + c_{13}^2 s_{12}^2 e^{2i\alpha_2} m_2 + s_{13}^2 m_3, \quad (1.6)$$

is extracted from the observed half-life of the process [29, 30] .

3. Direct determination of the neutrino mass by kinematics of the ordinary  $\beta$ -decay. The effective mass of the electron neutrino

$$m_\beta = \sqrt{\sum_{i=1}^3 U_{ei}^2 m_i^2} = \sqrt{c_{12}^2 c_{13}^2 m_1^2 + c_{13}^2 s_{12}^2 m_2^2 + s_{13}^2 m_3^2} \quad (1.7)$$

is obtained from precise investigation of the electron spectrum near its endpoint [31, 32].

Although methods 1 and 2 are very sensitive to neutrino masses, their results are model-dependent. On the other hand, direct neutrino mass determination from the kinematics of  $\beta$ -decays is essentially based on energy and momentum conservation only and thus model independent.

The above combinations of masses can be written as follows:

- I) For the normal hierarchy ( $m_1 \ll m_2 \ll m_3$ ):

- Restriction from cosmology and astrophysics:

$$m_{cosmo} = m_0 + \sqrt{\Delta m_{SUN}^2 + m_0^2} + \sqrt{\Delta m_{ATM}^2 + \Delta m_{SUN}^2 + m_0^2} \quad (1.8)$$

- $0\nu\beta\beta$ -decay:

$$m_{\beta\beta} = c_{12}^2 c_{13}^2 m_0 e^{2i\alpha_1} + s_{12}^2 c_{13}^2 e^{2i\alpha_2} \sqrt{\Delta m_{SUN}^2 + m_0^2} + s_{13}^2 \sqrt{\Delta m_{ATM}^2 + \Delta m_{SUN}^2 + m_0^2} \quad (1.9)$$

- Ordinary  $\beta$ -decay:

$$m_\beta = \sqrt{c_{12}^2 c_{13}^2 m_0^2 + s_{12}^2 c_{13}^2 (\Delta m_{SUN}^2 + m_0^2) + s_{13}^2 (\Delta m_{ATM}^2 + \Delta m_{SUN}^2 + m_0^2)} \quad (1.10)$$

By assuming normal hierarchy the mass  $m_1$  is negligibly small and we have

$$m_1 \ll \sqrt{\Delta m_{SUN}^2}, \quad m_2 \simeq \sqrt{\Delta m_{SUN}^2}, \quad m_3 \simeq \sqrt{\Delta m_{ATM}^2}. \quad (1.11)$$

Within these bounds an upper limit can be put on the effective Majorana neutrino mass

$$|m_{\beta\beta}| \simeq |c_{13}^2 s_{12}^2 \sqrt{\Delta m_{SUN}^2} + s_{13}^2 \sqrt{\Delta m_{ATM}^2} e^{-2i\alpha_2}| \leq 4 \cdot 10^{-3} \text{ eV}. \quad (1.12)$$

II) For the inverted hierarchy ( $m_3 \ll m_1 < m_2$ ):

- Restriction from cosmology and astrophysics:

$$m_{cosmo} = \sqrt{\Delta m_{ATM}^2 + m_0^2} + \sqrt{\Delta m_{ATM}^2 + \Delta m_{SUN}^2 + m_0^2} + m_0 \quad (1.13)$$

- $0\nu\beta\beta$ -decay:

$$m_{\beta\beta} = c_{12}^2 c_{13}^2 e^{2i\alpha_1} \sqrt{\Delta m_{ATM}^2 + m_0^2} + s_{12}^2 c_{13}^2 e^{2i\alpha_2} \sqrt{\Delta m_{ATM}^2 + \Delta m_{SUN}^2 + m_0^2} + s_{13}^2 m_0 \quad (1.14)$$

- Ordinary  $\beta$ -decay:

$$m_\beta = \sqrt{s_{13}^2 m_0^2 + s_{12}^2 c_{13}^2 (\Delta m_{ATM}^2 + m_0^2) + c_{12}^2 c_{13}^2 (\Delta m_{ATM}^2 - \Delta m_{SUN}^2 + m_0^2)} \quad (1.15)$$

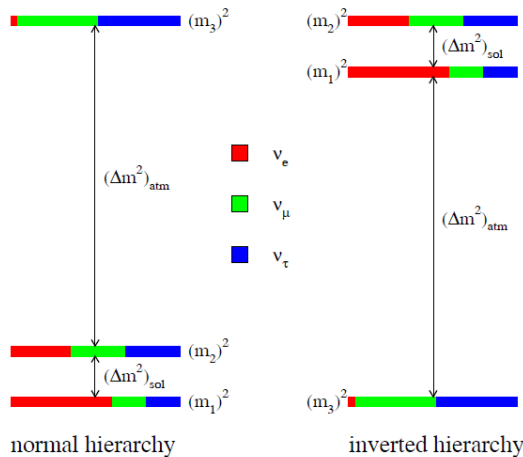


Figure 1.1: The normal and inverted hierarchy of neutrino masses are illustrated. We note that  $m_1 < m_2 < m_3$  in normal spectrum and  $m_3 < m_1 < m_2$  in inverted spectrum. Differences between masses are determined by  $\Delta m_{ATM}^2$  and  $\Delta m_{SUN}^2$  from neutrino oscillation experiments. The absolute scale of neutrino masses is not known.

By assuming inverted hierarchy the mass  $m_3$  is negligibly small and we have

$$m_1 \simeq m_2 \simeq \sqrt{\Delta m_{SUN}^2}, \quad m_3 \ll \sqrt{\Delta m_{ATM}^2}. \quad (1.16)$$

For the limit of the effective Majorana neutrino mass we find

$$|m_{\beta\beta}| \simeq \sqrt{\Delta m_{ATM}^2} c_{13}^2 (1 - \sin^2 2\theta_{12} \sin^2 \alpha_{12})^{\frac{1}{2}}, \quad (1.17)$$

where  $\alpha_{12} = \alpha_2 - \alpha_1$ . The phase difference  $\alpha_{12}$  is the only unknown parameter here. From [33] we obtain the following restriction

$$1.5 \cdot 10^{-2} \text{ eV} \leq |m_{\beta\beta}| \leq 5.0 \cdot 10^{-2} \text{ eV}. \quad (1.18)$$

III) For the quasi-degenerate hierarchy ( $m_0 = m_1 \simeq m_2 \simeq m_3$ ):

- Cosmology and ordinary  $\beta$ -decay:

$$m_{cosmo} = 3m_0 \quad \text{and} \quad m_{\beta} = 3m_0. \quad (1.19)$$

- $0\nu\beta\beta$ -decay:



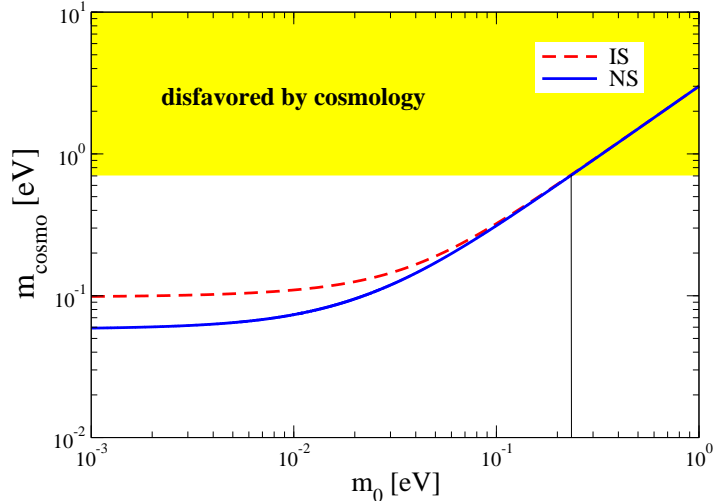


Figure 1.2: The neutrino mass limits as a function of the mass of the lightest neutrino  $m_0$  determined by cosmology. Corresponding mass  $m_0 = 0.23eV$  is extracted from astrophysical observations, which place a limit on a sum of neutrino masses  $m_{cosmo} = 0.71eV$  for both scenarios, normal and inverted spectrum.

The effective Majorana neutrino mass is relatively large in this case and for both scenarios of the neutrino mass spectrum is given by

$$m_0|1 - 2c_{12}^2c_{13}^2| \leq m_{\beta\beta} \leq m_0. \quad (1.20)$$

For the sake of illustration the normal and inverted hierarchy are shown in Fig. (1.1)

The above results for the cosmological limits as a function of the mass of the lightest neutrino are illustrated in Fig. (1.2) for both scenarios the normal and inverted spectrum. From global fit value  $m_{cosmo} = 0.71eV$  from astrophysical and cosmological observations a corresponding mass of the lightest neutrino  $m_0 = 0.23 eV$  is determined for both scenarios. The lowest value for the sum of the neutrino masses, which can be reached in future cosmological measurements [28, 34, 35] is about  $0.05 - 0.1eV$ . The corresponding values of the  $m_0$  are in the region, where the normal and inverted spectrum predictions for  $m_{cosmo}$  differ significantly from each other.

The allowed range of the values for the effective Majorana neutrino mass  $|m_{\beta\beta}|$  as a function of the mass of the lightest neutrino  $m_0$  is illustrated in Fig. (1.3) for normal and inverted spectrum. In case of inverted spectrum the allowed region for the  $|m_{\beta\beta}|$  is presented between two parallel lines in the upper part of Fig. (1.3). The allowed region for  $|m_{\beta\beta}| \approx \text{few } meV$  in case of the normal spectrum corresponds to the  $m_0$  smaller than  $10meV$ .

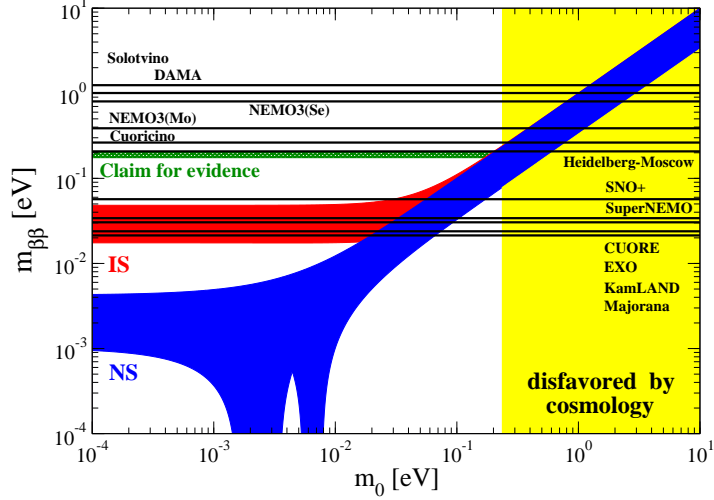


Figure 1.3: The allowed range for  $|m_{\beta\beta}|$  values is showed as a function of the mass of the lightest neutrino  $m_0$  for both scenarios the normal and inverted spectrum. The current experimental limits and the expected future results are shown [36] ( Nuclear matrix elements in quasiparticle random phase approximation with CD-Bonn short-range correlations and  $g_A = 1.25$  are assumed [37, 38]). It is worth mentioning that in the scenario of inverted spectrum there exist a lower bound, which means that  $0\nu\beta\beta$ -decay should be definitely observed, if the experiments reach the required level.

The strongest limits on the half-life of the  $0\nu\beta\beta$ -decay were set in Heidelberg-Moscow [39], NEMO3 [40], CUORICINO [41] and KamLAND-Zen [42] experiments:

$$\begin{aligned}
 T_{1/2}^{0\nu}({}^{76}\text{Ge}) &\geq 1.9 \times 10^{25} \text{ y} \\
 T_{1/2}^{0\nu}({}^{100}\text{Mo}) &\geq 1.0 \times 10^{24} \text{ y} \\
 T_{1/2}^{0\nu}({}^{130}\text{Te}) &\geq 3.0 \times 10^{24} \text{ y} \\
 T_{1/2}^{0\nu}({}^{136}\text{Xe}) &\geq 5.7 \times 10^{24} \text{ y}.
 \end{aligned} \tag{1.21}$$

From these experiments [39, 41, 42] by using of nuclear matrix elements of Ref. [37] calculated with Brueckner two-nucleon short-range correlations the following stringent bounds on effective Majorana mass were obtained

$$\begin{aligned}
 |m_{\beta\beta}| &< (0.20 - 0.32) \text{ eV } ({}^{76}\text{Ge}), \\
 &< (0.33 - 0.46) \text{ eV } ({}^{130}\text{Te}), \\
 &< (0.17 - 0.30) \text{ eV } ({}^{136}\text{Xe}).
 \end{aligned} \tag{1.22}$$

However, there exist a claim of the observation of the  $0\nu\beta\beta$ -decay of  ${}^{76}\text{Ge}$  made by some participants of the Heidelberg-Moscow collaboration [43]. Their estimated

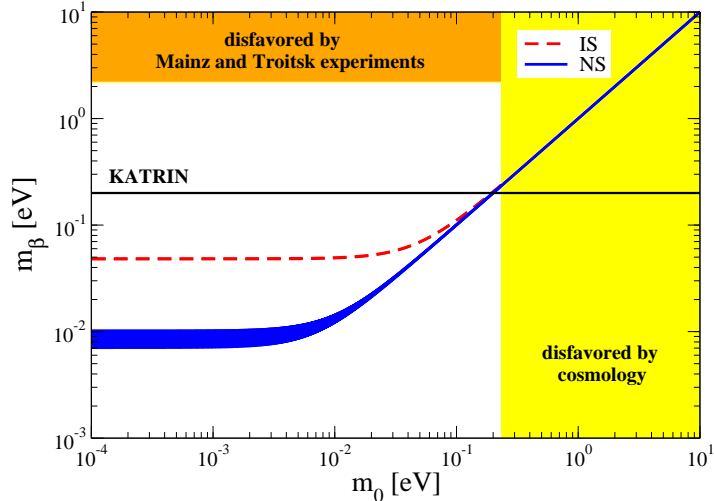


Figure 1.4: Limits of the effective mass of electron neutrino as a function of the mass of the lightest neutrino  $m_0$  extracted from the tritium  $\beta$ -decay. From the Mainz and Troitsk experiments a current upper limit  $m_\beta = 2.2 \text{ eV}$  a mass of the lightest neutrino  $m_0 = 2.2 \text{ eV}$  is deduced for both normal and inverted spectrum.

value of the effective Majorana mass (assuming a specific value for the NME) is  $|m_{\beta\beta}| \sim 0.4 \text{ eV}$ . This result will be checked by an independent experiment GERDA with germanium [44] and the Heidelberg-Moscow sensitivity will be reached in about one year of measuring time. In future experiments, CUORE [45], EXO [46], SuperNEMO [47], SNO+ [48], KamLAND-Zen [42] and others, a sensitivity  $|m_{\beta\beta}| \sim \text{a few } 10^{-2} \text{ eV}$  is planned to be reached, what is the region of the inverted hierarchy of neutrino masses. In the case of the normal mass hierarchy  $|m_{\beta\beta}|$  is too small in order to be probed in the  $0\nu\beta\beta$ -decay experiments of the next generation.

The determination of the effective mass of electron neutrino from ordinary  $\beta$ -decay is based on the very precise investigation of the electron energy spectrum near its endpoint. The relative number of events occurring in an interval of energy  $\Delta T$  near the endpoint is proportional to  $(\Delta T/Q)^3$ . Therefore isotopes with low  $Q$ -value are favorable, e.g. tritium ( $\sim 18.6 \text{ keV}$ ) and rhenium ( $\sim 2.47 \text{ keV}$ ).

The recent best upper limit  $m_\beta \leq 2.2 \text{ eV}$  is obtained by the Mainz [49] and Troitsk [50] experiments measuring the electron energy spectrum near its endpoint in tritium  $\beta$ -decay. A next-generation tritium  $\beta$ -decay experiment is the KARlsruhe TRItium Neutrino experiment (KATRIN) [31], which is planned to start data commissioning in 2013. This experiment is projected for measurement of the neutrino mass with a sensitivity of  $0.2 \text{ eV}$ , which can probe the quasi-degenerate hierarchy of neutrino masses.

The results for the limits of the effective mass of electron neutrino as a function of the mass of the highest neutrino are illustrated in Fig. (1.4) for both scenarios the normal and inverted hierarchy.

Complementary to the kinematical measurements of tritium  $\beta$ -decay appears the calorimetric measurement of the rhenium  $\beta$ -decay in MARE experiment [32], where all electron energy released in reaction is recorded. The achieved sensitivity of  $m_\beta < 15 eV$  was limited by statistics [51]. The success of rhenium experiments has encouraged the micro-calorimeter community to proceed with a competitive precision search for a neutrino mass. The ambitious project is planned in two steps, MARE I and MARE II. MARE II is to challenge the KATRIN goal of  $0.2 eV$  in future.

# Chapter 2

## Aims of the thesis

The aim of this thesis is to investigate the absolute scale of the neutrino masses and the statistics of neutrinos. The attention is paid to the determination of the neutrino mass from single  $\beta$ -decays of tritium, rhenium and indium, i.e.  $\beta$ -emitters with low  $Q$ -values. The effect of the neutrino mass on the shape of the electron energy spectrum near the kinematical endpoint is analyzed via the Kurie function. Further, the statistics of neutrinos is discussed in the context of the two-neutrino double  $\beta$ -decay. A possibility of neutrinos obeying at least partly Bose-Einstein statistics is addressed. The associated nuclear matrix elements are determined within the Single State Dominance (SSD) and Higher States Dominance (HSD) hypotheses. A possibility of realization of the SSD hypothesis for the  $2\nu\beta\beta$ -decay of  $^{150}\text{Nd}$  is studied as well.

- A relativistic description of the tritium  $\beta$ -decay:
  - For the  $\beta$ -decay of tritium the theoretical electron energy spectrum will be derived within the Elementary Particle Treatment approach of Kim and Primakoff. The effects of higher order terms of hadron currents and nuclear recoil will be considered.
  - The role of weak interactions beyond the Standard Model (the effective scalar and tensor) in the tritium  $\beta$ -decay will be investigated.
- Unique forbidden  $\beta$ -decays of rhenium and indium:
  - The theoretically unknown electron energy spectrum of the first unique forbidden  $\beta$ -decay of  $^{187}\text{Re}$  will be presented.
  - The dominance of the particular differential decay rate associated with the emission of p-wave electrons in the rhenium  $\beta$ -decay, which was found out in the MIBETA experiment, will be investigated.

- The second unique forbidden  $\beta$ -decay of  $^{115}\text{In}$  to the first nuclear excited state of  $^{115}\text{Sn}$  (with the lowest known  $Q$ -value) will be described theoretically.
- Single State Dominance hypothesis:
  - For the two-neutrino double  $\beta$ -decay of  $^{150}\text{Nd}$  with the  $1^-$  ground state of the intermediate nucleus  $^{150}\text{Pm}$  possible realization of the Single State Dominance hypothesis will be analyzed.
  - The energy distributions of emitted electrons in the  $2\nu\beta\beta$ -decay of  $^{150}\text{Nd}$  within the SSD (HSD) hypothesis will be calculated.
- Statistics of neutrinos:
  - The statistics of neutrinos will be studied within the two-neutrino double  $\beta$ -decay. For pure bosonic and partly bosonic neutrinos the normalized energy distributions of emitted electrons will be derived.
  - For pure bosonic or fermionic neutrinos the half-lives of  $2\nu\beta\beta$ -decay to the ground ( $0^+$ ) and first excited ( $2^+$ ) states of the final nucleus will be calculated.

# Chapter 3

## Neutrino mass and $\beta$ -decay of tritium

In a view of an enormous progress in the tritium  $\beta$ -decay experiments, which aim to determine the absolute scale of neutrino masses by precise investigation of the electron energy spectrum near its endpoint, there is a request for a highly accurate theoretical description of this spectrum near the endpoint. The subject of interest has been molecular effects in tritium  $\beta$ -decay [52], radiative corrections [53], Lorentz invariance violations [54], interactions beyond the Standard Model [55], relativistic form for the  $\beta$ -decay endpoint spectrum [56, 57] etc.

In connection with this, the theoretical description of tritium  $\beta$ -decay is presented in this chapter. First, a conventional approach to tritium  $\beta$ -decay is showed. Then, main focus is set on the relativistic description of this process in the Elementary Particle Treatment approach. The effect of recoil on the shape of the endpoint spectrum is discussed. In addition to the standard  $V - A$  interaction, the effective scalar and tensor, beyond the Standard Model interactions are taken into account. Their role in the tritium  $\beta$ -decay is discussed.

### 3.1 A conventional description of the $\beta$ -decay of tritium

A conventional theoretical description of the tritium  $\beta$ -decay is presented here. The effect of nuclear recoil is neglected in this formalism. For the sake of simplicity we neglect the neutrino mixing. The considered weak  $\beta$ -decay Hamiltonian takes the form,

$$\mathcal{H}^\beta(x) = \frac{G_\beta}{\sqrt{2}} \bar{e}(x) \gamma_\mu (1 - \gamma_5) \nu_e(x) j^\mu(x) + h.c.. \quad (3.1)$$

Here,  $G_\beta = G_F \cos \theta_C$ . The  $G_F$  stands for the Fermi coupling constant of the weak

interaction and the  $\cos\theta_C$  is the cosine of Cabbibo angle that is due to the mixing of up and down quarks. The field operators for the electron and neutrino are denoted as  $e(x)$  and  $\nu_e(x)$ , respectively. The field is defined as

$$\Psi(x) = \int \frac{d\vec{p}}{\sqrt{2E}} \sum_{\sigma} (u^{\sigma}(p)e^{-ipx}c^{\dagger}(p) + u^{\sigma}(-p)e^{ipx}d(p)). \quad (3.2)$$

Here,  $u^{\sigma}(p)$  is a Dirac spinor. Normalization of the spinor is  $u(p)^{\dagger}u(p) = 1$ . This normalization is used within the thesis, with only exception being made in sections 3.2 and 3.3 due to reasons mentioned therein.  $c^{\dagger}(p)$  is the creation operator of particle and  $d(p)$  is the anihilation operator of antiparticle. The free charged hadron current conserving the strangeness is given by

$$j_{\mu}(x) = \bar{p}(x)\gamma_{\mu}(g_V - g_A\gamma_5)n(x). \quad (3.3)$$

Here,  $p(x)$  and  $n(x)$  are the field operators of proton and neutron, respectively. The renormalization constants of vector and axial-vector currents are  $g_V = 1.0$  and  $g_A = 1.269$ , respectively.

The single  $\beta$ -decay occurs in the first order perturbation theory in the weak interaction. The corresponding S-matrix element is given by

$$S^{(1)} = -i \int dx T \left[ \mathcal{H}^{\beta}(x) e^{-i \int (\mathcal{H}^h(z) + \mathcal{H}^{h;\gamma}(z)) dz} \right]. \quad (3.4)$$

Here,  $\mathcal{H}^h(x)$  and  $\mathcal{H}^{h;\gamma}(x)$  is the Hamiltonian of strong interactions and the latter is the Hamiltonian of electromagnetic interactions of hadron fields involved. The strong and electromagnetic interactions are taken into account exactly in this way.

The initial and final states can be written in the Dirac notation as

$$\begin{aligned} |i\rangle &= |A\rangle \\ |f\rangle &= |e(p_e), \bar{\nu}(k_{\nu}), A'\rangle \\ &= c^{\dagger}(p_e)d^{\dagger}(k_{\nu})|A'\rangle. \end{aligned} \quad (3.5)$$

Here,  $|A\rangle$  and  $|A'\rangle$  denote mother and daughter nucleus. The creation operators of electron and antineutrino are denoted as  $c^{\dagger}(p_e)$  and  $d^{\dagger}(k_{\nu})$ , respectively.  $p_e$  and  $k_{\nu}$  are the electron and antineutrino four-momenta, respectively. For the S-matrix element of the process we get

$$\langle f|S^{(1)}|i\rangle = -i \int dx_{out} \langle e(p_e), \bar{\nu}(k_{\nu}), A' | \mathcal{H}_{h.r.}^{\beta}(x) | A \rangle_{in}, \quad (3.6)$$



with

$$\mathcal{H}_{h.r.}^\beta(x) = \frac{G_\beta}{\sqrt{2}} [\bar{e}(x)\gamma_\mu(1 - \gamma_5)\nu_e(x)] J^\mu(x) + h.c.. \quad (3.7)$$

Here,  $J_\mu(x)$  is the weak charged nuclear hadron current in the Heisenberg representation and we have used

$${}_{out} \langle A' | H_{h.r.}^\beta(x) | A \rangle_{in} = \langle A' | T(H^\beta(x) e^{-i \int (\mathcal{H}^h(x) + \mathcal{H}^{h;\gamma}(x)) dx}) | A \rangle. \quad (3.8)$$

For the sake of simplicity we will omit the indices "in" and "out" in the following text.

In the tritium  $\beta$ -decay the spin and parity of initial and final nuclei are equal. Therefore, it is classified as the super-allowed transition and the dominant contribution to the decay rate is determined by the s-wave states of emitted leptons

$$\begin{aligned} \Psi(\vec{x}, p_e) &\approx \sqrt{F_0(Z+1, E_e)} u(p_e) \\ \Phi^c(\vec{x}, k_\nu) &\approx u(-k_\nu). \end{aligned} \quad (3.9)$$

$\vec{x}$  stands for spatial coordinate vector of the lepton.  $e^{i\vec{p}\cdot\vec{x}} \approx 1$ , since the s-wave states of leptons are considered. The Fermi function  $F_0(Z+1, E_e)$  takes into account the electromagnetic interaction between the outgoing electron and the daughter nucleus. Finally, the matrix element of the process is given as

$$\begin{aligned} \langle f | S^{(1)} | i \rangle &= -i \frac{G_\beta}{\sqrt{2}} \sqrt{F_0(Z+1, E_e)} \frac{1}{\sqrt{2E_e}} \frac{1}{\sqrt{2E_\nu}} \bar{u}(p_e) \gamma_\alpha (1 - \gamma_5) u(-k_\nu) \\ &\quad \times \int dx e^{i(E_e + E_\nu)x_0} \langle A' | J^\alpha(x) | A \rangle \\ &= -i 2\pi \delta(E_f + E_e + E_\nu - E_i) \frac{G_\beta}{\sqrt{2}} \sqrt{F_0(Z+1, E_e)} \\ &\quad \times \frac{1}{\sqrt{2E_e}} \frac{1}{\sqrt{2E_\nu}} \bar{u}(p_e) \gamma_\alpha (1 - \gamma_5) u(-k_\nu) \langle A' | J^\alpha(0, \vec{x}) | A \rangle. \end{aligned} \quad (3.10)$$

We use the non-relativistic impulse approximation for the hadron current,

$$J_\mu(0, \vec{x}) = \sum_m \tau_m^+ [g_{\mu 0} + g_A g_{\mu k} (\vec{\sigma}_m)_k] \delta(\vec{x} - \vec{x}_m). \quad (3.11)$$

Here, the sum over  $m$  runs over all nucleons. The operator  $\tau_m^+$  is the isospin raising operator that turns the  $m$ -th neutron into a proton and  $\vec{\sigma}_m$  is the Pauli spin operator

of  $m$ -th neutron. The metric tensor is defined as  $g = \text{diag}(1, -1, -1, -1)$ . The matrix element of the process takes the form,

$$\begin{aligned}
\langle f|S^{(1)}|i\rangle &= -i2\pi\delta(E_f + E_e + E_\nu - E_i)\frac{G_\beta}{\sqrt{2}}\sqrt{F_0(Z+1, E_e)} \\
&\times \frac{1}{\sqrt{2E_e}}\frac{1}{\sqrt{2E_\nu}}\bar{u}(p_e)\gamma^\alpha(1-\gamma_5)u(-k_\nu) \\
&\times \left[ g_{\alpha 0}M_F + g_A g_{\alpha k}(\vec{M}_{GT})_k \right].
\end{aligned} \tag{3.12}$$

The Fermi and Gamow-Teller matrix elements are given as

$$\begin{aligned}
M_F &= \sum_{m,m'} \langle {}^3He(1/2^+)m' | \sum_n \tau_n^+ | {}^3H(1/2^+)m \rangle \\
\vec{M}_{GT} &= \sum_{m,m'} \langle {}^3He(1/2^+)m' | \sum_n \tau_n^+ \vec{\sigma}_n | {}^3H(1/2^+)m \rangle.
\end{aligned} \tag{3.13}$$

The subject of our interest is the non-polarized  $\beta$ -decay of tritium. Therefore, the sum over the  $z$ -projections ( $m, m'$ ) of spins of mother and daughter nuclei is performed. By performing the traces, the square of the matrix element is given as

$$\begin{aligned}
\sum_{spins} |\langle f|S|i\rangle|^2 &= \left( \frac{G_\beta}{\sqrt{2}} \right)^2 F_0(Z+1, E_e) 8(g^{\alpha 0}g^{\beta 0} + g^{kl}) \\
&\times \left[ g_{\alpha 0}M_F + g_A g_{\alpha k}(\vec{M}_{GT})_k \right] \left[ g_{\beta 0}M_F^* + g_A g_{\beta l}(\vec{M}_{GT}^*)_l \right] \\
&= \left( \frac{G_\beta}{\sqrt{2}} \right)^2 8F_0(Z+1, E_e) \\
&\times (|M_F|^2 + g_A^2 |M_{GT}|^2).
\end{aligned} \tag{3.14}$$

Here, the squares of Fermi and Gamow-Teller reduced nuclear matrix elements are given by

$$\begin{aligned}
|M_F|^2 &= \left| \langle {}^3He(1/2^+) || \sum_n \tau_n^+ || {}^3H(1/2^+) \rangle \right|^2 \\
|M_{GT}|^2 &= \left| \langle {}^3He(1/2^+) || \sum_n \tau_n^+ \sigma_n || {}^3H(1/2^+) \rangle \right|^2.
\end{aligned} \tag{3.15}$$

The Fermi matrix element can be evaluated by assuming the exact isospin symmetry and considering that the  ${}^3H$  and  ${}^3He$  form an isospin doublet. Isospin is given as

$T = 1/2$ , with the  $T_z = +1/2$  assigned to the  ${}^3He$  and the  $T_z = -1/2$  to the  ${}^3H$ . For the Fermi matrix element we get  $M_F = 1$ .

The absolute square of the Gamow-Teller matrix element can be estimated by using the Ikeda sum rule. For the ground state of tritium it is given as

$$\begin{aligned} 3(N - Z) &= \sum_m |\langle {}^3He_m | \tau^+ \sigma | {}^3H_{g.s.} \rangle|^2 + |\langle {}^3n_m | \tau^- \sigma | {}^3H_{g.s.} \rangle|^2 \\ &= 3. \end{aligned} \quad (3.16)$$

In  ${}^3H$  the 1s neutron level is already occupied by two neutrons. Therefore, the transition  $p \rightarrow n$  would need to be scattered into a higher orbit, e.g. 2s in the continuum. This is forbidden for the Gamow-Teller operator since it has no radial dependence. Thus only transition  ${}^3H \rightarrow {}^3He$  but not  ${}^3H \rightarrow 3n$  can contribute to the Ikeda sum rule. In addition, there are no excited states of  ${}^3He$ . As a consequence we have  $|M_{GT}|^2 = 3$ .

Usually, the Q-values of nuclear  $\beta$ -decays are small in comparison with nuclear masses. Therefore, recoil energy is replaced with rest mass of final nucleus. Thus only leptons, electron and neutrino, are considered in the phase space. The differential decay rate of the process takes the form

$$d\Gamma^\beta = \sum_{spins} |\langle f | S | i \rangle|^2 2\pi \delta(E_e + E_\nu + M_f - M_i) \frac{d\vec{p}_e}{(2\pi)^3} \frac{d\vec{k}_\nu}{(2\pi)^3}. \quad (3.17)$$

The integration over the neutrino variables is performed in order to obtain the electron energy distribution. For the sake of convenience the phase space is given in spherical coordinates.

$$\begin{aligned} d\Gamma^\beta &= \frac{1}{(2\pi)^5} G_\beta^2 F_0(Z + 1, E_e) (|M_F|^2 + g_A^2 |M_{GT}|^2) \\ &\quad \times \delta(E_e + E_\nu + M_f - M_i) p_e^2 dp_e d\Omega_{p_e} k_\nu^2 dk_\nu d\Omega_{k_\nu}. \end{aligned} \quad (3.18)$$

Next step is to integrate over the neutrino variables and electron angles  $d\Omega_{p_e}$ . Finally, the electron energy spectrum of tritium  $\beta$  decay is obtained. In more detail, the number of electrons  $N(E_e)$  emitted in narrow energy interval  $(E_e, E_e + dE_e)$  is given as

$$\begin{aligned} N(E_e) = \frac{d\Gamma^\beta}{dE_e} &= \frac{G_\beta^2}{2\pi^3} (|M_F|^2 + g_A^2 |M_{GT}|^2) \\ &\quad \times F_0(Z + 1, E_e) p_e E_e (E_0 - E_e) \sqrt{(E_0 - E_e)^2 - m_\beta^2}. \end{aligned} \quad (3.19)$$

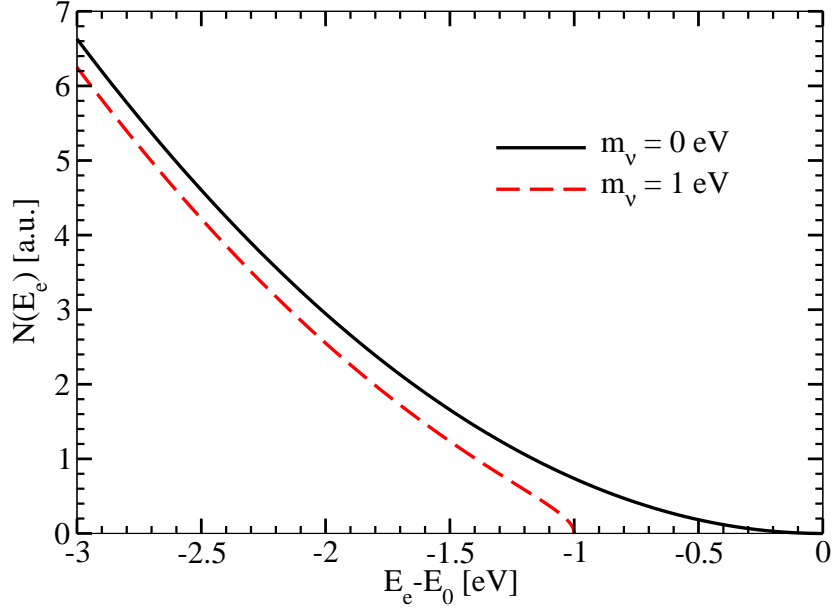


Figure 3.1: The endpoint electron energy spectrum is presented for various neutrino masses:  $m_\nu = 0, 1 \text{ eV}$ .

Here,  $p_e$ ,  $E_e$  and  $E_0 = M_i - M_f$  denote, respectively, the electron momentum, energy and maximal energy in case of zero neutrino mass.  $M_i$  and  $M_f$  stand for the rest masses of initial and final nuclei, respectively. For the non-zero neutrino mass the maximal electron energy shifts to  $E_e^{max} = E_0 - m_\nu$ . The Fermi function  $F_0(Z, E_e)$  takes into account the Coulomb interaction between the final nucleus and the emitted electrons. The electron energy spectrum near the endpoint is illustrated in Fig. 3.1. The effect of the neutrino mass is obvious. The spectrum is shifted and distorted near the endpoint. The connection between the decay rate and the half-life is given as

$$[T_{1/2}]^{-1} = \frac{\Gamma^\beta}{\ln 2} = \frac{1}{\ln 2} \int_{m_e}^{E_e^{max}} dE_e N(E_e). \quad (3.20)$$

In addition, the Kurie function is defined by

$$\begin{aligned} K(E_e, m_\nu) &\equiv \sqrt{\frac{d\Gamma^\beta/dE_e}{p_e E_e F_0(Z+1, E_e)}} \\ &= \frac{1}{2\pi^3} G_\beta^2 (|M_F|^2 + g_A^2 |M_{GT}|^2) (E_0 - E_e) \sqrt{(E_0 - E_e)^2 - m_\nu^2} \end{aligned} \quad (3.21)$$

The main aim of defining the Kurie function is its dependence on neutrino mass. For the case of zero neutrino mass it is a straight line crossing the electron energy

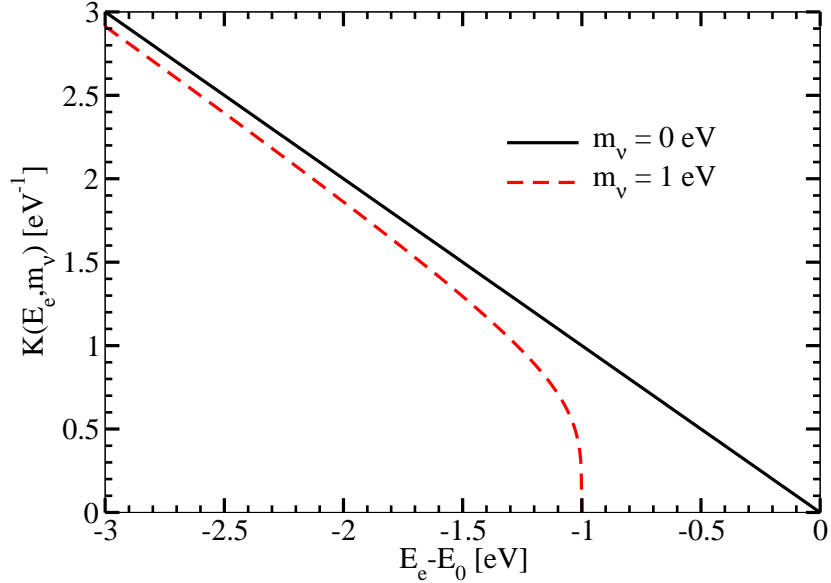


Figure 3.2: The Kurie function for allowed transitions is shown for two values of neutrino mass:  $m_\nu = 0, 1 \text{ eV}$ .

axis at the endpoint. For non-zero neutrino mass the linearity is lost, most apparently near the endpoint. The plot of the Kurie function for two different neutrino masses is illustrated in Fig. 3.2. The linearity might be lost also in case of forbidden transitions when the nuclear matrix elements become dependent on electron energy.

### 3.2 A relativistic treatment of tritium $\beta$ -decay

The relativistic description for the electron energy spectrum near the endpoint is presented in this section. The fact that the nuclei  ${}^3\text{H}$  and  ${}^3\text{He}$  are, respectively, the nuclear analogs of the neutron and the proton is taken into account. They form an isospin  $\text{SU}(2)$  doublet. The considered approach known as Elementary Particle Treatment which was developed by Kim and Primakoff [58] is revisited for the  $\beta$ -decay of tritium.

The process,



is performed in analogy with the  $\beta$ -decay of free neutron,



The kinematics of the two processes differ mostly due to different Q-values and the Coulomb corrections. The effects of higher order terms of hadron current and nuclear recoil are taken into account in this formalism.

The invariant  $\beta$ -decay amplitude is given by

$$\begin{aligned}
M &= \frac{G_\beta}{\sqrt{2}} \bar{u}(P_e) \gamma_\alpha (1 - \gamma_5) u(-P_\nu) \\
&\quad \times \bar{u}(P_f) \left[ G_V(q^2) \gamma^\alpha + i \frac{G_M(q^2)}{2M_i} \sigma^{\alpha\beta} q_\beta - G_A(q^2) \gamma^\alpha \gamma_5 - G_P(q^2) q^\alpha \gamma_5 \right] u(P_i).
\end{aligned} \tag{3.24}$$

Here,  $P_i = (M_i, 0)$ ,  $P_f = (E_f, \vec{p}_f)$ ,  $P_e = (E_e, \vec{p}_e)$  and  $P_\nu = (E_\nu, \vec{p}_\nu)$  are four-momenta of  ${}^3H$ ,  ${}^3He$ , electron and antineutrino in the laboratory frame, respectively.  $q_\alpha = (P_f - P_i)_\alpha = (P_e + P_\nu)_\alpha$  is the momentum transferred to the hadron vertex. In this section, an exception in the normalization of spinors is made with respect to the rest of the thesis. Namely, the sum over polarizations of spinors is  $\sum_{spins} u(P) \bar{u}(P) = \not{P} + M$ . The infinitesimal phase space volume is then given as  $d\vec{p}/(2E(2\pi)^3)$ . In this notation, both phase space and square of spin-summed amplitude are Lorentz invariant. The Lorentz invariance is important in the EPT approach of the reaction.

The form factors  $G_V(q^2)$ ,  $G_M(q^2)$ ,  $G_A(q^2)$ ,  $G_P(q^2)$  are real functions of the squared momentum  $q^2$ . They are parameterized as follows

$$G_V(q^2) = \frac{g_V}{\left(1 - \frac{q^2}{M_V^2}\right)^2}, \quad G_M(q^2) = \frac{g_M}{\left(1 - \frac{q^2}{M_V^2}\right)^2}, \quad G_A(q^2) = \frac{g_A}{\left(1 - \frac{q^2}{M_A^2}\right)^2}. \tag{3.25}$$

The two form-factor cut-offs  $M_V$  and  $M_A$  are in general different and their values are expected to be of the order of 1 GeV like it is in the case of nucleon form-factors. As it will be discussed later the  $q^2$ -dependence of these form-factors is not crucial for tritium  $\beta$ -decay.

The conserved vector current hypothesis (CVC) implies  $g_V = 1.0$ .  $g_M = -6.106$  is calculated from the values of magnetic moments of  ${}^3H$  and  ${}^3He$  using the CVC hypothesis as well [59]. The axial coupling constant  $g_A$  can be determined from the measured half-life of tritium. The induced pseudoscalar coupling is given by the partially conserved axial-vector current hypothesis (PCAC)

$$g_P(q^2) = \frac{2M_i}{m_\pi^2 - q^2} g_A(q^2). \tag{3.26}$$

$m_\pi$  is the mass of pion.

For the square of spin-summed, Lorentz-invariant amplitude we get

$$\begin{aligned} \frac{1}{2} \sum_{spins} |M|^2 = & 16G_\beta^2 \left[ G_V^2 \mathcal{P}_{VV} + G_A G_V \mathcal{P}_{AV} + G_A^2 \mathcal{P}_{AA} + \right. \\ & + G_A G_P \mathcal{P}_{AP} + G_P^2 \mathcal{P}_{PP} + G_V G_M \frac{\mathcal{P}_{VM}}{2M_i} \\ & \left. + G_A G_M \frac{\mathcal{P}_{AM}}{2M_i} + G_M^2 \frac{\mathcal{P}_{MM}}{4M_i^2} \right] \end{aligned} \quad (3.27)$$

with

$$\mathcal{P}_{VV} = P_{ef} P_{\nu i} + P_{ei} P_{\nu f} - M_i M_f P_{e\nu}, \quad (3.28)$$

$$\mathcal{P}_{AA} = P_{ef} P_{\nu i} + P_{ei} P_{\nu f} + M_i M_f P_{e\nu}, \quad (3.29)$$

$$\mathcal{P}_{AV} = 2(P_{ef} P_{\nu i} - P_{ei} P_{\nu f}), \quad (3.30)$$

$$\mathcal{P}_{AP} = M_f(m_e^2 P_{\nu i} + m_\nu^2 P_{ei}) - M_i(m_e^2 P_{\nu f} + m_\nu^2 P_{ef}), \quad (3.31)$$

$$\mathcal{P}_{PP} = \frac{1}{2}(P_{if} - M_i M_f)(P_{e\nu}(m_e^2 + m_\nu^2) + 2m_\nu^2 m_e^2), \quad (3.32)$$

$$\begin{aligned} \mathcal{P}_{VM} = & M_i [P_{e\nu}(P_{if} - M_f^2) + P_{ef}(P_{\nu i} - 2P_{\nu f}) + P_{ei} P_{\nu f}] \\ & + M_f [P_{e\nu}(P_{if} - M_i^2) + P_{ei}(P_{\nu f} - 2P_{\nu i}) + P_{ef} P_{\nu i}], \end{aligned} \quad (3.33)$$

$$\mathcal{P}_{AM} = 2(M_i + M_f)(P_{ef} P_{\nu i} - P_{ei} P_{\nu f}), \quad (3.34)$$

$$\begin{aligned} \mathcal{P}_{MM} = & \frac{1}{2} P_{if} (P_{e\nu}(m_e^2 + m_\nu^2) + 2m_e^2 m_\nu^2) - M_i M_f m_e^2 m_\nu^2 + 2P_{ei} P_{ef} (P_{e\nu} + m_\nu^2) \\ & + 2P_{\nu i} P_{\nu f} (P_{e\nu} + m_e^2) - \frac{1}{2} M_i M_f P_{e\nu} (3m_e^2 + 3m_\nu^2 + 4P_{e\nu}). \end{aligned} \quad (3.35)$$

Here,  $P_{kl} \equiv (P_k \cdot P_l)$  denotes the scalar product of two four-momenta. Indices  $i$ ,  $f$ ,  $e$  and  $\nu$  stand for initial nucleus, final nucleus, electron and antineutrino, respectively.

By neglecting the contribution from higher order currents (terms proportional to  $G_{M,P}$ ) it is found

$$\begin{aligned} \frac{1}{2} \sum_{spins} |M|^2 = & 16G_\beta^2 [(G_V + G_A)^2 (P_e \cdot P_f)(P_\nu \cdot P_i) \\ & + (G_V - G_A)^2 (P_e \cdot P_i)(P_\nu \cdot P_f) \\ & (-G_V^2 + G_A^2) M_i M_f (P_e \cdot P_\nu)]. \end{aligned} \quad (3.36)$$

The advantage of the presented formalism is that the squared Lorentz invariant amplitude is calculated exactly unlike in ref. [57], where an assumption about its

dominant constituent was considered. For  $G_V = G_A = 1$  the squared amplitude is proportional to  $(P_e \cdot P_f)(P_\nu \cdot P_i)$ , i.e., the structure is similar as, e.g., in the case of the muon decay.

For the tritium  $\beta$ -decay at rest the differential decay rate is

$$d\Gamma = \frac{1}{2M_i} F(Z, E_e) \left( \frac{1}{2} \sum_{spins} |M|^2 \right) \times \frac{(2\pi)^4}{(2\pi)^9} \delta^{(4)}(P_i - P_f - P_e - P_\nu) \frac{d^3 p_e}{2E_e} \frac{d^3 p_\nu}{2E_\nu} \frac{d^3 p_f}{2E_f}. \quad (3.37)$$

The factor  $1/2$  in front of the squared amplitude is for the average over the spin of the initial state.

The subject of interest is the energy distribution of the outgoing electrons. Hence, the integration over antineutrino and final nucleus momenta has to be performed in (3.37). It requires calculation of the following integrals,

$$\mathcal{K} = \int \frac{d^3 p_f}{E_f} \frac{d^3 p_\nu}{E_\nu} \delta^{(4)}(Q - P_f - P_\nu), \quad (3.38)$$

$$(\mathcal{L}_{\nu,f})^\rho = \int \frac{d^3 p_f}{E_f} \frac{d^3 p_\nu}{E_\nu} \delta^{(4)}(Q - P_f - P_\nu) (P_{\nu,f})^\rho, \quad (3.39)$$

$$(\mathcal{N}_{kl})^{\rho\sigma} = \int \frac{d^3 p_f}{E_f} \frac{d^3 p_\nu}{E_\nu} \delta^{(4)}(Q - P_f - P_\nu) (P_k)^\rho (P_l)^\sigma, \quad (3.40)$$

with  $Q = P_i - P_e$  and  $k, l = \nu, f$ . The detailed calculation of the integrals is given in the Appendix A.

The differential decay rate is found to be of the form,

$$\begin{aligned} \frac{d\Gamma}{dE_e} &= \frac{1}{2\pi^3} G_\beta^2 F(Z, E_e) p_e \frac{M_i^2}{(m_{12})^2} \sqrt{y \left( y + 2m_\nu \frac{M_f}{M_i} \right)} \\ &\times \left[ g_V^2 \mathcal{R}_{VV} + g_{AV} g_V \mathcal{R}_{AV} + g_A^2 \mathcal{R}_{AA} + g_{AP} g_V \mathcal{R}_{AP} \right. \\ &\left. + g_P^2 \mathcal{R}_{PP} + g_V g_M \mathcal{R}_{VM} + g_{AM} g_V \mathcal{R}_{AM} + g_M^2 \mathcal{R}_{MM} \right], \end{aligned} \quad (3.41)$$

where  $(m_{12})^2 = M_i^2 + m_e^2 - 2M_i E_e$  and  $y = E_e^{max} - E_e$ . The maximal electron energy,

$$E_e^{max} = \frac{1}{2M_i} (M_i^2 + m_e^2 - (M_f + m_\nu)^2), \quad (3.42)$$



gives value by about 3.4 eV lower than the conventional consideration  $E_e^{max} = E_0 - m_\nu$ . The energy of 3.4 eV is carried out by the recoiling nuclei. In the calculation we neglected  $q^2$  dependence of the form-factors as for the  $\beta$ -decay of tritium the value of  $q^2$  is rather small. Their consideration would lead only to small correction factors, which are not sensitive to neutrino mass. It is not of use to present here the explicit form of all  $\mathcal{R}_I$  ( $I = VV, VA, AA, AP, PP, VM, AM, MM$ ) factors. Instead of that the conclusion about their structure and importance is made.

The analysis showed that each term of  $\mathcal{R}_I$  is proportional to  $(y + m_\nu(M_f + m_\nu)/M_i)$  or  $(y + m_\nu M_f/M_i)$ . Hence, a common  $(y + m_\nu M_f/M_i)$  can be put in front of the bracket in (3.41) by neglecting a small term  $m_\nu/M_i$ . The importance of different  $\mathcal{R}_I$  contributions can be studied in the limit  $M_i = M_f$ ,  $E_e = m_e$  and by making Taylor expansion in  $m_\nu$ ,  $m_e$  ( $m_\nu \ll m_e \ll M_i$ ). The leading terms of different  $\mathcal{R}_I$  (without the common factor) are

$$\begin{aligned}
VV &: m_e M_i, & AA &: 3m_e M_i, & AV &: 2m_e^2, \\
VM &: \frac{1}{2} \frac{m_e^3}{M_i}, & MM &: \frac{3}{16} \frac{m_e^5}{M_i^3}, & AM &: 2m_e^2, \\
AP &: 2m_e M_i \frac{m_e^2}{m_\pi^2}, & PP &: \frac{1}{2} m_e M_i \frac{m_e^4}{M_i^2 m_\pi^2}.
\end{aligned} \tag{3.43}$$

From their comparison the conclusion that in fact the contributions coming from higher order terms of hadron current to the decay rate can be neglected is obtained.

The electron energy distribution is given as follows,

$$\begin{aligned}
\frac{d\Gamma}{dE_e} &= \frac{1}{2\pi^3} G_\beta^2 F(Z, E_e) p_e \frac{M_i^2}{(m_{12})^2} \sqrt{y \left( y + 2m_\nu \frac{M_f}{M_i} \right)} \\
&\times \left[ (g_V + g_A)^2 y \left( y + m_\nu \frac{M_f}{M_i} \right) \frac{M_i^2 (E_e^2 - m_e^2)}{3(m_{12})^4} \right. \\
&\quad + (g_V + g_A)^2 \left( y + m_\nu \frac{M_f + m_\nu}{M_i} \right) \frac{(M_i E_e - m_e^2)}{m_{12}^2} \\
&\quad \times \left( y + M_f \frac{M_f + m_\nu}{M_i} \right) \frac{(M_i^2 - M_i E_e)}{m_{12}^2} \\
&\quad - (g_V^2 - g_A^2) M_f \left( y + m_\nu \frac{(M_f + m_\nu)}{M_i} \right) \frac{(M_i E_e - m_e^2)}{(m_{12})^2} \\
&\quad \left. + (g_V - g_A)^2 E_e \left( y + m_\nu \frac{M_f}{M_i} \right) \right]. \tag{3.44}
\end{aligned}$$

The first term in the brackets in (3.44), which is quadratic in  $y$ , plays a subleading role. By keeping only the dominant contributions and by introducing a mass scale parameter  $M$  instead of the  $M_i$  and  $M_f$ , we get

$$\frac{d\Gamma}{dE_e} \simeq \frac{1}{2\pi^3} G_\beta^2 F(Z, E_e) p_e E_e (g_V^2 + 3g_A^2) \times \sqrt{y(y+2m_\nu)} (y+m_\nu). \quad (3.45)$$

The relativistic form of the Kurie function is defined by

$$K(y) = B \left( \sqrt{y(y+2m_\nu)} (y+m_\nu) \right)^{1/2}, \quad (3.46)$$

with

$$B = \frac{G_\beta}{\sqrt{2\pi^3}} \sqrt{g_V^2 + 3g_A^2}. \quad (3.47)$$

The unknown coupling constant  $g_A$  of the hadron current is fixed to the half-life of  ${}^3H$  [60, 61] with result  $g_A = 1.247$ . This value coincides well with that of the axial-vector coupling of the free nucleon. Then the  $\beta$ -strength is  $B = 3.43 \times 10^{-6} \text{ GeV}^{-2}$ . The numerical factors, 1 and 3, in front of constants  $g_V$  and  $g_A$  in eq. 3.47, respectively, correspond to the values of Fermi and Gamow-Teller matrix elements obtained in the conventional nuclear physics description of the process. Further, if  $y$  is replaced with  $(E_0 - E_e - m_\nu)$ , the relativistic Kurie function in eq. (3.46) is reduced to the commonly known Kurie function given in eq. (3.21).

The plot of the relativistic Kurie function versus  $y = E^{max} - E_e$  near the endpoint is illustrated in Fig. 3.3. Special attention is given to the effect of a small neutrino mass ( $m_\nu = 0.2, 0.4, 0.6$  and  $0.8 \text{ eV}$ ). For the zero neutrino mass the relativistic Kurie function is linear. Deviation from linearity depends on the magnitude of neutrino mass  $m_\nu$ . Though, there is no difference with the previously known dependences, it is worth to note that in this case the relativistic form of the  $\beta$ -decay Kurie function is used, which also takes the nuclear recoil into account.

In summary, it is found that the relativistic effects are small corrections to the results known in the conventional approach due to a small  $Q$ -value of the process. We found out that the recoil of the nucleus ( $\sim 3.4 \text{ eV}$ ) does not yield a significant change of the endpoint spectra if sub eV mass of neutrino is measured. It is found that there is no significant modification of the shape of the electron spectra close to the endpoint due to the nuclear recoil within the considered Elementary Particle Treatment of  $\beta$ -decay of tritium.

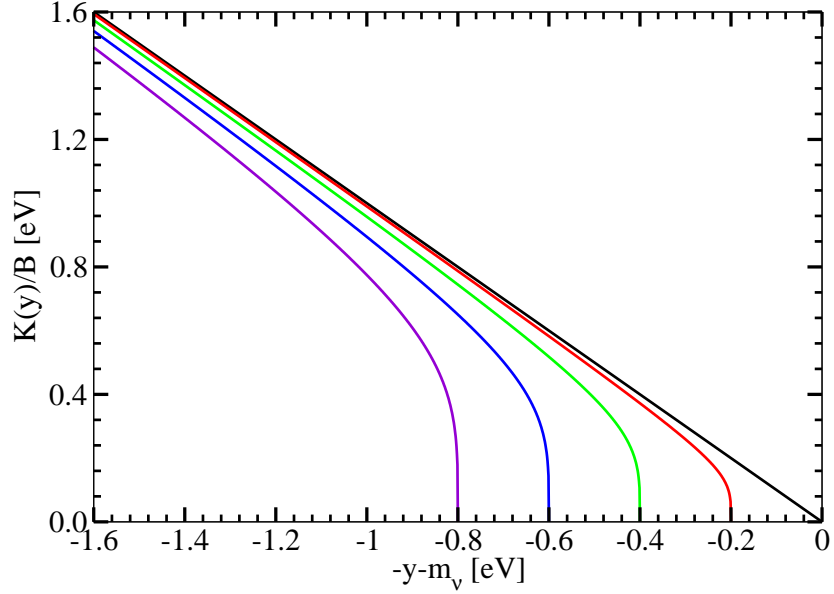


Figure 3.3: Endpoints of the relativistic Kurie plot [see Eqs. (3.46) and (3.47)] of the tritium beta decay for various values of the neutrino mass:  $m_\nu = 0, 0.2, 0.4, 0.6,$  and  $0.8 \text{ eV}$ .

### 3.3 Weak interactions beyond the Standard Model

The role of the weak interactions beyond the Standard Model, e.g. effective scalar and tensor interactions, is discussed here. It is worth to note that these exotic interactions appear naturally in theories beyond SM, e.g. within the R-parity breaking SUSY models. The constraints on the coupling constants of scalar and tensor interactions are given by the measurements of recoil spectrum in nuclear  $\beta$ -decays performed by the WITCH experiment at ISOLDE [62]. The theoretical framework used here is the Elementary Particle Treatment (EPT) of the tritium  $\beta$ -decay. The considered approach allows to perform the relativistic calculation for the electron energy spectrum close to the endpoint with the nuclear recoil taken into account.

The phenomenological Hamiltonian [63] of weak processes takes the form

$$H_\beta = (H_{V,A} + H_S + H_T), \quad (3.48)$$

with

$$\begin{aligned}
H_{V,A} &= \frac{G_\beta}{\sqrt{2}} [\bar{e}\gamma_\lambda(g_V + g'_V\gamma_5)\nu_e] [\bar{p}\gamma^\lambda n] \\
&\quad - [\bar{e}\gamma_\lambda\gamma_5(g_A + g'_A\gamma_5)\nu_e] [\bar{p}\gamma^\lambda\gamma_5 n] + h.c. \\
H_S &= \frac{G_\beta}{\sqrt{2}} [\bar{e}(g_S + g'_S\gamma_5)\nu_e] [\bar{p}n] + h.c. \\
H_T &= \frac{G_\beta}{\sqrt{2}} \frac{1}{2} [\bar{e}\sigma_{\lambda\mu}(g_T + g'_T\gamma_5)\nu_e] [\bar{p}\sigma^{\lambda\mu}n] + h.c.. \tag{3.49}
\end{aligned}$$

$H_{V,A}$ ,  $H_S$  and  $H_T$  are effective vector-axial, scalar and tensor Hamiltonians, respectively. The effective pseudoscalar Hamiltonian can be neglected due to the small energy release in the decay.  $g_{V,V'}$ ,  $g_{A,A'}$ ,  $g_S$  and  $g_T$  are vector, axial-vector, scalar and tensor coupling constants, respectively. Considering the time reversal invariance of the Hamiltonian the coupling constants  $g_{i,i'}$  are real parameters [62]. The standard  $V - A$   $\beta$ -decay Hamiltonian is restored from eq. (3.48) by the set of parameters given as  $g'_V = -g_V = -1$ ,  $g'_A = -g_A = 1.269$  and  $g'_S = g_S = g'_T = g_T = 0$ . In addition to the standard  $V - A$  interaction we add scalar or tensor interaction, respectively:

- i)  $g'_S = -g_S \neq 0$  and  $g'_T = g_T = 0$ ;
- ii)  $g'_S = g_S = 0$  and  $g'_T = -g_T \neq 0$ .

It is worth to mention that there exist constraints on scalar and tensor coupling constants,  $g_S/g_V = 0.0013$  and  $g_T/g_A = 0.0036$  [62], obtained from the WITCH experiment at ISOLDE.

For the sake of simplicity the neutrino mixing is neglected here. Within the considered EPT approach of tritium  $\beta$ -decay the differential decay rate takes the form

$$\frac{d\Gamma}{dE_e} = \frac{1}{(2\pi)^3\pi M_i} G_\beta^2 F(Z, E_e) p_e [C_{V-A} + C_{S,T}]. \tag{3.50}$$

Here, the  $C_{V-A}$  term in the differential decay rate is associated with the standard  $V - A$  interaction. The term  $C_S$  ( $C_T$ ) is due to the interference between standard  $V - A$  interaction and additional scalar (tensor) interaction. They take the following form

$$\begin{aligned}
C_{V-A} &= (g_A^2 - g_V^2) M_i M_f (P_e \cdot \mathcal{L}_\nu) + (g_V - g_A)^2 (P_e \cdot P_i) (P_\nu \cdot P_f) \mathcal{K} \\
&\quad + (g_V + g_A)^2 P_e^\rho P_i^\sigma \mathcal{N}_{\rho\sigma} \\
C_S &= g_V g_S m_e M_i (P_f \cdot P_\nu) \mathcal{K} + g_V g_S m_e M_f (P_i \cdot \mathcal{L}_\nu) \\
C_T &= -3g_T (g_A - g_V) m_e M_i (P_f \cdot P_\nu) \mathcal{K} - 3g_T (g_A + g_V) m_e M_f (P_i \cdot \mathcal{L}_\nu), \tag{3.51}
\end{aligned}$$

with the phase space integrals given as

$$\begin{aligned}
\mathcal{K} &= \int \frac{d^3 p_f}{E_f} \frac{d^3 p_\nu}{E_\nu} \delta^{(4)}(Q - P_f - P_\nu) \\
(\mathcal{L}_{\nu,f})^\rho &= \int \frac{d^3 p_f}{E_f} \frac{d^3 p_\nu}{E_\nu} \delta^{(4)}(Q - P_f - P_\nu) (P_{\nu,f})^\rho \\
(\mathcal{N}_{\nu,f})^{\rho\sigma} &= \int \frac{d^3 p_f}{E_f} \frac{d^3 p_\nu}{E_\nu} \delta^{(4)}(Q - P_f - P_\nu) (P_\nu)^\rho (P_f)^\sigma.
\end{aligned} \tag{3.52}$$

We recall that  $P_i = (M_i, 0)$ ,  $P_f = (E_f, p_f)$ ,  $P_e = (E_e, p_e)$  and  $P_\nu = (E_\nu, p_\nu)$  are four-momenta of the  ${}^3\text{H}$ ,  ${}^3\text{He}$ , electron and neutrino in the laboratory frame, respectively. The  $Q = P_f + P_\nu = P_i - P_e$  is the four-momentum of the system consisting of neutrino and recoiling nucleus. The next step is the integration over recoil and neutrino momentum. Details of calculation are given in Appendix A. The energy distribution of emitted electrons is given as

$$\begin{aligned}
\left(\frac{d\Gamma}{dE_e}\right)_{V-A,S} &\simeq \frac{1}{2\pi^3} G_\beta^2 F_0(Z, E_e) p_e \sqrt{y(y+2m_\nu)} (y+m_\nu) \\
&\times (E_e(g_V^2 + 3g_A^2) + m_e 2g_V g_S) \\
\left(\frac{d\Gamma}{dE_e}\right)_{V-A,T} &\simeq \frac{1}{2\pi^3} G_\beta^2 F_0(Z, E_e) p_e \sqrt{y(y+2m_\nu)} (y+m_\nu) \\
&\times (E_e(g_V^2 + 3g_A^2) - m_e 6g_A g_T).
\end{aligned} \tag{3.53}$$

The terms with coupling constants  $g_S$  ( $g_T$ ) in set of eqs. (3.53) are due to interference between the standard  $V - A$  and scalar (tensor) interaction. The subject of our interest is the impact of these additive terms on the shape of the spectrum. Let us analyze the terms in parentheses with coupling constants. We have

$$E_e(g_V^2 + 3g_A^2) + m_e 2g_V g_S = m_e(g_V^2 + 3g_A^2) + \frac{p_e^2}{2m_e}(g_V^2 + 3g_A^2) + m_e 2g_V g_S \tag{3.54}$$

and

$$E_e(g_V^2 + 3g_A^2) - m_e 6g_A g_T = m_e(g_V^2 + 3g_A^2) + \frac{p_e^2}{2m_e}(g_V^2 + 3g_A^2) - m_e 6g_A g_T \tag{3.55}$$

The first (constant) term on the right hand side of eqs. (3.54) and (3.55),  $m_e(g_V^2 + 3g_A^2)$ , is the dominant one. The second term, kinetic energy of electron, has a maximum

value of about 18.6 keV within  $\beta$ -decay of tritium. Considering the constraints on scalar ( $g_S = 1.3 \times 10^{-3}$ ) and tensor ( $g_T = 2.3 \times 10^{-3}$ ) coupling constants obtained from the WITCH experiment [62], a comparison of numerical values of expressions (3.54) and (3.55) is made.

$$\begin{aligned}
\frac{(p_e^{max})^2}{2m_e}(g_V^2 + 3g_A^2) &= 108 \text{ keV} \\
m_e 2g_V g_S &= 1.33 \text{ keV} \\
m_e 6g_A g_T &= 8.9 \text{ keV}.
\end{aligned}
\tag{3.56}$$

We get

$$\begin{aligned}
\frac{(p_e^{max})^2}{2m_e}(g_V^2 + 3g_A^2) &> m_e 2g_V g_S \\
\frac{(p_e^{max})^2}{2m_e}(g_V^2 + 3g_A^2) &> m_e 6g_A g_T
\end{aligned}
\tag{3.57}$$

and eventually we have

$$\begin{aligned}
E_e(g_V^2 + 3g_A^2) &\gg m_e 2g_V g_S \\
E_e(g_V^2 + 3g_A^2) &\gg m_e 6g_V g_T.
\end{aligned}
\tag{3.58}$$

We note that the kinetic energy term  $p_e^2/2m_e$  in eqs. (3.57) becomes smaller than the contribution  $m_e 2g_V g_S$  ( $m_e 6g_V g_T$ ) from the interference of scalar (tensor) interaction with  $V - A$  for  $p_e^2/2m_e < 0.23 \text{ keV}$  ( $p_e^2/2m_e < 1.5 \text{ keV}$  )

By analysis of the structure of (3.53) a conclusion is made that the effect of scalar and tensor interactions is significantly weaker than the well known  $V - A$  interaction on the spectrum of emitted electrons in the  $\beta$ -decay of tritium and can be therefore neglected.

## Conclusions

In this chapter, the relativistic calculation of the  $\beta$ -decay of tritium in a hadron model was presented. The elementary particle treatment of tritium  $\beta$ -decay follows from the analogy between  ${}^3H$  ( ${}^3He$ ) and the neutron (proton) having the same spin-isospin properties. It allowed us unlike in Ref. [57] to determine the squared  $\beta$ -decay amplitude

more accurately. The effects of higher order terms of hadron current and nuclear recoil are taken into account in this formalism. The relativistic Kurie function was derived and presented in a simple form suitable for the determination of neutrino masses from the shape of the endpoint spectrum. By comparing the relativistic and previously used Kurie functions a good agreement between them was established.

The relativistic form for the endpoint spectrum of tritium  $\beta$ -decay was derived within EPT approach by taking into account beyond the SM, effective scalar and tensor, interactions. It was found that these interactions, weaker than the V-A SM interaction, with the SM interaction cannot produce effects near the endpoint of the tritium  $\beta$ -decay spectrum which are of different character from those produced by the purely kinematic effect of the neutrino mass expected within the SM. These findings were published in Refs. [V,VIII] given in the *List of publications*.

# Chapter 4

## Neutrino mass and forbidden unique $\beta$ -decays of rhenium and indium

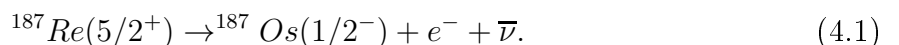
The aim of this chapter is to derive the form of the endpoint spectrum of emitted electrons for the  $\beta$ -decay of  $^{187}\text{Re}$ , which is needed to extract the effective electron neutrino mass  $m_\beta$  or to place a limit on this quantity from future MARE I and II experiments. The unique first forbidden  $\beta$ -decay of rhenium is particularly promising due to its low transition energy of  $\sim 2.47 \text{ keV}$  and the large isotopic abundance of  $^{187}\text{Re}$  (62.8%), which allows the use of absorbers made with natural Rhenium.

Recent measurement with Penning traps [64] has established that the  $\beta$ -decay of  $^{115}\text{In}(9/2+)$  to the first excited state of  $^{115}\text{Sn}(3/2+)$  is a transition with the smallest Q value ( $\sim 155\text{eV}$ ) among  $\beta$ -decays. The theoretical spectral shape of emitted electrons associated with the second unique forbidden  $\beta$ -decay transition  $^{115}\text{In}(9/2+) \rightarrow ^{115}\text{Sn}(3/2+)$  is presented.

The Kurie function of these transitions is discussed in the context of neutrino mass and the Kurie function of superallowed  $\beta$ -decay of tritium.

### 4.1 Theoretical treatment of the first unique forbidden $\beta$ -decay of rhenium

We present the first unique forbidden  $\beta$ -decay of the rhenium here. The subject of our interest is the process



The energy release of this reaction is the smallest known among all the ground state to ground state  $\beta$ -decaying nuclei. The spin-parity change between mother and



daughter nuclear ground states,  $^{187}\text{Re}(5/2^+) \rightarrow ^{187}\text{Os}(1/2^-)$ , is  $\Delta J^\pi = 2^-$ , i.e. this transition is classified as the first unique forbidden. The change of nuclear spin and parity is carried out by the emitted leptons involved in the reaction. Therefore, for the sake of convenience, the lepton wave functions are expressed in terms of spherical waves,

$$\Psi(E_e, \vec{x}) = \Psi_S(E_e, \vec{x}) + \Psi_P(E_e, \vec{x}) + \Psi_D(E_e, \vec{x}) \dots \quad (4.2)$$

Here, the indices  $S, P, D, \dots$  stand for the angular momentum values  $l = 0, 1, 2, \dots$ , i.e. we adopted the atomic physics notation. The parity of the particular spherical wave is given by  $\pi = (-1)^l$ . Considering the first order of  $G_\beta$  in the perturbation theory of weak interaction, for the amplitude of the process we get

$$\mathcal{M}_{Re} = -i \frac{G_\beta}{\sqrt{2}} \int d\vec{x} \langle J_f, M_f | J^\alpha(0, \vec{x}) | J_i, M_i \rangle \bar{\Psi}_e(\vec{x}) \gamma_\alpha (1 - \gamma_5) \Psi_\nu(\vec{x}). \quad (4.3)$$

Here, the  $J^\alpha(0, \vec{x})$  (see eq. 3.11 for the explicit form) is the nuclear charge changing weak hadron current. The main contribution to the amplitude arises from the  $s$  and  $p$  waves of the emitted leptons. The change of the angular momentum of 2 units can be achieved either by

- i) the emission of the electron in the  $s_{1/2}$ -state and antineutrino in the  $p_{3/2}$ -state simultaneously, or
- ii) the emission of the electron in the  $p_{3/2}$ -state and antineutrino in the  $s_{1/2}$ -state simultaneously.

Due to the centrifugal repulsion and small energy release in the above mentioned reaction (4.1) is the contribution from higher spherical waves of the leptons negligible. Both of the above mentioned channels for lepton states contribute coherently to the amplitude of the reaction (4.1). Thus, the amplitude is given as

$$\begin{aligned} \mathcal{M}_{Re} &= -i \frac{G_\beta}{\sqrt{2}} \int d\vec{x} \langle J_f, M_f | J^\alpha(0, \vec{x}) | J_i, M_i \rangle \\ &\times \left[ \bar{\Psi}_e^{(s_{1/2})}(\vec{x}) \gamma_\alpha (1 - \gamma_5) \Psi_\nu^{(p)}(\vec{x}) + \bar{\Psi}_e^{(p_{3/2})}(\vec{x}) \gamma_\alpha (1 - \gamma_5) \Psi_\nu^{(s)}(\vec{x}) \right]. \end{aligned} \quad (4.4)$$

The experimental observable is the energy of electron that is emitted in the rhenium  $\beta$ -decay (4.1). In order to obtain the electron energy spectrum we have to perform several procedures that are common for  $\beta$ -decay treatment.

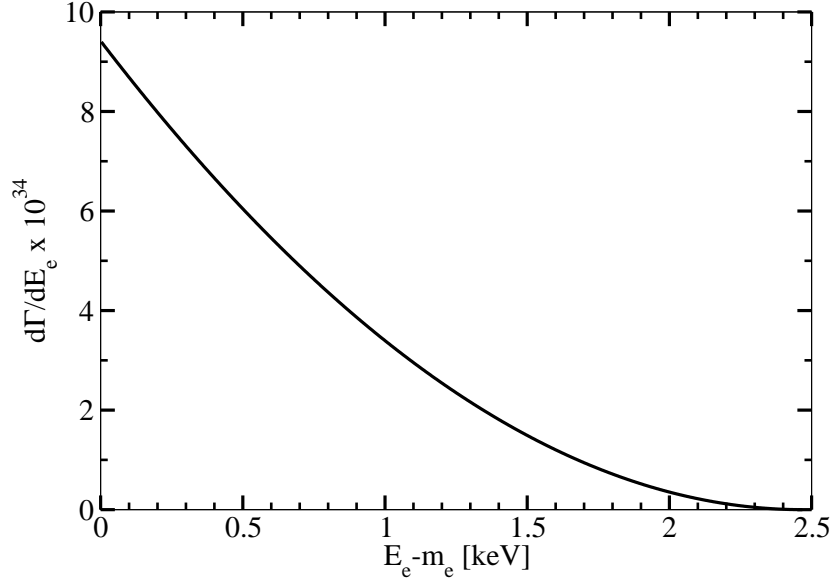


Figure 4.1: The electron energy spectrum of  $^{187}\text{Re}$  beta decay normalized to the experimental value of half-life  $T_{1/2}^{\text{exp}} = 4.35 \times 10^{10} \text{ y}$  [65].

Thus, we neglect the recoil effect here for the sake of smallness of energy release in the rhenium decay. As far as the neutrino is not observed we have to perform the integration over the neutrino momentum. Subject of our interest is the non-polarized  $\beta$ -decay of rhenium, i.e. we sum over the spin polarizations of constituents involved and finally we integrate over the electron momentum direction. After these steps we end up with the differential decay rate with respect to the electron energy  $E_e$ , that is measured experimentally indeed. The theoretical shape of electron energy spectrum of the  $\beta$ -decay of  $^{187}\text{Re}$  is

$$\begin{aligned}
 N(E_e) &= \frac{d\Gamma}{dE_e} = \frac{1}{2\pi^3} G_\beta^2 B R^2 p_e E_e (E_0 - E_e) \sqrt{(E_0 - E_e)^2 - m_\beta^2} \\
 &\times \frac{1}{3} \left( F_1(Z, E_e) p^2 + F_0(Z, E_e) ((E_0 - E_e)^2 - m_\beta^2) \right). \quad (4.5)
 \end{aligned}$$

with

$$B = \frac{g_A^2}{6} | \langle O_{s_{1/2}^-} | \sqrt{\frac{4\pi}{3}} \sum_n \tau_n^+ \frac{r_n}{R} \{ \sigma_1(n) \otimes Y_1(n) \}_2 | | Re_{5/2}^+ \rangle |^2. \quad (4.6)$$

$G_\beta = G_F V_{ud}$ , where  $G_F$  is the Fermi constant and  $V_{ud}$  is the element of the Cabbibo-Kobayashi-Maskawa (CKM) matrix.  $p_e$ ,  $E_e$  and  $E_0$  are the momentum, energy, and maximal endpoint energy (in the case of zero neutrino mass) of the electron, respectively.  $R$  is the nuclear radius. The Fermi functions  $F_0(Z, E)$  and  $F_1(Z, E)$  in (4.5)

are present due to a distortion of the  $s_{1/2}$  and the  $p_{3/2}$  electron wave states in the Coulomb field of final nucleus, respectively. We note that due to the fact of the first unique forbidden transition there is only one nuclear matrix element involved. The value of nuclear matrix element in (4.6) ( $B = 3.573 \times 10^{-4}$ ) can be determined from the measured value of half-life  $T_{1/2}^{exp} = 4.35 \times 10^{10}y$  of the  $\beta$ -decay of  $^{187}\text{Re}$  [65].

However, it is the shape of the electron energy spectrum, especially near the endpoint, that is so important for the neutrino mass estimation. The area beneath this spectrum negligibly depends on neutrino mass.

It is worth to mention that derived theoretical shape of the electron energy spectrum of  $^{187}\text{Re}$   $\beta$ -decay (4.5) has not been presented with relativistic electron wave function previously. The shape of the electron energy spectrum is shown in Fig. 4.1. It was already found out by the experiment [66] that the electrons are preferably emitted in the  $p_{3/2}$ -wave state. In forthcoming, we present the reasons that clarify the electron p-wave dominance in case of rhenium  $\beta$ -decay.

## 4.2 The dominance of electron $p$ -wave in the first unique forbidden $\beta$ -decay of rhenium

The differential decay rate of  $\beta$ -decay of  $^{187}\text{Re}$  (4.5) with respect to the electron energy is found to be a sum of two contributions.

$$\frac{d\Gamma}{dE_e} = \frac{d\Gamma^{s_{1/2}}}{dE_e} + \frac{d\Gamma^{p_{3/2}}}{dE_e}, \quad (4.7)$$

where  $d\Gamma^{s_{1/2}}$  and  $d\Gamma^{p_{3/2}}$  are the individual parts of differential decay rate associated to electrons to be in the  $s_{1/2}$  and  $p_{3/2}$  wave states, respectively. It is noteworthy that the interference between electron  $s$ - and  $p$ - wave states does not appear in the decay rate due to the fact that these are two distinguishable physical states. The explicit form of these particular parts of differential decay rate is given as

$$\frac{d\Gamma^{s_{1/2}}}{dE_e} = \frac{B}{6\pi^3} G_\beta^2 R^2 p_e F_0(Z, E_e) E_e (E_0 - E_e) ((E_0 - E_e)^2 - m_\beta^2)^{3/2} \quad (4.8)$$

and

$$\frac{d\Gamma^{p_{3/2}}}{dE_e} = \frac{B}{6\pi^3} G_\beta^2 R^2 p_e^3 F_1(Z, E_e) E_e (E_0 - E_e) \sqrt{(E_0 - E_e)^2 - m_\beta^2}. \quad (4.9)$$

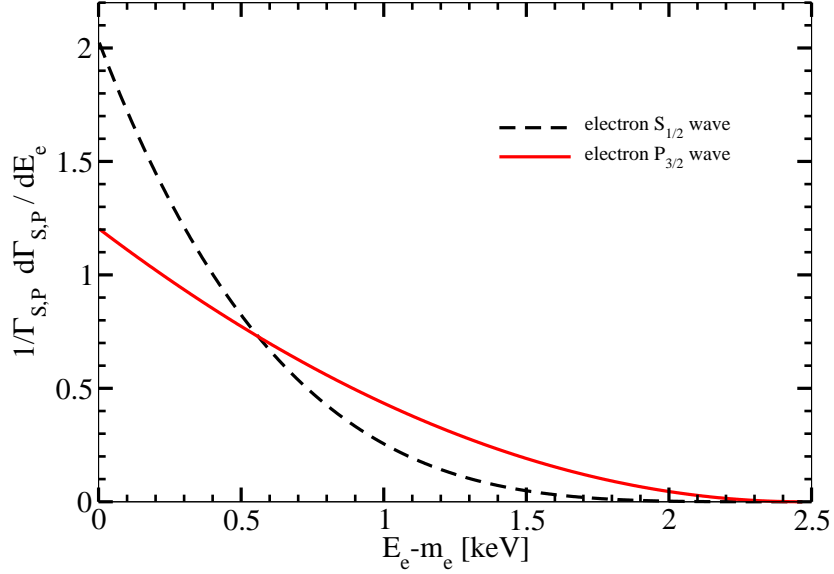


Figure 4.2: The particular decay rates associated with electron  $s_{1/2}$  and  $p_{3/2}$  wave states normalized to unity versus electron kinetic energy in rhenium  $\beta$ -decay.

The notation used here is the same as in the previous section. The particular differential decay rates (4.8, 4.9) normalized to unity are shown in Fig. 4.2 as a function of electron kinetic energy. We see that the partial decay rate associated with electron in  $p_{3/2}$ -state is rather smooth function and becomes dominant especially near the endpoint that is crucial for neutrino mass estimation.

One can naturally asks what is the relative strenght of the individual parts of the decay rate entering to the rhenium  $\beta$ -decay rate. For this purpose it is convenient to define

$$R(E_e) = \frac{d\Gamma^{s_{1/2}}/dE_e}{d\Gamma^{p_{3/2}}/dE_e}, \quad (4.10)$$

the ratio of the individual parts of differential decay rate (4.8, 4.9) as a function of the electron energy. The ratio 4.10 allows to see the relative strength as a function of energy for the whole energy region of few  $keV$  interesting for case of rhenium  $\beta$ -decay.

The function (4.10) is shown in the Fig. 4.3 against the electron kinetic energy. As far as we might see the electron  $s_{1/2}$  wave contribution to the decay rate is negligible with respect to the  $p_{3/2}$  wave contribution. In addition, for the ratio of decay rates associated with  $p_{3/2}$  and  $s_{1/2}$  electron waves we get

$$\frac{\Gamma^{s_{1/2}}}{\Gamma^{p_{3/2}}} = 1.011 \times 10^{-4}, \quad (4.11)$$

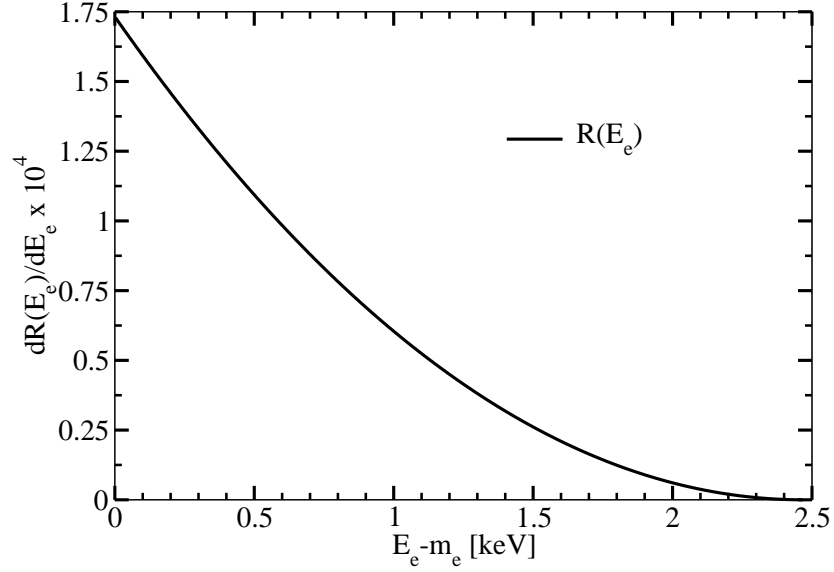


Figure 4.3: The ratio of the particular differential decay rates associated with electron in  $s_{1/2}$  and  $p_{3/2}$  wave states versus electron kinetic energy for the rhenium  $\beta$ -decay.

with

$$\begin{aligned}\Gamma^{s_{1/2}} &= \int_{m_e}^{E_0} dE_e \left( \frac{d\Gamma^{s_{1/2}}}{dE_e} \right) \\ \Gamma^{p_{3/2}} &= \int_{m_e}^{E_0} dE_e \left( \frac{d\Gamma^{p_{3/2}}}{dE_e} \right)\end{aligned}\tag{4.12}$$

This result means that the electron p-wave is dominant in the  $\beta$ -decay of rhenium, fact that can be seen from the energy behavior of the ratio defined in eq. 4.10 also.

In order to understand the dominant behavior of the particular differential decay rate  $d\Gamma^{p_{3/2}}/dE_e$  associated with the electron emission in  $p_{3/2}$  wave state we start our analysis with the plane wave limit for the sake of simplicity. In more detail, we "switch off" the electromagnetic interaction between the emitted electron and the final nucleus. This limit also establish the symmetry between the two emitted leptons with the rest mass being the only difference. By use of the property of the Fermi functions

$$\lim_{\alpha Z \rightarrow 0} F_k(Z, E_e) \rightarrow 1\tag{4.13}$$

we obtain for the electron energy spectrum in plane wave approximation (PWA)

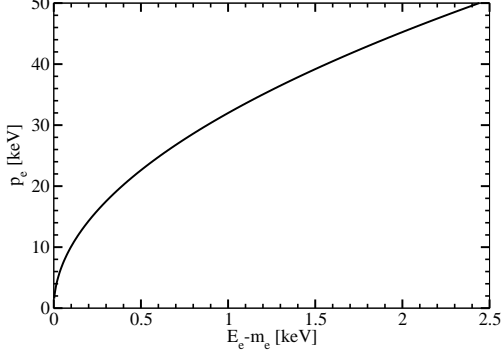


Figure 4.4: The electron momentum as a function of electron kinetic energy in the single  $\beta$ -decay of  $^{187}\text{Re}$ .

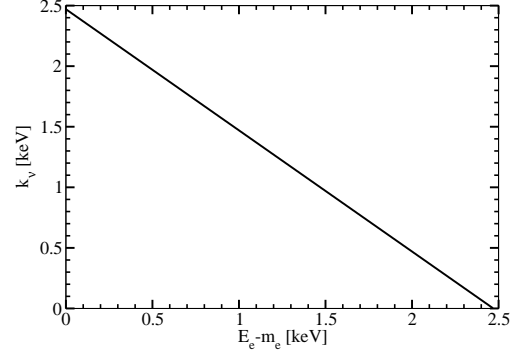


Figure 4.5: The neutrino momentum as a function of electron kinetic energy in the single  $\beta$ -decay of  $^{187}\text{Re}$ .

$$\begin{aligned} \left(\frac{d\Gamma}{dE_e}\right)_{PWA} &= \frac{1}{2\pi^3} G_\beta^2 B R^2 p_e E_e (E_0 - E_e) \sqrt{(E_0 - E_e)^2 - m_\beta^2} \\ &\times \frac{1}{3} (p_e^2 + k_\nu^2), \end{aligned} \quad (4.14)$$

with the square of neutrino momentum obtained from the energy conservation of the process (4.1), given as

$$k_\nu^2 = (E_0 - E_e)^2 - m_\beta^2. \quad (4.15)$$

The differential decay rate is expressed with respect to the electron kinetic energy that is observed experimentally indeed. The integration over the neutrino momentum and direction of electron momentum was already performed in (4.14).

The individual parts of the decay rate (4.8, 4.9) in the limit of no Coulomb interaction take the following form

$$\begin{aligned} \left(\frac{d\Gamma}{dE_e}\right)_{PWA} &= \left(\frac{d\Gamma^{s_{1/2}}}{dE_e}\right)_{PWA} + \left(\frac{d\Gamma^{p_{3/2}}}{dE_e}\right)_{PWA} \\ \left(\frac{d\Gamma^{s_{1/2}}}{dE_e}\right)_{PWA} &= C_S(E_e) k_\nu^2 \\ \left(\frac{d\Gamma^{p_{3/2}}}{dE_e}\right)_{PWA} &= C_S(E_e) p_e^2, \end{aligned} \quad (4.16)$$

where the common function is defined as

$$C_S(E_e) = \frac{1}{6\pi^3} G_\beta^2 B R^2 p_e E_e (E_0 - E_e) \sqrt{(E_0 - E_e)^2 - m_\beta^2}. \quad (4.17)$$

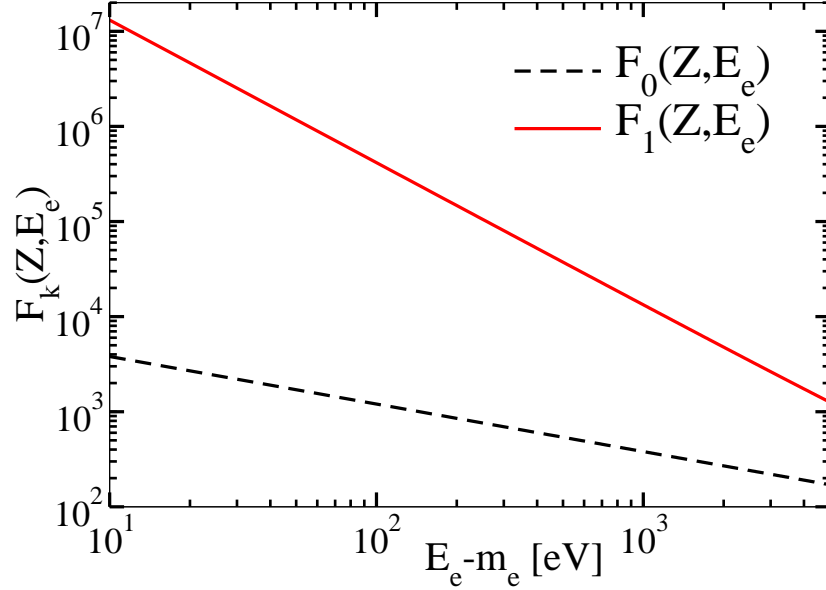


Figure 4.6: Relativistic Fermi functions for  $k = 0$  and  $k = 1$  as functions of electron energy  $E_e$  in energy interval relevant for the  $\beta$ -decay of  $^{187}\text{Re}$ .

We see that both individual differential decay rates contain common function given in eq. 4.17. The particular differential decay rates associated with electrons in  $s_{1/2}$  and  $p_{3/2}$  states in plane wave approximation (4.16) are obtained by multiplying the function (4.17) with square of neutrino ( $k_\nu^2$ ) and electron ( $p_e^2$ ) momenta, respectively. It is clear that behavior of particular differential decay rates in plane wave approximation obey the behavior of lepton momenta. Therefore it is worth to turn more attention to lepton momenta as a function of electron energy.

The  $Q$ -value ( $\sim 2.5 \text{ keV}$ ) is the maximal kinetic energy of electron (and neutrino simultaneously) that might be achieved in the decay. The  $Q$ -value in the rhenium decay is rather small with respect to the electron rest mass but still large with respect to the recent upper limit on neutrino rest mass ( $\sim 2.2 \text{ eV}$ ). As a consequence: i) the maximal neutrino momentum (energy) is  $\sim 2.5 \text{ keV}$ . ii) the maximal electron momentum is  $\sim 50 \text{ keV}$ . However, it is worth mentioning that neutrino and electron do not achieve the maximal momenta (kinetic energies) simultaneously. From energy conservation follows that if electron reaches maximum kinetic energy, neutrino is at rest and vice versa. For the sake of completeness the electron and neutrino momenta versus the electron kinetic energy are illustrated in Figs. 4.4 and 4.5, respectively. It is obvious that electron momentum dominates over neutrino momentum for almost the whole energy region with only exception in the low energy region.

We see that the kinematics is enhancing the electron p-wave contribution to the decay rate.

However, the electromagnetic interaction between the emitted electron and final nucleus takes place, eventually. Therefore, we have to investigate the behavior of relativistic Fermi functions  $F_k(Z, E_e)$  ( $k = 0, 1$ ) at least in the few  $keV$  region that is interesting for the case of rhenium  $\beta$ -decay. The explicit analytical form of these functions is given in (B.14). We would rather point out the behavior of the relativistic Fermi functions versus electron energy that is illustrated in Fig. 4.6. It is clear that the Fermi function  $F_1(Z, E_e)$  associated with  $p_{3/2}$  electron waves dominates over the Fermi function  $F_0(Z, E_e)$  associated with  $s_{1/2}$  electron waves for the energy region sufficient for the rhenium  $\beta$ -decay.

In summary, we found out that electrons in rhenium  $\beta$ -decay are emitted preferably in  $p_{3/2}$ -wave states. This can be understood as a direct consequence of small  $Q$ -value in rhenium  $\beta$ -decay. The fact that  $Q$ -value is small with respect to the electron rest mass and yet still large with respect to neutrino rest mass limit allow us to see the electron p-wave dominance in the reaction. There are two reasons for the enhancement of electron p-wave. These are: i) the kinematics of the reaction and ii) relativistic Fermi functions behavior in low energy region. These two effects sum up coherently into the decay rate.

### 4.3 The Kurie function

The Kurie function (3.21) has been introduced in order to resolve the issue of neutrino mass non-zerosness. For the allowed  $\beta$ -transitions the nuclear matrix elements are independent of the energy carried out by emitted electrons. Therefore, they contribute only as a scaling factor to the differential decay rate and henceforth do not change the shape of the electron energy spectrum. On the contrary, for forbidden transitions the nuclear matrix elements are dependent on energy [67]. In spite of this the Kurie function (3.21) deviates from linearity even for zero neutrino mass. Nevertheless, as becomes clear in forthcoming, we define the Kurie function for the rhenium  $\beta$ -decay in a standard way

$$K(E_e, m_\beta) = \sqrt{\frac{N(E_e)}{p_e E_e F_0(Z, E_e)}}. \quad (4.18)$$

The behavior of the Kurie function (4.18) defined is shown in Fig. 4.7 against the electron kinetic energy for the zero neutrino mass in case of rhenium  $\beta$ -decay. As a surprise, one may see that it is a straight line, within a good accuracy, crossing the energy axis at the endpoint.



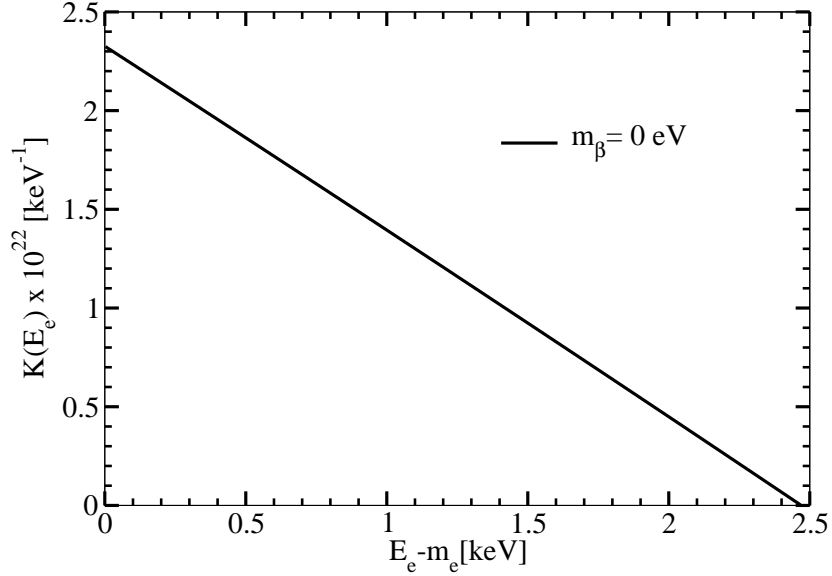


Figure 4.7: The Kurie function versus electron kinetic energy for rhenium  $\beta$ -decay in case of zero neutrino mass.

In order to understand this result we present here our analysis of the behavior of the Kurie function (4.18). The explicit analytical form of the relativistic Fermi functions  $F_k(Z, E_e)$ , taking into account the Coulomb interaction between the emitted electrons and final nucleus, lead us to the following approximation

$$\frac{p_e^2 F_1(Z, E_e)}{F_0(Z, E_e)} \approx m_e^2 \left[ 1 + 2 \frac{(E_e - m_e)}{m_e} \right]. \quad (4.19)$$

We note that the maximal electron kinetic energy (Q-value  $\sim 2.5$  keV) with respect to the electron rest mass is of the order of  $\sim 1\%$  and therefore the ratio (4.19) can be approximated as a constant within a good accuracy. Neglecting the electron  $s_{1/2}$  wave contribution to the decay rate we define for the rhenium  $\beta$ -decay

$$\mathcal{B}_{Re} = \frac{G_\beta \sqrt{B}}{\sqrt{2\pi^3}} \sqrt{\frac{R^2 p_e^2 F_1(Z, E_e)}{3 F_0(Z, E_e)}}. \quad (4.20)$$

Here, the  $B$  stands for the nuclear matrix element defined in (4.6). Considering aforementioned we assume the factor in (4.20) to be a constant. We might turn back to the linearity of Kurie function for the rhenium  $\beta$ -decay at this point. However, before we proceed further, we would like to point out the explicit form of the experimental observables, e.g. electron energy spectrum and Kurie function, in case of three neutrino mixing here. For the sake of simplicity we assume the normal mass hierarchy of neutrino masses ( $m_3 > m_2 > m_1$ ). For the electron energy spectrum we then get

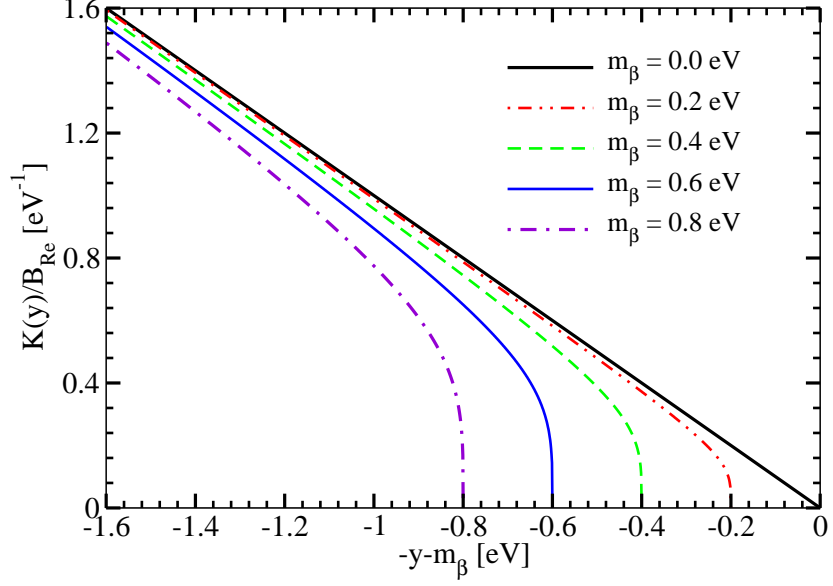


Figure 4.8: Endpoints of the Kurie function of the rhenium  $\beta$ -decay for various values of the effective neutrino mass:  $m_\beta = 0, 0.2, 0.4, 0.6$  and  $0.8$  eV.

$$\begin{aligned}
N(E_e) &= \frac{d\Gamma}{dE_e} = \sum_{k=1}^3 |U_{ek}|^2 \frac{G_F^2 V_{ud}^2}{2\pi^3} BR^2 p_e E_e (E_0 - E_e) \sqrt{(E_0 - E_e)^2 - m_k^2} \\
&\times \frac{1}{3} [F_1(Z, E_e) p_e^2 + F_0(Z, E_e) ((E_0 - E_e)^2 - m_k^2)] \theta(E_0 - E_e - m_k).
\end{aligned} \tag{4.21}$$

The nuclear matrix element is the same as in (4.6).

The Kurie function for forbidden  $\beta$ -decay of rhenium takes the form

$$\begin{aligned}
K(y) &= \mathcal{B}_{Re} \sqrt{y + m_1} \left[ |U_{e1}|^2 \sqrt{y(y + 2m_1)} \right. \\
&\quad + |U_{e2}|^2 \sqrt{(y + m_1 - m_2)(y + m_1 + m_2)} \theta(y + m_1 - m_2) \\
&\quad \left. + |U_{e3}|^2 \sqrt{(y + m_1 - m_3)(y + m_1 + m_3)} \theta(y + m_1 - m_3) \right]^{1/2},
\end{aligned} \tag{4.22}$$

with  $y = (E_0 - E_e - m_1) \geq 0$  as the independent variable instead of electron energy  $E_e$  and  $\theta$  is the common step function.

For the recent rhenium  $\beta$ -decay experiments is the energy resolution far beyond the limit to see the effect of small differences of the neutrino masses  $m_i - m_j$ . It is well possible to estimate the mass of neutrino below the energy resolution of detectors  $m_k \ll \delta E$ . For the Kurie function we obtain the following form

$$K(y) \simeq \mathcal{B}_{Re} \left( (y + m_\beta) \sqrt{y(y + 2m_\beta)} \right)^{1/2}, \quad (4.23)$$

where  $m_\beta$  is the effective mass of electron neutrino.

The Kurie function (4.23) is illustrated in Fig. 4.8 for various neutrino masses versus  $y$  near the endpoint. We see that for zero neutrino mass the Kurie plot is linear function.

We come to the conclusion, that the Kurie function of rhenium  $\beta$ -decay reveals the same functional dependence on neutrino mass, near the endpoint, as those for the allowed  $\beta$ -transitions. These findings are important for the planned experiment MARE II that aims to reach sub  $eV$  sensitivity.

## 4.4 Second unique forbidden $\beta$ -decay of indium

In this section the theoretical spectral shape of emitted electrons in the second unique forbidden  $\beta$ -decay,

$$^{115}\text{In}(9/2^+) \rightarrow ^{115}\text{Sn}(3/2^+) + e^- + \bar{\nu}_e \quad (4.24)$$

is presented. Recent measurements performed with Penning traps showed that the Q-value of this reaction is the smallest known  $\sim 155 eV$  [64].

The spin-parity change between the ground state of  $^{115}\text{In}(9/2^+)$  and the first nuclear excited state of  $^{115}\text{Sn}(3/2^+)$  is  $\Delta J^\pi = 3^+$ . Hence, the  $\beta$ -decay of  $^{115}\text{In}$  to the first excited state of  $^{115}\text{Sn}$  is classified as the second unique forbidden transition. The emitted electrons and antineutrinos are expected to be, respectively, in  $d_{5/2^-}$  and  $s_{1/2^-}$  states,  $p_{3/2^-}$  and  $p_{3/2^-}$  states and  $s_{1/2^-}$  and  $d_{5/2^-}$  states.

The  $\beta$ -decay rate is a sum of contributions associated with the  $d_{5/2}$ ,  $p_{3/2}$  and  $s_{1/2}$  wave electrons (see B). We get

$$\begin{aligned} \frac{d\Gamma}{dE_e} &= \sum_{k=1}^3 |U_{ek}|^2 \frac{G_\beta^2}{2\pi^3} B_{In} p_e E_e (E_0 - E_e) k_\nu \\ &\times \frac{1}{9} (p_e^4 F_2(Z, E_e) + 4p_e^2 k_\nu^2 F_1(Z, E_e) + k_\nu^4 F_0(Z, E_e)) \theta(E_0 - E_e - m_k). \end{aligned} \quad (4.25)$$

Here,  $k_\nu = \sqrt{(E_0 - E_e)^2 - m_k^2}$  is the neutrino momentum.  $F_k(Z, E_e)$  ( $k=1,2,3$ ) is the relativistic Fermi function.  $B_{In}$  takes the form

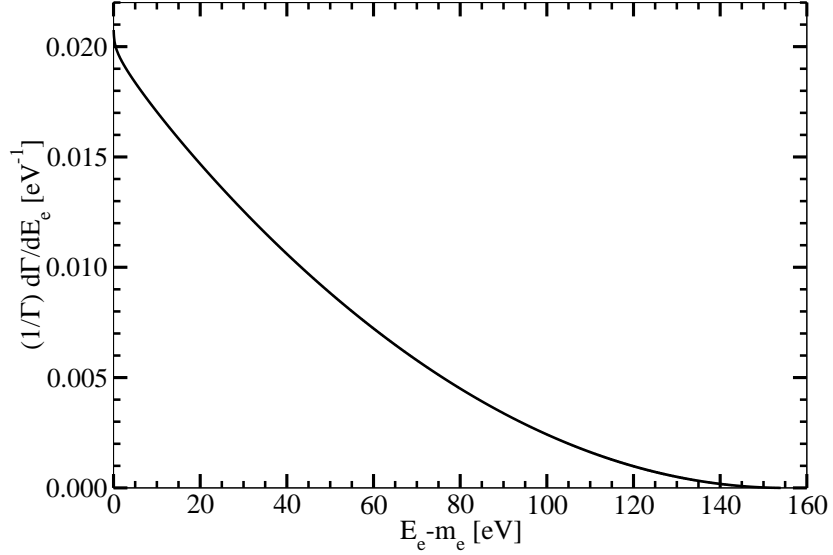


Figure 4.9: The single electron differential decay rate normalized to the total decay rate versus electron energy  $E_e$  for  $\beta$  transition  $^{115}\text{In}(9/2^+) \rightarrow ^{115}\text{Sn}(3/2^+)$ .

$$B_{In} = \frac{g_A^2}{10} \left| \langle ^{115}\text{Sn}(3/2^+) || \sqrt{\frac{8\pi}{15}} \sum_n r_n^2 \tau_n^+ \{ \sigma_1(n) \otimes Y_2(n) \}_3 || ^{115}\text{In}(9/2^+) \rangle \right|^2. \quad (4.26)$$

It contains single squared nuclear matrix element due to the uniqueness of the decay. Its value can be determined from the measured half-life of  $^{115}\text{In}(9/2^+) \rightarrow ^{115}\text{Sn}(3/2^+)$  transition.  $g_A$  is the axial-vector coupling constant.  $r_n$  is a coordinate of the  $n$ -th nucleon.

In Fig. 4.9 the single electron differential decay rate normalized to the total decay rate is shown as function of electron energy. This quantity is free of the nuclear matrix element of the process.

By performing numerical analysis of partial decay rates associated with emission of the  $d_{5/2}$ ,  $p_{3/2}$  and  $s_{1/2}$  electrons (terms associated with  $F_2(Z, E_e)$ ,  $F_1(Z, E_e)$  and  $F_0(Z, E_e)$  in Eq. (4.25), respectively) we conclude that about  $\sim 10^5$  times more  $d_{5/2}$ -state electrons are emitted when compared with other -state electrons. The reason for it is a small  $Q$ -value resulting to a fact that maximal electron momentum ( $\sim 12.6 \text{ keV}$ ) is much larger than the maximal momentum of neutrino ( $\sim 155 \text{ eV}$ ). In addition,  $F_2(Z, E_e) \gg F_1(Z, E_e) \gg F_0(Z, E_e)$  for  $E_e - m_e < Q$ . Thus, one can safely neglect small contributions to the total decay rate given by an emission of the  $p_{3/2}$ - and  $s_{1/2}$ -state electrons.

For a normal hierarchy of neutrino masses with  $m_3 > m_2 > m_1$  the Kurie function

of the unique second forbidden  $\beta$ -decay of  $^{115}\text{In}$  is given by

$$\begin{aligned}
K(y) &= \sqrt{\frac{d\Gamma/dE_e}{p_e E_e F_0(Z, E_e)}} \\
&= \mathcal{B}_{In} \sqrt{y + m_1} \left[ |U_{e1}|^2 \sqrt{y(y + 2m_1)} \right. \\
&\quad + |U_{e2}|^2 \sqrt{(y + m_1 - m_2)(y + m_1 + m_2)} \theta(y + m_1 - m_2) \\
&\quad \left. + |U_{e3}|^2 \sqrt{(y + m_1 - m_3)(y + m_1 + m_3)} \theta(y + m_1 - m_3) \right]^{1/2}, \quad (4.27)
\end{aligned}$$

with

$$\mathcal{B}_{In} = \frac{G_\beta \sqrt{B_{In}}}{\sqrt{2\pi^3}} \sqrt{\frac{1}{9} \frac{p_e^4 F_2(Z, E_e)}{F_0(Z, E_e)}}, \quad (4.28)$$

and  $y = (E_0 - E_e - m_1) \geq 0$ . With a good accuracy the factor  $\mathcal{B}_{In}$  can be considered to be a constant.

For the degenerate neutrino mass region ( $m_1 \simeq m_2 \simeq m_3 \simeq m_0$  with  $m_0 = \sum_{i=1}^3 |U_{ei}|^2 m_i$ ) we get

$$K(y) \simeq \mathcal{B}_{In} \left( (y + m_0) \sqrt{y(y + 2m_0)} \right)^{1/2}, \quad (4.29)$$

where  $y = (E_0 - E_e - m_0)$ . We see that the Kurie function for unique second forbidden  $\beta$ -decay of  $^{115}\text{In}$  is linear near the endpoint for  $m_0 = 0$ . However, the linearity of the Kurie plot is lost if  $m_0$  is not equal to zero.

In summary, for the second unique forbidden  $\beta$ -decay of  $^{115}\text{In}$  to the first excited state of  $^{115}\text{Sn}$ , the theoretical spectral shape is presented. The decay rate of this process is a sum of particular decay rates associated with emissions of  $d_{5/2^-}$ ,  $p_{3/2^-}$  and  $s_{1/2}$ -state electrons with a clear dominance of the  $d_{5/2^-}$ -state contribution. The Kurie function, defined by Eq. (4.27), coincides up to a factor to the Kurie function of superallowed  $\beta$ -decay of tritium.

## Conclusions

The theoretical spectral shape of emitted electrons for the first unique forbidden  $\beta$ -decay of  $^{187}\text{Re}$  to the ground state of  $^{187}\text{Os}$  was presented. The decay rate of the process was found to be a sum of particular decay rates associated with emissions of  $s_{1/2}$  and  $p_{3/2}$  electrons, which depend in a different way on the neutrino mass. The  $p$ -wave emission dominates over the  $s$ -wave. Kurie function for the rhenium  $\beta$ -decay was

derived. It was shown that the Kurie plot near the endpoint is within a good accuracy linear in the limit of massless neutrinos like the Kurie plot of the superallowed  $\beta$ -decay of tritium.

The theoretical spectral shape for the second unique forbidden  $\beta$ -decay of  $^{115}\text{In}$  to the first excited state of  $^{115}\text{Sn}$  was presented. Our investigation showed that in this transition electrons are predominantly emitted in  $d_{5/2}$  partial waves. In addition, it was found that the Kurie function associated with this transition near the end point within a good accuracy reflects a behavior the Kurie function of superallowed  $\beta$ -transitions.

Based on these findings we conclude that behavior of the Kurie function of an arbitrary n-th unique forbidden  $\beta$ -decay with sufficiently small  $Q$ -value is to a good accuracy the same as the behavior of Kurie function of superallowed  $\beta$ -decay transitions.

These findings were published in Refs. [I-IV,VI,VII] given in the *List of publications*.

# Chapter 5

## Double $\beta$ -decay within Single State Dominance hypothesis

The main interest in the double  $\beta$  decay is connected with the neutrinoless mode as a probe for physics beyond the Standard Model of electroweak interactions. On the other hand, the detection of double  $\beta$ -decay with emission of two neutrinos, which is an allowed process in the SM, provides the possibility for experimental determination of the corresponding nuclear matrix elements.

A subject of interest is the Single State Dominance (SSD) hypothesis proposed by Abad et al. [68], which suggests that the amplitude of  $2\nu\beta\beta$ -transition, where the ground state of intermediate nucleus is  $1^+$  state, is determined by two step transition, which connects initial and final states through this  $1^+$  ground state of intermediate nucleus. A discussion is given on possible realization of the SSD hypothesis in the case of the two-neutrino double  $\beta$ -decay of  $^{150}\text{Nd}$  with  $1^-$  ground state of the intermediate nucleus  $^{150}\text{Pm}$ .

The characteristics of the  $2\nu\beta\beta$ -decay of  $^{150}\text{Nd}$ , e.g. half-life and energy distributions of emitted electrons, are derived within SSD hypothesis.

### 5.1 Theoretical description of the double $\beta$ -decay

We present here the derivation of decay rate of the double  $\beta$  decay. The subject of our interest is the two-neutrino double  $\beta$ -decay,

$$(A, Z) \rightarrow (A, Z + 2) + 2e^- + 2\bar{\nu}. \quad (5.1)$$

This reaction is governed by the Hamiltonian of weak interaction given as

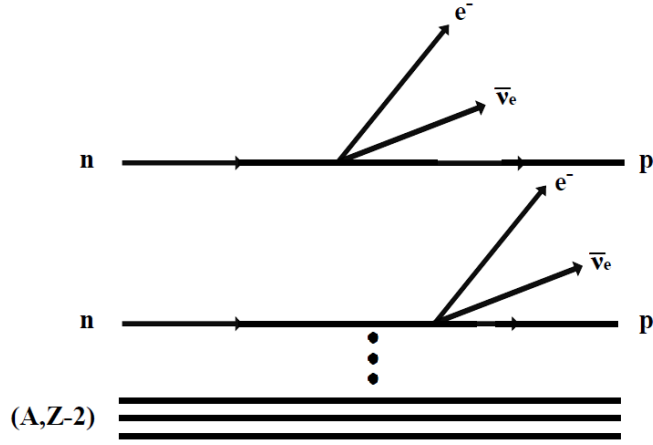


Figure 5.1: The Feynman diagram of the two-neutrino double  $\beta$ -decay process.

$$\mathcal{H}^\beta(x) = \frac{G_\beta}{\sqrt{2}} \bar{e}(x) \gamma^\alpha (1 - \gamma_5) \nu_e(x) j_\alpha(x) + h.c.. \quad (5.2)$$

Here,  $G_\beta = G_F \cos \theta_C$  is the weak interaction coupling constant.  $G_F$  and  $\theta_C$  are Fermi constant and Cabbibo angle, respectively.  $e(x)$  and  $\nu_e(x)$  represent the electron and neutrino field. The free hadron current takes the form

$$j_\alpha(x) = \bar{p}(x) \gamma_\alpha (g_V - g_A \gamma_5) n(x). \quad (5.3)$$

Here  $p(x)$ ,  $n(x)$  are the proton, neutron fields respectively and  $g_V = 1$  and  $g_A = 1.269$  are renormalization constants of vector and axial-vector hadron current, respectively.

Double  $\beta$ -decay is a second order process in theory of weak interaction given by Hamiltonian (5.2). Therefore, the relevant contribution to the S-matrix element is given as

$$S^{(2)} = \frac{(-i)^2}{2} \int dx_1 dx_2 T \left[ \mathcal{H}^\beta(x_1) \mathcal{H}^\beta(x_2) e^{-i \int (\mathcal{H}^h(z) + \mathcal{H}^{h;\gamma}(z)) dz} \right]. \quad (5.4)$$

$\mathcal{H}^h(x)$  a  $\mathcal{H}^{h;\gamma}(x)$  stand for the Hamiltonian of strong interaction and electromagnetic interaction of hadrons, respectively. The strong and electromagnetic interaction is considered here exactly.

The Feynman diagram for this nuclear process is illustrated in Fig. 5.1. For the initial and final states we may write



$$\begin{aligned}
|i\rangle &= |A\rangle \\
|f\rangle &= |e(p_{e1}), e(p_{e2}), \bar{\nu}(k_{\nu1}), \bar{\nu}(k_{\nu2}), A'\rangle \\
&= c^\dagger(p_{e1})c^\dagger(p_{e2})d^\dagger(k_{\nu1})d^\dagger(k_{\nu2})|A'\rangle.
\end{aligned} \tag{5.5}$$

Here,  $|A\rangle$  and  $|A'\rangle$  denote initial  $(A, Z)$  and final  $(A, Z + 2)$  nucleus.  $p_{e1}$  and  $p_{e2}$  correspond to the electron four-momenta and  $k_{\nu1}$  and  $k_{\nu2}$  stand for the neutrino four-momenta, respectively. For the electron and antineutrino operators,  $c^\dagger$  and  $d^\dagger$ , the anticommutation relations are given by

$$\begin{aligned}
c^\dagger(p_{e1})c^\dagger(p_{e2}) &= -c^\dagger(p_{e2})c^\dagger(p_{e1}) \\
d^\dagger(k_{\nu1})d^\dagger(k_{\nu2}) &= -d^\dagger(k_{\nu2})d^\dagger(k_{\nu1}).
\end{aligned} \tag{5.6}$$

For the matrix element of the two neutrino double  $\beta$ -decay we have

$$\begin{aligned}
\langle f|S^{(2)}|i\rangle &= \frac{(-i)^2}{2} \times \\
&\int dx_1 dx_2 \text{out} \langle e(p_{e1}), e(p_{e2}), \bar{\nu}(k_{\nu1}), \bar{\nu}(k_{\nu2}), A'|T [\mathcal{H}_{h.r.}^\beta(x_1)\mathcal{H}_{h.r.}^\beta(x_2)] |A\rangle_{in},
\end{aligned} \tag{5.7}$$

with

$$\mathcal{H}_{h.r.}^\beta(x) = \frac{G_\beta}{\sqrt{2}} [\bar{e}(x)\gamma^\alpha(1 - \gamma_5)\nu_e(x)] J_\alpha(x) + h.c.. \tag{5.8}$$

Here,  $J_\alpha(x)$  is the weak hadron current in Heisenberg representation. We have also used the relation

$$\begin{aligned}
&\text{out} \langle A'|T(H_{h.r.}^\beta(x_1)H_{h.r.}^\beta(x_2))|A\rangle_{in} \\
&= \langle A'|T(H^\beta(x_1)H^\beta(x_2)e^{-i\int(\mathcal{H}^h(x)+\mathcal{H}^{h;\gamma}(x))dx})|A\rangle.
\end{aligned} \tag{5.9}$$

For the sake of simplicity we will omit the indices "in" and "out". In order to perform the integration over the time we have to rewrite the T-product with help of the step function defined as

$$\vartheta(t) = \begin{cases} 0 & t \leq 0 \\ 1 & t > 0 \end{cases}$$

The T-product can be expressed as

$$T(H_{h.r.}^\beta(x_1)H_{h.r.}^\beta(x_2)) = \vartheta(x_{10} - x_{20})H_{h.r.}^\beta(x_1)H_{h.r.}^\beta(x_2) + \vartheta(x_{20} - x_{10})H_{h.r.}^\beta(x_2)H_{h.r.}^\beta(x_1). \quad (5.10)$$

It is worth mentioning that both terms of the expressed T-product contribute equally to the double  $\beta$ -decay matrix element (5.7). We shall take the advantage of the completeness of states ( $\sum_n |n\rangle\langle n| = 1$ ) of the intermediate nucleus ( $A, Z + 1$ ). Moreover, the nuclear states of parent, daughter and intermediate nuclei are eigenstates of the nuclear Hamiltonian  $H$ . Considering the time dependent form of the hadron current operator in Heisenberg representation given as

$$J_\mu(x) = e^{iHx_0} J_\mu(0, \vec{x}) e^{-iHx_0} \quad (5.11)$$

with the above mentioned considerations we get

$$\begin{aligned} & \langle e(p_{e1}), e(p_{e2}), \bar{\nu}(k_{\nu1}), \bar{\nu}(k_{\nu2}), A' | H_{h.r.}^\beta(x_1) H_{h.r.}^\beta(x_2) | A \rangle = \\ & \left( \frac{G_\beta}{\sqrt{2}} \right)^2 e^{(E_{e1} + E_{\nu1})x_{10}} e^{(E_{e2} + E_{\nu2})x_{20}} \times \\ & \bar{\Psi}(\vec{x}_1, p_{e1}) \gamma_\mu (1 - \gamma_5) \Phi^c(\vec{x}_1, k_{\nu1}) \bar{\Psi}(\vec{x}_2, p_{e2}) \gamma_\nu (1 - \gamma_5) \Phi^c(\vec{x}_2, k_{\nu2}) \times \\ & \sum_n e^{i(E_f - E_n)x_{10}} e^{i(E_n - E_i)x_{20}} \langle A' | J^\mu(0, \vec{x}_1) | n \rangle \langle n | J^\nu(0, \vec{x}_2) | A \rangle \\ & - (p_{e1} \leftrightarrow p_{e2}) - (k_{\nu1} \leftrightarrow k_{\nu2}) + (p_{e1} \leftrightarrow p_{e2})(k_{\nu1} \leftrightarrow k_{\nu2}). \end{aligned} \quad (5.12)$$

$E_i$ ,  $E_f$  and  $E_n$  are the initial, final and intermediate nuclear state energies, respectively. The sum  $\sum_n$  runs over all discrete states of the intermediate nucleus assuming their completeness. By use of adiabatic switch off of interaction at infinity ( $x_0 \rightarrow \pm\infty$ )

$$\begin{aligned} \int_{-\infty}^0 e^{ia\tau} d\tau & \implies \lim_{\varepsilon \rightarrow 0} \int_{-\infty}^0 e^{i(a-i\varepsilon)\tau} d\tau = \lim_{\varepsilon \rightarrow 0} \frac{-i}{a - i\varepsilon}, \\ \int_0^{\infty} e^{-ia\tau} d\tau & \implies \lim_{\varepsilon \rightarrow 0} \int_0^{\infty} e^{-i(a-i\varepsilon)\tau} d\tau = \lim_{\varepsilon \rightarrow 0} \frac{-i}{a - i\varepsilon} \end{aligned} \quad (5.13)$$

we may perform the integration over the time variables. We end up with

$$\begin{aligned}
& \langle f|S^{(2)}|i \rangle = i 2\pi\delta(E_{e1} + E_{e2} + E_{\nu1} + E_{\nu2} + E_f - E_i) \left( \frac{G_\beta}{\sqrt{2}} \right)^2 \\
& \int d\vec{x}_1 d\vec{x}_2 \bar{\Psi}(\vec{x}_1, p_{e1}) \gamma_\mu (1 - \gamma_5) \Phi^c(\vec{x}_1, k_{\nu1}) \bar{\Psi}(\vec{x}_2, p_{e2}) \gamma_\nu (1 - \gamma_5) \Phi^c(\vec{x}_2, k_{\nu2}) \\
& \quad \times \sum_n \frac{\langle A'|J^\mu(0, \vec{x}_1)|n \rangle \langle n|J^\nu(0, \vec{x}_2)|A \rangle}{E_n - E_i + E_{e2} + E_{\nu2}} \\
& \quad - (p_{e1} \leftrightarrow p_{e2}) - (k_{\nu1} \leftrightarrow k_{\nu2}) + (p_{e1} \leftrightarrow p_{e2})(k_{\nu1} \leftrightarrow k_{\nu2}).
\end{aligned} \tag{5.14}$$

For the sake of simplicity we introduce the following approximations as far as they will not reduce the value of further results.

i) We consider only the  $s_{1/2}$  and  $p_{1/2}$  electron waves and  $s_{1/2}$  neutrino wave (see App. B).

$$\begin{aligned}
\Psi(\vec{x}, p_e) & \approx \sqrt{F_0(Z+2, E_e)} \left( 1 + \frac{\alpha(Z+2)}{2} \gamma_0 \vec{\gamma} \cdot \frac{\vec{x}}{R} \right) u(p_e) \\
\Phi^c(\vec{x}, k_\nu) & \approx u(-k_\nu).
\end{aligned} \tag{5.15}$$

$\vec{x}$  is the lepton coordinate vector and  $R$  is the nuclear radius.

ii) The non-relativistic approximation of hadron current is given as

$$J_\nu(0, \vec{x}) = \sum_m \tau_m^+ [g_{\nu0} + g_A g_{\nu k} (\vec{\sigma}_m)_k] \delta(\vec{x} - \vec{x}_m), \tag{5.16}$$

where the sum is running over all nucleons.

iii) The subject of our interest are only the transitions to the ground state  $0^+$  and first excited state  $2_1^+$  of daughter nucleus. Due to the previous assumptions on lepton wave functions these transitions can be realized only via the  $0^+$ ,  $1^+$ ,  $0^-$  and  $1^-$  states of the intermediate nucleus.

By use of the relation

$$\vec{\gamma} \cdot \vec{a} \vec{\gamma} \cdot \vec{b} = \vec{a} \cdot \vec{b} + \gamma_0 \vec{\gamma} \cdot (\vec{a} \times \vec{b}) \tag{5.17}$$

for the transitions  $0^+ \rightarrow 0^+$  and  $0^+ \rightarrow 2^+$  we get

$$\begin{aligned}
\langle f|S^{(2)}|i\rangle &= i \left( \frac{G_\beta}{\sqrt{2}} \right)^2 2\pi\delta(E_{e1} + E_{e2} + E_{\nu1} + E_{\nu2} + E_f - E_i) \\
&\times \sqrt{F_0(Z+2, E_{e1})} \sqrt{F_0(Z+2, E_{e2})} \frac{1}{\sqrt{2E_{e1}}} \frac{1}{\sqrt{2E_{e2}}} \frac{1}{\sqrt{2E_{\nu1}}} \frac{1}{\sqrt{2E_{\nu2}}} \\
&\quad \times \bar{u}(p_{e1})\gamma_\mu(1-\gamma_5)u(-k_{\nu1}) \bar{u}(p_{e2})\gamma_\nu(1-\gamma_5)u(-k_{\nu2}) \\
&\quad \times \left[ g^{\mu0}g^{\nu0}\mathcal{M}^{(0)}(J^+) + g^{\mu k}g^{\nu l}\mathcal{M}_{kl}^{(1)}(J^+) \right] \\
&\quad - (p_{e1} \leftrightarrow p_{e2}) - (k_{\nu1} \leftrightarrow k_{\nu2}) + (p_{e1} \leftrightarrow p_{e2})(k_{\nu1} \leftrightarrow k_{\nu2}),
\end{aligned} \tag{5.18}$$

with

$$\begin{aligned}
\mathcal{M}^{(0)}(J^+) &= \sum_{\mathcal{J}^\pi=0^+,0^-} \sum_n \frac{\langle J_f^+ | \mathcal{O}(\mathcal{J}^\pi) | \mathcal{J}^\pi, n \rangle \langle \mathcal{J}^\pi, n | \mathcal{O}(\mathcal{J}^\pi) | 0_i^+ \rangle}{E_n - E_i + E_{e2} + E_{\nu2}} \\
\mathcal{M}_{kl}^{(1)}(J^+) &= \sum_{\mathcal{J}^\pi=1^+,1^-} \sum_n \frac{\langle J_f^+ | \mathcal{O}_k(\mathcal{J}^\pi) | \mathcal{J}^\pi, n \rangle \langle \mathcal{J}^\pi, n | \mathcal{O}_l(\mathcal{J}^\pi) | 0_i^+ \rangle}{E_n - E_i + E_{e2} + E_{\nu2}}.
\end{aligned} \tag{5.19}$$

The transition operators are given as

$$\begin{aligned}
\mathcal{O}(0^+) &= \sum_m \tau_m^+, \quad \mathcal{O}_k(1^+) = g_A \sum_m \tau_m^+ (\vec{\sigma}_m)_k \\
\mathcal{O}(0^-) &= -g_A \left( \frac{\alpha Z'}{2} \right) \sum_m \tau_m^+ \left( \frac{\vec{x}_m \cdot \vec{\sigma}_m}{R} \right), \\
\mathcal{O}_k(1^-) &= \left( \frac{\alpha Z'}{2} \right) \sum_m \tau_m^+ \frac{1}{R} (\vec{x}_m - g_A \vec{x}_m \times \vec{\sigma}_m)_k.
\end{aligned} \tag{5.20}$$

Here  $\mathcal{O}(0^+)$  and  $\mathcal{O}_k(1^+)$  are the operators of Fermi and Gamow-Teller transitions.  $\mathcal{O}(0^-)$  and  $\mathcal{O}_k(1^-)$  are operators involved in the first forbidden  $\beta$ -decays.  $Z'$  stands for the proton number of final nucleus ( $Z' = Z + 2$ ).

We shall take the advantage of the Fierz transformation (for details see Appendix C) in order to recouple the electron and neutrino spinors together

$$\begin{aligned}
&\bar{u}(p_{e1})\gamma_\mu(1-\gamma_5)u(-k_{\nu1}) \bar{u}(p_{e2})\gamma_\nu(1-\gamma_5)u(-k_{\nu2}) = \\
&-\frac{1}{2}\bar{u}(p_{e1})(1+\gamma_5)u(-p_{e2}) \bar{u}(k_{\nu1})\gamma_\nu\gamma_\mu(1-\gamma_5)u(-k_{\nu2}) \\
&+\frac{1}{8}\bar{u}(p_{e1})\sigma^{\alpha\beta}(1+\gamma_5)u(-p_{e2}) \bar{u}(k_{\nu1})\gamma_\nu\sigma_{\alpha\beta}\gamma_\mu(1-\gamma_5)u(-k_{\nu2}).
\end{aligned} \tag{5.21}$$

For the double  $\beta$ -decay amplitude we then have

$$\begin{aligned}
& \langle f|S^{(2)}|i \rangle = 2\pi\delta(E_{e1} + E_{e2} + E_{\nu1} + E_{\nu2} + E_f - E_i) \times \\
& \frac{-i}{2} \left( \frac{G_\beta}{\sqrt{2}} \right)^2 \sqrt{F_0(Z', E_{e1})} \sqrt{F_0(Z', E_{e2})} \frac{1}{\sqrt{2E_{e1}}} \frac{1}{\sqrt{2E_{e2}}} \frac{1}{\sqrt{2E_{\nu1}}} \frac{1}{\sqrt{2E_{\nu2}}} \times \\
& \left[ (\mathcal{K}^{(0)} + \mathcal{L}^{(0)}) \bar{u}(p_{e1})(1 + \gamma_5)u(-p_{e2}) \bar{u}(k_{\nu1})(1 - \gamma_5)u(-k_{\nu2}) \right. \\
& - \frac{(\mathcal{K}^{(0)} - \mathcal{L}^{(0)})}{4} \bar{u}(p_{e1})\sigma^{\alpha\beta}(1 + \gamma_5)u(-p_{e2}) \bar{u}(k_{\nu1})\gamma_0\sigma_{\alpha\beta}\gamma_0(1 - \gamma_5)u(-k_{\nu2}) \\
& + (\mathcal{K}_{kl}^{(1)} + \mathcal{L}_{kl}^{(1)}) \bar{u}(p_{e1})(1 + \gamma_5)u(-p_{e2}) \bar{u}(k_{\nu1})\gamma^l\gamma^k(1 - \gamma_5)u(-k_{\nu2}) \\
& \left. - \frac{(\mathcal{K}_{kl}^{(1)} - \mathcal{L}_{kl}^{(1)})}{4} \bar{u}(p_{e1})\sigma_{\alpha\beta}(1 + \gamma_5)u(-p_{e2}) \bar{u}(k_{\nu1})\gamma^l\sigma^{\alpha\beta}\gamma^k(1 - \gamma_5)u(-k_{\nu2}) \right], \tag{5.22}
\end{aligned}$$

with

$$\begin{aligned}
\mathcal{K}^{(0)} &= \sum_{\mathcal{J}^\pi=0^+,0^-} \sum_n \langle J_f^+ | \mathcal{O}(\mathcal{J}^\pi) | \mathcal{J}^\pi, n \rangle \langle \mathcal{J}^\pi, n | \mathcal{O}(\mathcal{J}^\pi) | 0_i^+ \rangle K_n \\
\mathcal{L}^{(0)} &= \sum_{\mathcal{J}^\pi=0^+,0^-} \sum_n \langle J_f^+ | \mathcal{O}(\mathcal{J}^\pi) | \mathcal{J}^\pi, n \rangle \langle \mathcal{J}^\pi, n | \mathcal{O}(\mathcal{J}^\pi) | 0_i^+ \rangle L_n \\
\mathcal{K}_{kl}^{(1)} &= \sum_{\mathcal{J}^\pi=1^+,1^-} \sum_n \langle J_f^+ | \mathcal{O}_k(\mathcal{J}^\pi) | \mathcal{J}^\pi, n \rangle \langle \mathcal{J}^\pi, n | \mathcal{O}_l(\mathcal{J}^\pi) | 0_i^+ \rangle K_n \\
\mathcal{L}_{kl}^{(1)} &= \sum_{\mathcal{J}^\pi=1^+,1^-} \sum_n \langle J_f^+ | \mathcal{O}_k(\mathcal{J}^\pi) | \mathcal{J}^\pi, n \rangle \langle \mathcal{J}^\pi, n | \mathcal{O}_l(\mathcal{J}^\pi) | 0_i^+ \rangle L_n. \tag{5.23}
\end{aligned}$$

The energy denominators are given as

$$\begin{aligned}
K_n &= \frac{1}{E_n - E_i + E_{e1} + E_{\nu1}} + \frac{1}{E_n - E_i + E_{e2} + E_{\nu2}} \\
L_n &= \frac{1}{E_n - E_i + E_{e1} + E_{\nu2}} + \frac{1}{E_n - E_i + E_{e2} + E_{\nu1}}. \tag{5.24}
\end{aligned}$$

For the differential decay rate the relation,

$$\begin{aligned}
d\Gamma^{2\nu} &= \sum_{spins} | \langle f|S|i \rangle |^2 2\pi\delta(E_i - E_f - E_{e1} - E_{e2} - E_{\nu1} - E_{\nu2}) \\
&\times \frac{d\vec{p}_{e1}}{(2\pi)^3} \frac{d\vec{p}_{e2}}{(2\pi)^3} \frac{d\vec{k}_{\nu1}}{(2\pi)^3} \frac{d\vec{k}_{\nu2}}{(2\pi)^3}, \tag{5.25}
\end{aligned}$$

holds. We recall the relationship between the total decay rate and half-life for the sake of completeness.

$$\Gamma^{2\nu} = \frac{\ln 2}{T_{1/2}^{2\nu}}. \quad (5.26)$$

## 5.2 Double $\beta$ -decay to the $0^+$ ground state

We present here the half-life of the double  $\beta$ -decay to the  $0^+$  ground state of daughter nucleus. Based on the calculations presented in previous section (5.1) we may write

$$(T_{1/2}^{2\nu}(0^+))^{-1} = \frac{m_e}{32\pi^7 \ln 2} (G_\beta m_e^2)^4 I^{2\nu}(0^+) \quad (5.27)$$

for the half-life. The integral is given as

$$I^{2\nu}(0^+) = \frac{1}{m_e^9} \int_{m_e}^{E_i - E_f - m_e} dE_{e1} F_0(Z', E_{e1}) p_{e1} E_{e1} \times \int_{m_e}^{E_i - E_f - E_{e1}} dE_{e2} F_0(Z', E_{e2}) p_{e2} E_{e2} \int_0^{E_i - E_f - E_{e1} - E_{e2}} dE_{\nu 1} E_{\nu 1}^2 E_{\nu 2}^2 |M^{2\nu}(0^+)|^2. \quad (5.28)$$

Here, the neutrino energy, following the energy conservation law, is given as  $E_{\nu 2} = E_i - E_f - E_{e1} - E_{e2} - E_{\nu 1}$ .  $p_e = |\vec{p}_e|$  stands for the electron momentum. For the matrix element of nuclear transition we have

$$\begin{aligned} |M^{2\nu}(0^+)|^2 &= |M_K^{(0)}(0^+) + M_L^{(0)}(0^+)|^2 + 3|M_K^{(0)}(0^+) - M_L^{(0)}(0^+)|^2 + \\ &|M_K^{(1)}(0^+) + M_L^{(1)}(0^+)|^2 - \frac{1}{3}|M_K^{(1)}(0^+) - M_L^{(1)}(0^+)|^2 + \\ &2\text{Re}\{(M_K^{(0)}(0^+) + M_L^{(0)}(0^+))(M_K^{(1)}(0^+) + M_L^{(1)}(0^+))\} - \\ &2\text{Re}\{(M_K^{(0)}(0^+) - M_L^{(0)}(0^+))(M_K^{(1)}(0^+) - M_L^{(1)}(0^+))\}, \end{aligned} \quad (5.29)$$

with

$$\begin{aligned} M_K^{(0)}(0^+) &= M_K^{(0^+)}(0^+) + M_K^{(0^-)}(0^+) = \\ &\sum_{\mathcal{J}^\pi=0^+,0^-} \sum_n \langle 0_f^+ || \mathcal{O}(\mathcal{J}^\pi) || \mathcal{J}^\pi, n \rangle \langle \mathcal{J}^\pi, n || \mathcal{O}(\mathcal{J}^\pi) || 0_i^+ \rangle K_n \\ M_K^{(1)}(0^+) &= M_K^{(1^+)}(0^+) + M_K^{(1^-)}(0^+) = \\ &- \sum_{\mathcal{J}^\pi=1^+,1^-} \sum_n \langle 0_f^+ || \mathcal{O}(\mathcal{J}^\pi) || \mathcal{J}^\pi, n \rangle \langle \mathcal{J}^\pi, n || \mathcal{O}(\mathcal{J}^\pi) || 0_i^+ \rangle K_n. \end{aligned} \quad (5.30)$$

When replacing  $K_n$  with  $L_n$  in  $M_K^{(0)}(0^+)$ ,  $M_K^{(1)}(0^+)$  we get  $M_L^{(0)}(0^+)$ ,  $M_L^{(1)}(0^+)$ .

The presented form of half-life in (5.27) includes the forbidden  $\beta$ -transitions through the intermediate nucleus. Also, the exact energy dependence of the energy denominators have been kept so far. The  $\beta$ -transitions  $M_{K,L}^{(0^-)}(0^+)$  and  $M_{K,L}^{(1^-)}(0^+)$  enter to the double  $\beta$ -decay matrix element of Fermi ( $M_{K,L}^{(0^+)}(0^+)$ ) and Gamow-Teller ( $M_{K,L}^{(1^+)}(0^+)$ ) throughout the  $0^-$  and  $1^-$  states of intermediate nucleus. We neglect the double Fermi matrix element due to the fact, that initial and final nuclei belong to the different isospin multiplets [69]. The matrix elements  $M_{K,L}^{(0^-)}(0^+)$  and  $M_{K,L}^{(1^-)}(0^+)$  associated with the forbidden transitions are suppressed by a factor  $((\alpha Z')/2)^2$  with respect to the allowed transitions connecting the intermediate nucleus states with ground states of initial and final nuclei. This suppression has its origin in  $p_{1/2}$  electron wave function that has to be included in order to change parity between the state of intermediate nucleus and ground state of mother and daughter nucleus ( $0^+$ ). The suppression for typical double  $\beta$ -decaying nuclei is roughly  $\sim 1/40$ .

There exist an approximation that replaces the energy of leptons with a mean value associated with the energy release of the decay.

$$\begin{aligned}\Delta &\equiv (E_i - E_f)/2 \\ E_{ei} + E_{\nu j} &\approx \Delta.\end{aligned}\tag{5.31}$$

Here,  $i, j = 1, 2$ . This approximation is called the energy denominators closure and its advantage is the denominator independence of lepton energies. Taking into account this advantage we can write the half-life (see 5.27) as a product of the phase space integral and nuclear matrix element. By the use of the above mentioned approximation we get

$$\begin{aligned}|M^{2\nu}(0^+)|^2 &= |M^{(0)}(0^+) + M^{(1)}(0^+)|^2 \\ &= \left| 2 \sum_{\mathcal{J}^\pi=0^+,0^-,1^+,1^-} (-1)^{\mathcal{J}} \sum_n \frac{\langle 0_f^+ || \mathcal{O}(\mathcal{J}^\pi) || \mathcal{J}^\pi, n \rangle \langle \mathcal{J}^\pi, n || \mathcal{O}(\mathcal{J}^\pi) || 0_i^+ \rangle}{E_n - E_i + \Delta} \right|^2.\end{aligned}\tag{5.32}$$

The energy denominators closure is usually involved in case when considering Higher States Dominance (HSD) hypothesis, i.e. when the main contribution to the double  $\beta$ -decay matrix element comes from higher lying states of intermediate nucleus with spin and parity  $1^+$ . Considering only the  $s_{1/2}$  electron wave states and neglecting the double Fermi matrix element due to isospin symmetry we have

$$\begin{aligned}
|M^{2\nu}(0^+)|^2 &= g_A^4 |M_{GT}^{2\nu}(0^+)|^2 \\
&= 4g_A^4 \left| \sum_n \frac{\langle 0_f^+ || \sum_m \tau_m^+ \sigma_m || 1^+, n \rangle \langle 1^+, n || \sum_m \tau_m^+ \sigma_m || 0_i^+ \rangle}{E_n - E_i + \Delta} \right|^2.
\end{aligned} \tag{5.33}$$

The half-life is then given as

$$(T_{1/2}^{2\nu}(0^+))^{-1} = \frac{m_e}{8\pi^7 \ln 2} (G_\beta m_e^2)^4 g_A^4 |m_e M_{GT}^{2\nu}(0^+)|^2 J^{2\nu}(0^+), \tag{5.34}$$

with the phase space integral given as

$$\begin{aligned}
J^{2\nu}(0^+) &= \frac{1}{m_e^{11}} \int_{m_e}^{E_i - E_f - m_e} dE_{e1} F_0(Z', E_{e1}) p_{e1} E_{e1} \times \\
&\int_{m_e}^{E_i - E_f - E_{e1}} dE_{e2} F_0(Z', E_{e2}) p_{e2} E_{e2} \int_0^{E_i - E_f - E_{e1} - E_{e2}} dE_{\nu 1} E_{\nu 1}^2 E_{\nu 2}^2.
\end{aligned} \tag{5.35}$$

### 5.3 Double $\beta$ -decay to the $2_1^+$ excited state

The aim of this section is to present the half-life of the double  $\beta$ -decay to the first excited state ( $2_1^+$ ) of daughter nucleus. Based on the calculations presented in previous sections (5.1,5.2), for the half-life we may write

$$(T_{1/2}^{2\nu}(2^+))^{-1} = \frac{m_e}{32\pi^7 \ln 2} (G_\beta m_e^2)^4 I^{2\nu}(2^+), \tag{5.36}$$

with the integral defined as

$$\begin{aligned}
I^{2\nu}(2^+) &= \frac{1}{m_e^9} \int_{m_e}^{E_i - E_f - m_e} dE_{e1} F_0(Z', E_{e1}) p_{e1} E_{e1} \times \\
&\int_{m_e}^{E_i - E_f - E_{e1}} dE_{e2} F_0(Z', E_{e2}) p_{e2} E_{e2} \int_0^{E_i - E_f - E_{e1} - E_{e2}} dE_{\nu 1} E_{\nu 1}^2 E_{\nu 2}^2 |M^{2\nu}(2^+)|^2.
\end{aligned} \tag{5.37}$$

The matrix element of the transition  $0^+ \rightarrow 2^+$  is given as

$$|M^{2\nu}(2^+)|^2 = |M_K^{(1)}(2^+) - M_L^{(1)}(2^+)|^2, \tag{5.38}$$

with



$$\begin{aligned}
M_K^{(1)}(2^+) &= M_K^{(1^+)}(2^+) + M_K^{(1^-)}(2^+) = \\
\frac{1}{\sqrt{3}} \sum_{\mathcal{J}^\pi=1^+,1^-} \sum_n &< 2_f^+ || \mathcal{O}(\mathcal{J}^\pi) || \mathcal{J}^\pi, n \rangle \langle \mathcal{J}^\pi, n || \mathcal{O}(\mathcal{J}^\pi) || 0_i^+ \rangle K_n. \quad (5.39)
\end{aligned}$$

Replacing  $K_n$  with  $L_n$  from  $M_K^{(1)}(2^+)$  matrix element we get  $M_L^{(1)}(2^+)$ .

By introducing the replacement of energy of leptons with the half of the energy release of the decay we have

$$\begin{aligned}
|M^{2\nu}(2^+)|^2 &= \frac{4(E_{e1} - E_{e2})^2(E_{\nu1} - E_{\nu2})^2}{m_e^4} |M^{(1)}(2^+)|^2 \\
&= \frac{4(E_{e1} - E_{e2})^2(E_{\nu1} - E_{\nu2})^2}{m_e^4} \times \\
&\left| \frac{m_e^2}{\sqrt{3}} \sum_{\mathcal{J}^\pi=1^+,1^-} \sum_n \frac{\langle 2_f^+ || \mathcal{O}(\mathcal{J}^\pi) || \mathcal{J}^\pi, n \rangle \langle \mathcal{J}^\pi, n || \mathcal{O}(\mathcal{J}^\pi) || 0_i^+ \rangle}{(E_n - E_i + \Delta)^3} \right|^2. \quad (5.40)
\end{aligned}$$

As previously we consider only the  $s_{1/2}$  electron wave function. So we get

$$\begin{aligned}
|M^{2\nu}(2^+)|^2 &= 4(E_{e1} - E_{e2})^2(E_{\nu1} - E_{\nu2})^2 g_A^4 |M_{GT}^{2\nu}(2^+)|^2 \\
&= 4(E_{e1} - E_{e2})^2(E_{\nu1} - E_{\nu2})^2 g_A^4 \times \\
&\left| \frac{1}{\sqrt{3}} \sum_n \frac{\langle 2_f^+ || \sum_m \tau_m^+ \sigma_m || 1^+, n \rangle \langle 1^+, n || \sum_m \tau_m^+ \sigma_m || 0_i^+ \rangle}{(E_n - E_i + \Delta)^3} \right|^2. \quad (5.41)
\end{aligned}$$

The half-life then takes the form

$$(T_{1/2}^{2\nu}(2^+))^{-1} = \frac{m_e}{8\pi^7 \ln 2} (G_\beta m_e^2)^4 g_A^4 m_e^3 |M_{GT}^{2\nu}(2^+)|^2 J^{2\nu}(2^+), \quad (5.42)$$

with the phase space integral defined as

$$\begin{aligned}
J^{2\nu}(2^+) &= \frac{1}{m_e^{15}} \int_{m_e}^{E_i - E_f - m_e} dE_{e1} F_0(Z', E_{e1}) p_{e1} E_{e1} \times \\
&\int_{m_e}^{E_i - E_f - E_{e1}} dE_{e2} F_0(Z', E_{e2}) p_{e2} E_{e2} (E_{e1} - E_{e2})^2 \times \\
&\int_0^{E_i - E_f - E_{e1} - E_{e2}} dE_{\nu1} E_{\nu1}^2 E_{\nu2}^2 (E_{\nu1} - E_{\nu2})^2. \quad (5.43)
\end{aligned}$$

## 5.4 Nuclear electron capture and $\beta$ -decay

The aim of this section is to present brief exposition of nuclear single  $\beta$ -decay and electron capture on nuclei in order to show the connection between nuclear matrix elements and the  $\log ft$  values. The advantage of the results gained herein will become more obvious in theoretical treatment of the double  $\beta$ -decay within SSD hypothesis. We will omit some details of the theoretical description of the single  $\beta$ -decay because the theoretical treatment of single  $\beta$ -decay is presented in Sec. (3.1) for the tritium decay.

### Nuclear $\beta$ -decay

We present here the derivation of the single  $\beta$ -decay half-life. The subject of our interest is the nuclear  $\beta$ -decay with the change of spin and parity  $\Delta J^\pi = 1^+, 1^-$  between initial and final nuclei. Therefore we consider the electron  $s_{1/2}$  and  $p_{1/2}$  wave functions only. The non-relativistic hadron current approximation is also taken into account. For the transitions  $J_i^{\pi_i} \rightarrow 0_f^+$  the  $\beta$ -decay amplitude is given as

$$\begin{aligned}
 \langle f | S^{(1)} | i \rangle &= -i \frac{G_\beta}{\sqrt{2}} 2\pi \delta(E_e + E_\nu + E_f - E_i) \\
 &\times \sqrt{F_0(Z', E_e)} \frac{1}{\sqrt{2E_e}} \frac{1}{\sqrt{2E_\nu}} \bar{u}(p_e) \gamma^\mu (1 - \gamma_5) u(-k_\nu) \\
 &\times \left[ g_{\mu k} \left( \vec{\mathcal{M}}_\beta^{(1^+)} + \vec{\mathcal{M}}_\beta^{(1^-)} \right)^k \right],
 \end{aligned} \tag{5.44}$$

with

$$\vec{\mathcal{M}}_\beta^{(1^\pm)} = \langle 0_f^+ | \vec{\mathcal{O}}(1^\pm) | J_i^{\pi_i} \rangle. \tag{5.45}$$

$Z'$  is the proton number of final nucleus and operators  $\mathcal{O}(1^\pm)$  are the same as in (5.20). For the half-life we eventually get

$$\begin{aligned}
 &\left[ T_{1/2}^\beta (J_i^{\pi_i} \rightarrow 0_f^+) \right]^{-1} = \\
 &\frac{m_e}{2\pi^3 \ln 2} (G_\beta m_e^2)^2 \left( \frac{1}{2J_i + 1} B_\beta^{(1^\pm)} \right) f_\beta(Z', E_i - E_f) \quad (\pi_i \pi_f = \pm 1).
 \end{aligned} \tag{5.46}$$

The phase space integral is here included in the Fermi integral function

Table 5.1: The matrix element values of transitions  $^{100}Tc(1^+_{g.s.}) \rightarrow ^{100}Ru(0^+_{g.s.})$  and  $^{150}Pm(1^-_{g.s.}) \rightarrow ^{150}Sm(0^+_{g.s.})$  are presented here with the use of eq. (5.49).  $Z'$  is the proton number of final nucleus [70].

Transition	$E_i - E_f$ [MeV]	$Z'$	$T_{1/2}$ [s]	$ \langle 0^+    \mathcal{O}(1^\pm)    1^\pm \rangle $
$^{100}Tc(1^+) \rightarrow ^{100}Ru(0^+)$	3.713	44	15.8	0.695
$^{150}Pm(1^-) \rightarrow ^{150}Sm(0^+)$	3.965	64	9648	0.0159

$$f_\beta(Z', E_i - E_f) = \frac{1}{m_e^5} \int_{m_e}^{E_i - E_f} dE_e F_0(Z', E_e) p_e E_e (E_i - E_f - E_e)^2, \quad (5.47)$$

that depends on the proton number  $Z'$  and the energy release of the reaction. The  $\beta$ -strength is given throughout the value of matrix element as

$$B_\beta^{(\mathcal{J}^\pi)} = |\langle 0^+_f || \mathcal{O}(\mathcal{J}^\pi) || 1^\pm_i \rangle|^2 \quad (\mathcal{J}^\pi = 1^+, 1^-). \quad (5.48)$$

The above presented calculations are helpful tool for the experimental estimation of the single  $\beta$ -decay matrix element. Collecting previous results we finally may write for the matrix element

$$|\langle 0^+_f || \mathcal{O}(\mathcal{J}^\pi) || 1^\pm_i \rangle| = \sqrt{\frac{3D}{f_\beta(Z', E_i - E_f) T_{1/2}}}. \quad (5.49)$$

Inserting the known  $Q$ -value and half-life  $T_{1/2}$  into the eq. (5.49) we extract the bare value of the nuclear matrix element. The  $D = (2\pi^3 \ln 2)/(G_\beta^2 m_e^5)$  is a constant factor.

The two nuclear transitions

$$^{100}Tc(1^+) \rightarrow ^{100}Ru(0^+) \text{ and } ^{150}Pm(1^-) \rightarrow ^{150}Sm(0^+)$$

are the subject of particular interest. By use of the relation (5.49) we evaluate the matrix elements of these transitions.

The matrix element values are presented in Tab. (5.1). It is clearly seen that the forbidden  $\beta$ -transition  $^{150}Pm(1^-) \rightarrow ^{150}Sm(0^+)$  is suppressed nearly by a factor of  $\sim 44$  against the allowed  $\beta$ -transition  $^{100}Tc(1^+) \rightarrow ^{100}Ru(0^+)$ . This is just a consequence of the  $p_{1/2}$  electron containing the factor  $\alpha Z'/2$ .

Table 5.2:  $\log ft$  values for transitions  $^{100}\text{Tc}(1^+) \rightarrow ^{100}\text{Mo}(0^+)$ ,  $^{150}\text{Pm}(1^-) \rightarrow ^{150}\text{Nd}(0^+)$  are shown herein. ( $\dagger$  - estimated value.)

transition	$\log ft$
$^{100}\text{Tc}(1^+) \rightarrow ^{100}\text{Mo}(0^+)$	4.59
$^{150}\text{Pm}(1^-) \rightarrow ^{150}\text{Nd}(0^+)$	7.87 $\dagger$

## Electron capture on nucleus

We present here the theoretical description of the electron capture from atomic shell by nucleus

$$e_b^- + (A, Z) \rightarrow (A, Z + 1) + \nu_e. \quad (5.50)$$

We consider only the electrons from  $K_I$  and  $L_{II}$  shells. The contribution from other shells can be neglected due to the small overlap of the electron wave function with the bulk of the nucleus. For the sake of simplicity we adopt the bound atomic electron wave functions from [71] in the form

$$\begin{aligned} \Psi_{K_I}(x) &= N_{K_I} e^{-\frac{Z}{a_e}|\vec{x}|} e^{-i\varepsilon_b x_0} u_e, & N_{K_I}^2 &= \frac{Z^3}{\pi a_e^3} \\ \Psi_{L_{II}}(x) &= N_{L_{II}} e^{-\frac{Z}{2a_e}|\vec{x}|} e^{-i\varepsilon_b x_0} \gamma_0 \vec{\gamma} \cdot \frac{\vec{x}}{R} u_e, & N_{L_{II}}^2 &= \frac{Z^5 R^2}{96\pi a_e^5}, \end{aligned} \quad (5.51)$$

with

$$u_e^s = \begin{pmatrix} \chi^s \\ 0 \end{pmatrix}, \quad a_e = \frac{1}{\alpha} \frac{\hbar c}{m_e} = 5.28 \times 10^4 \text{ fm}. \quad (5.52)$$

$\varepsilon_b$  is the energy of bound electron. We get the half-life of electron capture as follows

$$\begin{aligned} [T_{1/2}^{EC}(1_i^\pm \rightarrow 0_f^+)]^{-1} &= \frac{m_e}{2\pi^3 \ln 2} (G_\beta m_e^2)^2 \\ &\times \frac{1}{2J_i + 1} B_{EC}^{(1^\pm)} f_{EC-K_I, L_{II}}(Z, E_i - E_f) \end{aligned} \quad (5.53)$$

The phase space integration is included in the function

$$f_{EC-K_I, L_{II}}(Z, E_i - E_f) = 2\pi^2 \left( \frac{1}{m_e^3} N_{K_I, L_{II}}^2 \right) \xi(Z) \frac{(E_i - E_f + \varepsilon_b)^2}{m_e^2}. \quad (5.54)$$

The proton number of initial nucleus enters into the normalization factor  $N_{K_I, L_{II}}^2$  and factor  $\xi(Z) = 1, \xi(Z) = (2/(\alpha Z))^2$  for  $K_I, L_{II}$  electrons, respectively. The  $\beta$ -strength is given as

$$B_{EC}^{(\mathcal{J}^\pi)} = |\langle 0_f^+ || \mathcal{O}(\mathcal{J}^\pi) || 1_i^\pm \rangle|^2 \quad (\mathcal{J}^\pi = 1^+, 1^-). \quad (5.55)$$

The half-life value of the electron capture of  $^{100}\text{Tc}(1_{g.s.}^+) \rightarrow ^{100}\text{Mo}(0_{g.s.}^+)$  was already experimentally measured. By evaluation of the function (5.54) we get for the bare value of the matrix element of the transition

$$|\langle 0^+ || \mathcal{O}(1^+) || 1^+ \rangle| = \sqrt{\frac{3D}{f_{EC}(43, -0.343 \text{ MeV}) 243.8h}} = 0.82. \quad (5.56)$$

The corresponding *logft* value is presented in Tab. 5.2. We note that measured value of the electron capture is *logft* =  $4.45_{-0.3}^{+0.18}$  [72], i.e. our estimation is not far from the measured value indeed.

The electron capture of  $^{150}\text{Pm}(1_{g.s.}^-) \rightarrow ^{150}\text{Nd}(0^+)$  has not been observed experimentally yet. In order to estimate the *logft* value for this reaction we assume that the value of bare nuclear matrix element for the electron capture is of the same order as the bare nuclear matrix element value of the single  $\beta$  decay of  $^{150}\text{Pm}(1_{g.s.}^-) \rightarrow ^{150}\text{Sm}(0^+)$ . A justification of such an approach can be seen in comparison of the electron capture and  $\beta$ -decay matrix elements of  $^{100}\text{Tc} \rightarrow ^{100}\text{Mo}$  (0.8) and  $^{100}\text{Tc} \rightarrow ^{100}\text{Ru}$  (0.7), respectively. For the *logft* value of electron capture by  $^{150}\text{Pm}(1^-)$  we get *logft* = 7.87. The implication for the half-life value is at the level of  $T_{1/2}^{EC} \approx 6.10^{16}$  years. Regrettably we have to conclude that this value of half-life would not be reached, most likely, in near future experiments.

## 5.5 Double $\beta$ -decay within the Single State Dominance hypothesis

The Single State Dominance (SSD) hypothesis was presented for the first time in [68] by Abad, et al. The SSD hypothesis states that for the double  $\beta$ -decaying nuclear

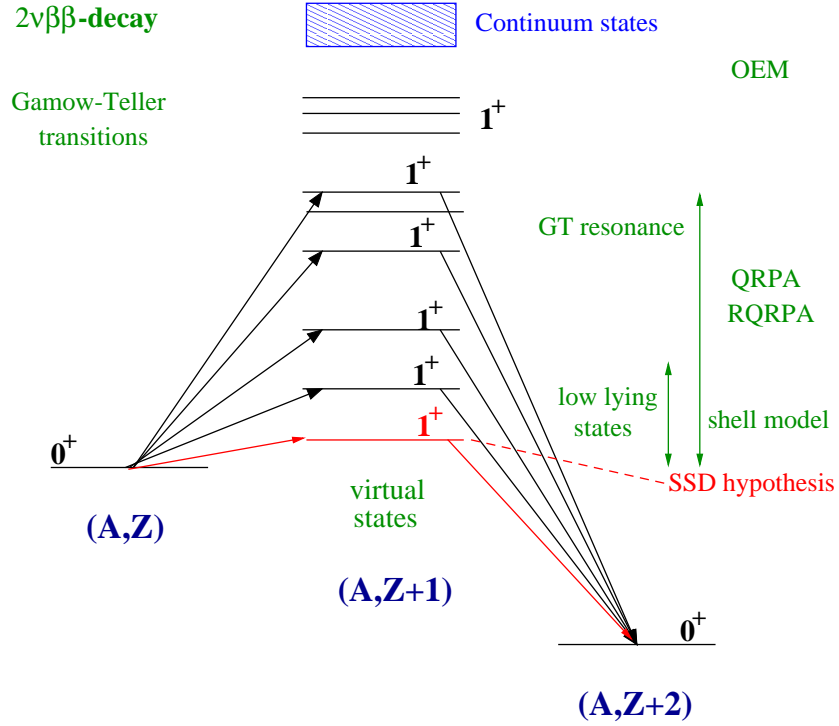


Figure 5.2: The double  $\beta$ -decay transition illustrated as a sum of virtual single  $\beta$ -decay transitions through the intermediate nucleus. The SSD hypothesis assumes only the transitions throughout the ground state of intermediate nucleus.

systems with the spin and parity of the ground state of intermediate nucleus  $1^+$  is possible to consider the double  $\beta$ -decay transition as two respective virtual single  $\beta$ -decay transitions.

- i) The first transition connects the ground state of initial nucleus ( $0^+$ ) with the ground state of intermediate nucleus ( $1^+$ ).
- ii) The second one connects the ground state of intermediate nucleus ( $1^+$ ) with the ground state of final nucleus ( $0^+$ ).

This assumption is known as the Single State Dominance hypothesis. The virtual transitions are illustrated in Fig. 5.2.

The main aim of the SSD hypothesis is the nuclear model independent way of estimating the double  $\beta$ -decay nuclear matrix element. The advantage is the possibility to extract the matrix elements of the two individual virtual single  $\beta$ -transitions from the known  $\log ft$  values [73, 74]. The available experimental data show that there exist some double  $\beta$ -decaying nuclear systems when the SSD hypothesis is realised. The idea of ruling out or confirming the SSD hypothesis by precise measurement of double  $\beta$ -decay differential characteristics was introduced in [74]. The experimental data from NEMO 3 experiment confirm the realisation of SSD hypothesis in case of  $^{100}\text{Mo}$  for

Table 5.3: The evaluated values ( $T_{1/2}^{SSD}$ ) of double  $\beta$ -decay half-life of  $^{100}\text{Mo}$  and  $^{150}\text{Nd}$  are presented here. The experimentally measured values ( $T_{1/2}^{exp}$ ) are shown also [75].

Nucleus	$E_i - E_f$ [MeV]	$T_{1/2}^{SSD}$ [years]	$T_{1/2}^{exp}$ [years]
$^{100}\text{Mo}$	4.05	$7.16 \times 10^{19}$	$7.1 \times 10^{18}$
$^{150}\text{Nd}$	4.39	$4.02 \times 10^{24}$	$8.2 \times 10^{18}$

instance. Previous theoretical studies involved the approximation that replaces the energy of leptons with the mean value in order to examine the SSD hypothesis [76, 77]. It was found in [69] that for some nuclear systems this approximation is inappropriate and more adequate approach was suggested therein.

The subject of our interest is the double  $\beta$ -decay to the ground state ( $0^+$ ) and to the first excited state ( $2_1^+$ ) of final nucleus. We investigate herein two isotopes of particular interest, namely  $^{100}\text{Mo}$  and  $^{150}\text{Nd}$ . The intermediate nuclei  $^{100}\text{Tc}$ ,  $^{150}\text{Pm}$  have the ground state spin and parities  $1^+$  and  $1^-$ , respectively. The nuclear structure of  $^{150}\text{Pm}$  is still an open task from both theoretical and experimental point of view. So with use of double  $\beta$ -decay differential characteristics we may conclude whether there exist a low lying  $1^+$  state of  $^{150}\text{Pm}$  or not.

We take the advantage of results of previous sections (5.1,5.2, 5.3,5.4) and write for the two-neutrino double  $\beta$ -decay half-life of  $0^+ \rightarrow 0^+, 2_1^+$  transitions following

$$\left(T_{1/2}^{2\nu-SSD}(J_f^+)\right)^{-1} = \frac{m_e}{8\pi^7 \ln 2} (G_\beta m_e^2)^4 I^{2\nu-SSD}(J_f^+) \times \\ | \langle J_f^+ | \mathcal{O}(1^\pi) | 1^\pi \rangle |^2 | \langle 1^\pi | \mathcal{O}(1^\pi) | 0_i^+ \rangle |^2. \quad (5.57)$$

Here,  $\pi = \pm 1$  and the phase space integral is given as

$$I^{2\nu-SSD}(J_f^+) = \frac{1}{m_e^9} \int_{m_e}^{E_i - E_f - m_e} dE_{e1} F_0(Z', E_{e1}) p_{e1} E_{e1} \times \\ \int_{m_e}^{E_i - E_f - E_{e1}} dE_{e2} F_0(Z', E_{e2}) p_{e2} E_{e2} \int_0^{E_i - E_f - E_{e1} - E_{e2}} dE_{\nu1} E_{\nu1}^2 E_{\nu2}^2 \mathcal{D}_{KL}^{SSD}(J_f^+). \quad (5.58)$$

The difference between the decay to the ground and excited state is given by integrand,

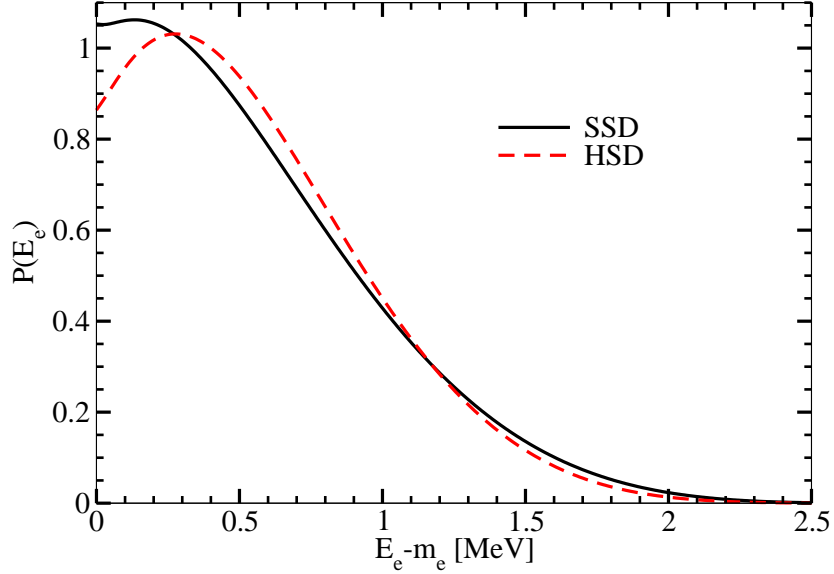


Figure 5.3: The single electron energy spectrum of the two neutrino double  $\beta$ -decay of  $^{100}\text{Mo}$  to the ground state of final nuclues  $^{100}\text{Ru}(0^+)$  is illustrated for the SSD and HSD approach.

$$\begin{aligned}
 \mathcal{D}_{KL}^{SSD}(J_f^+) &= \frac{1}{3}(K_1^2 + K_1 L_1 + L_1^2) \quad (J_f^+ = 0^+) \\
 &= \frac{1}{3}(K_1 - L_1)^2 \quad (J_f^+ = 2_1^+). \quad (5.59)
 \end{aligned}$$

The energy denominators  $K_1, L_1$  are given in eq. (5.24).

We see here the advantage of the SSD approach. The only nuclear matrix element involved herein consists from two  $\beta$ -strenghts that could be determined from the *logft* values of single  $\beta$ -transitions of the intermediate nucleus. The evaluation of the  $\beta$ -strenghts,  $|\langle 1\pi || \mathcal{O}(1\pi) || 0_i^+ \rangle|^2$  and  $|\langle J_f^+ || \mathcal{O}(1\pi) || 1\pi \rangle|^2$ , for the two isotopes  $^{100}\text{Tc}$  and  $^{150}\text{Pm}$  of particular interest has been already performed in previous section (see 5.4). Calculated values of half-life of the two-neutrino double  $\beta$ -decay of  $^{100}\text{Mo}$  and  $^{150}\text{Nd}$  are presented in Tab. 5.3. We see the discrepancy between the theoretically predicted value of half-life ( $T_{1/2}^{SSD}$ ) calculated within the SSD assumption and the measured value  $T_{1/2}^{exp}$  for  $^{150}\text{Nd}$ . This can be naturally taken into account as a proof of non-realization of SSD for the case of  $^{150}\text{Nd}$ . Although it is worth mentioning that relatively high uncertainty of double  $\beta$ -decay matrix element has its origin in poor estimation of matrix element of the electron capture by  $^{150}\text{Pm}$  nucleus. This effect can lead to a difference between the phenomenologically estimated value of half-life and the measured one in the end.

It is worth to note that the half-life is only one of the observables in the two neutrino



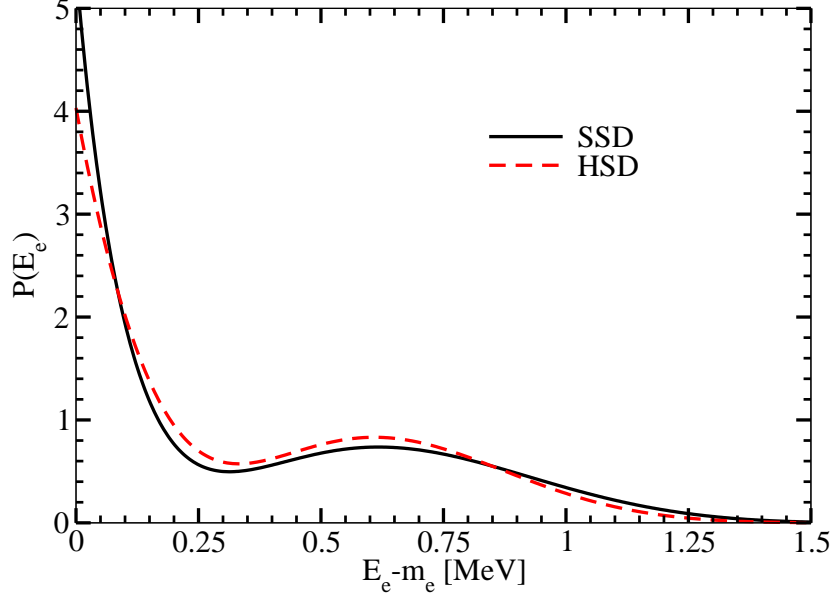


Figure 5.4: The single electron energy spectrum of the two neutrino double  $\beta$ -decay of  $^{100}\text{Mo}$  to the first excited state of final nucleus  $^{100}\text{Ru}(2_1^+)$  is illustrated for the SSD and HSD approach.

double  $\beta$ -decay. Therefore, our attention will be focused on the differential characteristics of the process, also. For instance, the single electron energy spectrum. There exist a Higher States Dominance (HSD) hypothesis introduced in [74]. As a competitive approach versus SSD, the HSD hypothesis assumes the dominant contribution from higher lying  $1^+$  states even in the region of Gamow-Teller resonance. The energy of leptons entering into the denominators (5.24) can be replaced with their average value. The advantage of this approach is the separation of the nuclear matrix element with respect to the phase space integration. We present the way how to verify both approaches (SSD, HSD) with the single electron energy spectrum in two-neutrino double  $\beta$ -decay.

The single electron energy spectrum normalized to unity is given as

$$\begin{aligned}
 \mathcal{P}_{J_f^+}^{2\nu-N}(E_{e1}) &= \frac{1}{\Gamma_{J_f^+}^{2\nu-N}} \frac{d\Gamma_{J_f^+}^{2\nu-N}}{dE_{e1}} \quad (N = \text{SSD}, \text{HSD}) \\
 &= \frac{1}{I^{2\nu-N}(J_f^+)} F_0(Z', E_{e1}) p_{e1} E_{e1} \times \\
 &\int_{m_e}^{E_i - E_f - E_{e1}} dE_{e2} F_0(Z', E_{e2}) p_{e2} E_{e2} \int_0^{E_i - E_f - E_{e1} - E_{e2}} dE_{\nu 1} E_{\nu 1}^2 E_{\nu 2}^2 \mathcal{D}_{KL}^N(J_f^+).
 \end{aligned} \tag{5.60}$$

Here, we distinguish two different approaches, namely SSD and HSD hypothesis.

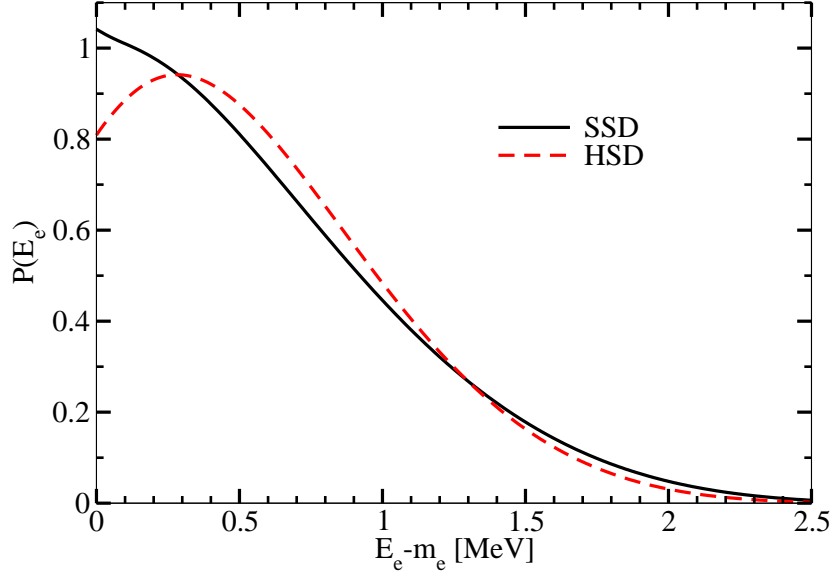


Figure 5.5: The single electron energy spectrum of the two-neutrino double  $\beta$ -decay of  $^{150}\text{Nd}$  to the ground state of final nuclues  $^{150}\text{Sm}(0^+)$  is illustrated for the SSD and HSD approach.

The factor  $N = SSD$  is defined in (5.59) and for  $N = HSD$  we have

$$\begin{aligned} \mathcal{D}_{KL}^N(J_f^+) &= 1 & (J_f^+ = 0^+), \\ &= (E_{e1} - E_{e2})^2 (E_{\nu1} - E_{\nu2})^2 & (J_f^+ = 2^+). \end{aligned} \quad (5.61)$$

The single electron energy distribution (5.60) is independent of the value of double  $\beta$ -decay nuclear matrix element, axial-vector constant  $g_A$  and Fermi constant  $G_F$  for the SSD and HSD assumptions. Therefore this phenomenological approach for the description of two-neutrino double  $\beta$ -decay is free of any nuclear model structure assumptions. This shall be taken into account as an advantage. Recent observations approve the SSD to be realised in case of  $^{100}\text{Mo}$  double  $\beta$ -decay [78, 79]. The single electron energy spectrum normalized to unity (5.60) of  $^{100}\text{Mo}$  double  $\beta$ -decay to the ground ( $0^+$ ) and first excited ( $2_1^+$ ) state of final nucleus  $^{100}\text{Ru}$  is illustrated in Fig. 5.3 and 5.4, respectively. The different approach (SSD, HSD hypothesis) is leading to deviation of the spectrum most apparently at the low electron energies. From the comparison of measured and evaluated half-life of  $^{150}\text{Nd}$  (see Tab. 5.3) one can conclude that SSD is not realized in this particular nuclear system. With the single electron energy spectrum we gain much stronger tool for confirming or ruling out the SSD hypothesis of  $^{150}\text{Nd} \rightarrow ^{150}\text{Sm}$  process because spectrum is free of any nuclear matrix elements. Moreover, we may probe the validity of the HSD too. The single

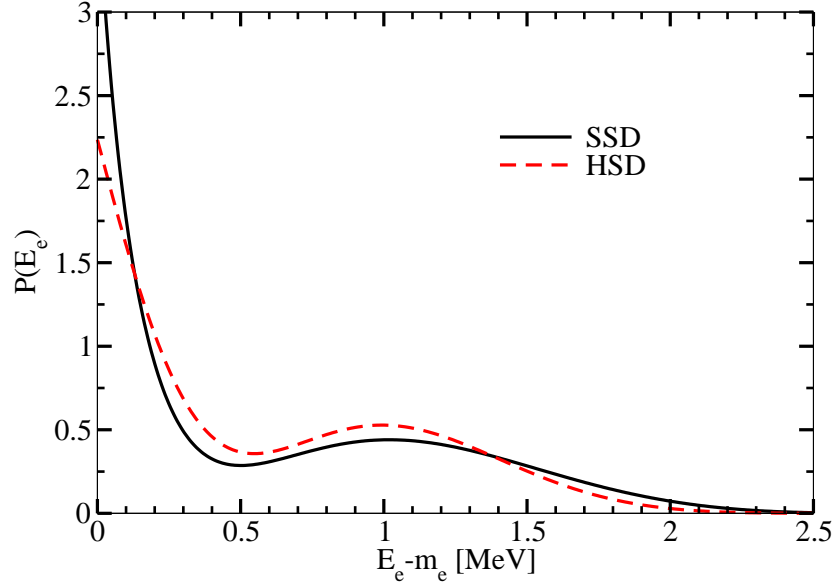


Figure 5.6: .The single electron energy spectrum of the two-neutrino double  $\beta$ -decay of  $^{150}\text{Nd}$  to the first excited state of final nucleus  $^{150}\text{Sm}(2_1^+)$  is illustrated for the SSD and HSD approach.

electron energy spectrum of  $^{150}\text{Nd}$  double  $\beta$ -decay to the ground ( $0^+$ ) and first excited state ( $2_1^+$ ) of daughter nucleus  $^{150}\text{Sm}$  is illustrated in Fig. 5.5 and 5.6, respectively. As in the case of  $^{100}\text{Mo}$  spectrum we see that the pattern is different for the SSD and HSD approaches.

By Comparing the theoretically predicted and experimentally measured half-life we conclude that SSD approach is not realised in the two-neutrino double  $\beta$ -decay of  $^{150}\text{Nd}$ .

## Conclusions

In this chapter, we have presented the theoretical description of the double  $\beta$ -decay to the ground ( $0^+$ ) and excited ( $2^+$ ) state of final nucleus. The probe of the SSD hypothesis for the  $2\nu\beta\beta$ -decay of  $^{150}\text{Nd}$  with energy distributions of emitted electrons was presented. A conclusion was made that the SSD hypothesis is expected to be ruled out by precision measurements of differential characteristics of the  $2\nu\beta\beta$ -decay of  $^{150}\text{Nd}$  in planned SuperNEMO experiment unlike some unknown low-lying  $1^+$  state of  $^{150}\text{Pm}$  does exist.

These findings were published in Ref. [IX,XI,XII] given in the *List of publications*.

# Chapter 6

## Statistics of neutrinos and two-neutrino double $\beta$ -decay

We discuss here the possibility of Pauli exclusion principle violation for neutrinos, and thus, possibility that neutrinos obey at least partly the Bose-Einstein statistics. The parameter  $\sin^2 \chi$  is introduced that characterizes the bosonic (symmetric) fraction of the neutrino wave function. Consequences of the violation of the exclusion principle for the two-neutrino double beta decay are considered. This violation strongly changes the rates of the decay and modifies the energy distributions of the emitted electrons.

We assume that Pauli exclusion principle is violated for neutrinos and therefore neutrinos obey (at least partly) the Bose-Einstein statistics. Possible violation of the exclusion principle was discussed in a series of papers [80] though no satisfactory and consistent mechanism of the violation has been proposed so far. The assumption of violation of the Pauli exclusion principle leads to a number of fundamental problems which include loss of a positive definiteness of energy, violation of the CPT invariance, and possibly, of the Lorentz invariance as well as of the unitarity of S-matrix. (For a critical review see ref. [81].) Experimental searches of the effects of the Pauli principle violation for electrons [82] and nucleons [83] have given negative results, leading to extremely strong bounds on the magnitude of violation.

It may happen however that due to unique properties of neutrinos (neutrality, smallness of mass associated to some high mass scales), a violation of the Pauli principle in the neutrino sector is much stronger than in other particle sectors. Therefore one may expect that effects of this violation can be first seen in neutrino physics.

A possibility of the Bose statistics for neutrinos has been first considered in ref. [84] where its effects on the Big Bang Nucleosynthesis (BBN) have been studied. According to [84] the change of neutrino statistics from pure fermionic to pure bosonic diminishes the primordial  ${}^4\text{He}$  abundance by  $\sim 4\%$ .

The idea of bosonic neutrinos has been proposed independently in ref. [85] where cosmological and astrophysical consequences of this hypothesis have been studied. Bosonic neutrinos might form a cosmological Bose condensate which could account for all (or a part of) the dark matter in the universe.

As far as the astrophysical consequences are concerned, dynamics of the supernova collapse would be influenced and spectra of the supernova neutrinos may change [85, 93]. The presence of neutrino condensate would enhance contributions of the Z-bursts to the flux of the UHE cosmic rays and lead to substantial refraction effects for neutrinos from remote sources [85].

We assume that the Pauli principle is violated substantially for neutrinos, while the violation is negligible for other particles. In particular, for electrons we will assume the usual Fermi-Dirac (FD) statistics. How to reconcile this pattern of the violation with the fact that in the standard model the left-handed neutrino and electron belong to the same doublet? The answer may be connected to the fact that neutrinos are the only known neutral leptons and thus they can have substantially different properties from those of the charged leptons. In particular, neutrinos can be the Majorana particles and violate lepton number conservation. The difference between charged leptons and neutrinos should be related to breaking of the electro-weak (EW) symmetry, and it can originate from some high mass scale of Nature. One may consider scenario where violation of the Pauli principle occurs in a hidden sector of theory related to the Planck scale physics or strings physics. It could be mediated by some singlets of the Standard model - (heavy) neutral fermions which mix with neutrinos when the EW symmetry is broken. Since only neutrinos can mix with the singlets, effects of the Pauli principle violation would show up first in the neutrino sector and then communicate to other particles. In this way a small or partial violation of the relation between spin and statistics might occur. A violation of the spin-statistics theorem for other particles can be suppressed by an additional power of a small parameter relevant for the violation in the neutrino sector and due to weak coupling of neutrino to other particle sectors.

A violation of the Pauli principle for neutrinos should show up in the elementary processes where identical neutrinos are involved. A realistic process for this test is the two-neutrino double beta decay,

$$(A, Z) \rightarrow (A, Z + 2) + 2\bar{\nu} + 2e^{-}. \quad (6.1)$$

It was shown in [85] that the probability of the decay as well as the energy spectrum of electrons should be affected. Qualitative conclusions were that the pure bosonic neutrino is excluded, whereas large fraction of the bosonic component in a neutrino state is still allowed by the present data. In this connection, a possibility of partly

bosonic (mixed-statistics) neutrinos can be considered.

In this chapter we perform a detailed study of the effects of bosonic neutrinos on the double beta decay. We consider the general case of partly bosonic neutrinos. We introduce a phenomenological parameter  $\sin^2 \chi$  which describes the fraction of bosonic neutrinos in such a way that a smooth change of  $\sin^2 \chi$  from 0 to 1 transforms fermionic neutrinos into bosonic ones. So, in general, neutrinos may possess a kind of mixed or more general statistics than Bose or Fermi ones [86, 87]. We present an analytic study of the double beta decay probabilities. The exact expressions for the two-neutrino double  $\beta$ -decay rates to ground ( $0^+$ ) and excited ( $2_1^+$ ) states are shown. The results of numerical calculations of the total rates and energy distributions for the two-neutrino double  $\beta$ -decays of  $^{100}\text{Mo}$  are presented herein. The obtained bounds on  $\sin^2 \chi$  from the existing data are presented.

## 6.1 Bosonic neutrinos in two-neutrino double $\beta$ -decay

First, let us discuss the case of pure bosonic neutrinos, i.e. the neutrinos possess the spin 1/2 but obey the Bose-Einstein statistics. The subject of our interest here is the two-neutrino double  $\beta$ -decay. The detailed calculation of this reaction for the fermionic neutrinos was already given in Chap. 5. We shall take the advantage of this treatment therein with the assumption on fermionic neutrinos and thus present here only the differences for the bosonic neutrinos. By introducing bosonic neutrinos we have to make change in (5.6) by changing the anticommutation relations for fermionic neutrinos to commutation relations for bosonic neutrinos, i.e.

$$\begin{aligned} c^\dagger(p_{e1})c^\dagger(p_{e2}) &= -c^\dagger(p_{e2})c^\dagger(p_{e1}) \\ d^\dagger(k_{\nu1})d^\dagger(k_{\nu2}) &= +d^\dagger(k_{\nu2})d^\dagger(k_{\nu1}). \end{aligned} \quad (6.2)$$

Some of the common approximations have been made in the derivation of the two neutrino double  $\beta$ -decay rate:

- i) We take into account only the  $s_{1/2}$  wave of the outgoing leptons.
- ii) The double  $\beta$ -decay Fermi nuclear matrix element is neglected because the initial and final nuclei belong to the different isospin multiplets.
- iii) The non-relativistic hadron current approximation (see 5.16) is used therefore only Gamow-Teller operators (5.20) are considered.

We present the differential decay rate of two neutrino double  $\beta$ -decay to the  $0^+$  ground state and  $2_1^+$  excited state of final nucleus for bosonic and fermionic neutrinos, simultaneously. In this way we gain a very compact formula useful for the comparison

of bosonic effect of neutrinos on the decay rates. The main purpose of this treatment will become more clear in forthcoming. Following the steps made in Chap. 5, for the differential decay rate of two neutrino double  $\beta$  decay to the ground and excited state of final nucleus we get

$$d\Gamma_{f,b}(J^+) = a_{2\nu} F_0(Z+2, E_{e1}) F_0(Z+2, E_{e2}) \mathcal{M}_{J^\pi}^{f,b} d\Omega. \quad (6.3)$$

Here,  $a_{2\nu} = (G_\beta g_A)^4 m_e^9 / (64\pi^7)$  and  $G_\beta = G_F \cos \theta_c$  ( $G_F$  is Fermi constant,  $\theta_c$  is Cabbibo angle) are constants.  $F_0(Z+2, E_e)$  denotes the relativistic Fermi function and  $g_A$  stands for the axial-vector coupling constant. The index  $f$  and  $b$  stands for fermionic and bosonic neutrinos, respectively. The phase space is given as

$$d\Omega = \frac{1}{m_e^{11}} E_{e1} p_{e1} E_{e2} p_{e2} E_{\nu 1}^2 E_{\nu 2}^2 \delta(E_{e1} + E_{e2} + E_{\nu 1} + E_{\nu 2} + E_f - E_i) \times dE_{e1} dE_{e2} dE_{\nu 1} dE_{\nu 2} d\cos\theta. \quad (6.4)$$

$\theta$  denotes the angle between the two emitted electrons. The expression  $\mathcal{M}_{J^\pi}^{f,b}$  with  $J^\pi = 0^+, 2^+$  arises as a result of product of nuclear matrix elements,

$$\begin{aligned} \mathcal{M}_{0^+}^{f,b} &= \frac{m_e^2}{4} \left[ |\mathcal{K}_{0^+}^{f,b} + \mathcal{L}_{0^+}^{f,b}|^2 + \frac{1}{3} |\mathcal{K}_{0^+}^{f,b} - \mathcal{L}_{0^+}^{f,b}|^2 \right] \\ &\quad - \frac{m_e^2}{4} \left[ |\mathcal{K}_{0^+}^{f,b} + \mathcal{L}_{0^+}^{f,b}|^2 - \frac{1}{9} |\mathcal{K}_{0^+}^{f,b} - \mathcal{L}_{0^+}^{f,b}|^2 \right] \frac{\vec{p}_{e1} \cdot \vec{p}_{e2}}{E_{e1} E_{e2}}, \\ \mathcal{M}_{2^+}^{f,b} &= m_e^2 |\mathcal{K}_{2^+}^{f,b} - \mathcal{L}_{2^+}^{f,b}|^2 \left( 1 + \frac{1}{3} \frac{\vec{p}_{e1} \cdot \vec{p}_{e2}}{E_{e1} E_{e2}} \right). \end{aligned} \quad (6.5)$$

With

$$\begin{aligned} \mathcal{K}_{J^+}^{f,b} &= \frac{m_e}{\sqrt{s}} \sum_m \langle J_f^\pi || \sum_j \tau_j^+ \sigma_j || 1_m^+ \rangle \langle 1_m^+ || \sum_k \tau_k^+ \sigma_k || 0_i^+ \rangle K_m^{f,b} \\ \mathcal{L}_{J^+}^{f,b} &= \frac{m_e}{\sqrt{s}} \sum_m \langle J_f^\pi || \sum_j \tau_j^+ \sigma_j || 1_m^+ \rangle \langle 1_m^+ || \sum_k \tau_k^+ \sigma_k || 0_i^+ \rangle L_m^{f,b}. \end{aligned} \quad (6.6)$$

Here, factor  $s = 1, 3$  for the  $J_f^\pi = 0^+, 2^+$ , respectively. The  $E_i, E_f$  and  $E_m$  stand for the initial ( $|0_i^+ \rangle$ ), final ( $|J_f^+ \rangle$ ) and intermediate ( $|1_m^+ \rangle$ ) nuclei energies. The energy denominators for the fermionic neutrinos are the same as in (5.24)

$$\begin{aligned} K_m^f &= \frac{1}{E_m - E_i + E_{e1} + E_{\nu 1}} + \frac{1}{E_m - E_i + E_{e2} + E_{\nu 2}} \\ L_m^f &= \frac{1}{E_m - E_i + E_{e1} + E_{\nu 2}} + \frac{1}{E_m - E_i + E_{e2} + E_{\nu 1}}. \end{aligned} \quad (6.7)$$

For the bosonic neutrinos the energy denominators take the form

$$\begin{aligned} K_m^b &= \frac{1}{E_m - E_i + E_{e1} + E_{\nu1}} - \frac{1}{E_m - E_i + E_{e2} + E_{\nu2}} \\ L_m^b &= \frac{1}{E_m - E_i + E_{e1} + E_{\nu2}} - \frac{1}{E_m - E_i + E_{e2} + E_{\nu1}}. \end{aligned} \quad (6.8)$$

Essentially the difference between the amplitude of the two-neutrino double  $\beta$ -decay for the bosonic neutrinos and for the case of fermionic neutrinos is in the minus sign in energy denominators indeed (see 6.7,6.8). This can be understood when considering the pictorial way for amplitude from the Feynman diagram of the two-neutrino double  $\beta$ -decay (see Fig. 5.1). The change of two lepton legs for the identical particles with given four-momenta in Feynman diagram leads to a relative minus or plus sign according to the statistical feature of that particles. In more detail, for fermions we have relative minus sign and for bosons we have relative plus sign. For particular case of our interest, the two-neutrino double  $\beta$ -decay, we have three permutations in addition to Feynman diagram shown in Fig. 5.1 associated with interchange of lepton legs in Feynman diagram.

- i) No change for neutrinos and interchange for electrons give a relative minus sign.
- ii) Interchange for neutrinos and no change for electrons give a relative plus sign.
- iii) Interchange for neutrinos and interchange for electrons give a relative minus sign.

We see the uniqueness of the process as far as two neutrinos as identical particles are involved in reaction. Therefore the statistical characteristics can be explored with the two-neutrino double  $\beta$ -decay directly. In order to understand this bosonic effect, given so far as a relative minus sign in the energy denominators, we have to analyze the differential decay rates.

Following the final result for the decay rate (6.5) we may see that there exist a significant difference between the double  $\beta$ -decay to the ground ( $0^+$ ) and excited state ( $2_1^+$ ) of final nucleus. The combinations of  $\mathcal{K}_m^{f,b} + \mathcal{L}_m^{f,b}$  and  $\mathcal{K}_m^{f,b} - \mathcal{L}_m^{f,b}$  enter to the decay rate in case of decay to the ground state of final nucleus. On the other hand only the latter term ( $\mathcal{K}_m^{f,b} - \mathcal{L}_m^{f,b}$ ) is involved in case of decay to the excited state of final nucleus. This feature is independent of statistical behavior of neutrinos, i.e. common for fermionic and bosonic neutrinos. Therefore, we shall study the energy denominators in such combinations in more detail. Let us introduce the energy denominators approximation. This procedure consists of replacing the lepton energy with the mean value, equal to the half of the energy release of reaction

$$\begin{aligned} \Delta &= (E_i - E_f)/2 \\ E_{ei} + E_{\nu j} &\approx \Delta, \quad i, j = 1, 2. \end{aligned} \quad (6.9)$$



With this approximation for the combinations of  $K_m^b$  and  $L_m^b$  we get

$$\begin{aligned} K_m^b + L_m^b &\approx 2 \frac{E_{\nu 2} - E_{\nu 1}}{(E_m - E_i + \Delta)^2}, \\ K_m^b - L_m^b &\approx 2 \frac{E_{e 2} - E_{e 1}}{(E_m - E_i + \Delta)^2} \end{aligned} \quad (6.10)$$

for the bosonic neutrinos. It is obvious that the structure of both terms is very similar. As a consequence of this similarity is the fact that qualitatively the transitions to the ground ( $0^+$ ) and excited ( $2^+$ ) state are of the same order for bosonic neutrinos. We note that energy differences in the numerators in (6.10) lead to the significant suppression of the total decay rate of the process at the level of 1-3 orders of magnitude. The impact is also observable on the electron energy distribution. Corresponding combinations for the fermionic neutrinos are given as

$$\begin{aligned} K_m^f + L_m^f &\approx 4 \frac{1}{E_m - E_i + \Delta}, \\ K_m^f - L_m^f &\approx 2 \frac{(E_{e 2} - E_{e 1})(E_{\nu 2} - E_{\nu 1})}{(E_m - E_i + \Delta)^3}. \end{aligned} \quad (6.11)$$

Unlike the case of bosonic neutrinos the combinations of  $K_m^f$  and  $L_m^f$  have significantly different behavior. The term  $K_m^f - L_m^f$  has an additional factor  $(E_{e 2} - E_{e 1}) / (E_m - E_i + \Delta)$  that suppress it even stronger against the term  $K_m^f + L_m^f$ . By summing the above mentioned facts yield that double  $\beta$ -decay to the ground and excited state represents an outstanding tool for study of the bosonic feature of neutrinos.

The kinematical factors  $K_m^{f,b}$  and  $L_m^{f,b}$  entering to the decay rates are weighted with the corresponding nuclear matrix elements.

We introduce the ratio

$$r_0(J^\pi) \equiv \frac{\Gamma_b(J^\pi)}{\Gamma_f(J^\pi)}, \quad (6.12)$$

of the decay probabilities to ground ( $J^\pi = 0_{g.s.}^+$ ) and excited ( $J^\pi = 2_1^+$ ) state for pure bosonic  $\Gamma_b(J^\pi)$  and pure fermionic  $\Gamma_f(J^\pi)$  neutrinos. In general case for the ratio  $r_0(J^\pi)$  one needs to evaluate the corresponding nuclear matrix elements for a given transition within an appropriate nuclear model. The situation is quite simplified for those nuclear systems where the transition via only the ground state of the intermediate nuclei  $m = 1$  dominates [68, 74, 88]. For such nuclear systems the Single State Dominance (SSD) hypothesis is considered. Then we may factor out the nuclear matrix elements and take the advantage that they vanish in the ratio  $r_0(J^\pi)$ .

## 6.2 Single State Dominance hypothesis

The Single State Dominance hypothesis states that for those nuclear systems with the ground state of intermediate nucleus  $1^+$  the two-neutrino double  $\beta$ -decay is realized by two virtual transitions:

- i) first one is connecting the ground state of initial nucleus with the ground state ( $1^+$ ) of intermediate nucleus,
- ii) the second one is connecting the ground state ( $1^+$ ) of intermediate nucleus with the ground state of final nucleus.

Assuming the SSD hypothesis we get

$$\begin{aligned}\mathcal{M}_{0^+}^{f,b} &= |M_{g.s.}(0^+)|^2 m_e^2 \left[ \frac{1}{3} (K_1^{f,b} K_1^{f,b} + L_1^{f,b} L_1^{f,b} + K_1^{f,b} L_1^{f,b}) \right. \\ &\quad \left. - \frac{1}{9} (2K_1^{f,b} K_1^{f,b} + 2L_1^{f,b} L_1^{f,b} + 5K_1^{f,b} L_1^{f,b}) \frac{\vec{p}_{e1} \cdot \vec{p}_{e2}}{E_{e1} E_{e2}} \right], \\ \mathcal{M}_{2^+}^{f,b} &= m_e^2 |M_{g.s.}(2^+)|^2 (K_1^{f,b} - L_1^{f,b})^2 \left( 1 + \frac{1}{3} \frac{\vec{p}_{e1} \cdot \vec{p}_{e2}}{E_{e1} E_{e2}} \right).\end{aligned}\quad (6.13)$$

The sum of the complete set of nuclear states of intermediate nucleus is replaced only with transition throughout the  $1^+$  ground state of intermediate nucleus, i.e.  $m = 1$ . The nuclear matrix element is given as

$$M_{g.s.}(J^\pi) = \frac{1}{\sqrt{s}} \langle J_f^\pi || \sum_j \tau_j^+ \sigma_j || 1_1^+ \rangle \langle 1_1^+ || \sum_k \tau_k^+ \sigma_k || 0_i^+ \rangle. \quad (6.14)$$

The main advantage of the SSD hypothesis is the nuclear model independent way of estimating the value of the nuclear matrix element  $M_{g.s.}(J^\pi)$ . The individual matrix elements of the two virtual transitions are determined from the  $\log ft$  values for the electron capture on intermediate nucleus and the single  $\beta$ -decay to the ground (excited  $2_1^+$ ) state of final nucleus, simultaneously. Details of the extraction of the nuclear matrix element from the  $\log ft$  values of electron capture and single  $\beta$ -decay are given in Sec. (5.4).

The total decay rate within the SSD approximation is given as

$$\Gamma_{f,b}(J^\pi) = |M_{g.s.}(J^\pi)|^2 \mathcal{I}_{SSD}^{f,b}(J^\pi). \quad (6.15)$$

The integral over the phase space takes the form

$$\mathcal{I}_{SSD}^{f,b}(J^\pi) = \frac{2a_{2\nu}}{m_e^{11}} \int_{m_e}^{E_i - E_f - m_e} dE_{e1} g_{J^\pi}^{f,b}(E_{e1}, E_{e2}, E_{\nu1}, E_{\nu2}) F_0(Z_f, E_{e1}) p_1 E_{e1} \times \int_{m_e}^{E_i - E_f - E_{e1}} dE_{e2} F_0(Z_f, E_{e2}) p_2 E_{e2} \int_0^{E_i - E_f - E_{e1} - E_{e2}} dE_{\nu1} E_{\nu2}^2 E_{\nu1}^2, \quad (6.16)$$

with

$$\begin{aligned} g_{0^+}^{f,b}(E_{e1}, E_{e2}, E_{\nu1}, E_{\nu2}) &= m_e^2 \left[ \frac{1}{3} (K_1^{f,b} K_1^{f,b} + L_1^{f,b} L_1^{f,b} + K_1^{f,b} L_1^{f,b}) \right] \\ g_{2^+}^{f,b}(E_{e1}, E_{e2}, E_{\nu1}, E_{\nu2}) &= m_e^2 \left( K_1^{f,b} - L_1^{f,b} \right)^2. \end{aligned} \quad (6.17)$$

The two-neutrino double  $\beta$ -decay half-life is given as

$$T_{1/2}^{f,b}(J^\pi) = \frac{\ln 2}{\Gamma_{f,b}(J^\pi)}. \quad (6.18)$$

### 6.3 Higher States Dominance hypothesis

The Higher States Dominance hypothesis suggests that the dominant contribution to the double  $\beta$ -decay nuclear matrix element has its origin in higher lying  $1^+$  states of intermediate nucleus. Within this assumption there exist a commonly used approximation called energy closure that replaces the lepton energies in the denominators with an average value equal half of the reaction energy release

$$E_m - E_i + E_{ek} + E_{\nu j} \approx E_m - E_i + \Delta \quad (k, j = 1, 2). \quad (6.19)$$

The main aim of this approach is to separate the nuclear and lepton parts in the decay rate of two-neutrino double  $\beta$ -decay. With the use of HSD hypothesis for fermionic neutrinos we get

$$\begin{aligned} \mathcal{M}_{0^+}^f &\simeq |M_{GT}^{(1)}(0^+)|^2 \left( 1 - \frac{\vec{p}_{e1} \cdot \vec{p}_{e2}}{E_{e1} E_{e2}} \right), \\ \mathcal{M}_{2^+}^f &= |M_{GT}^{(3)}(2^+)|^2 \frac{(E_{e1} - E_{e2})^2 (E_{\nu1} - E_{\nu2})^2}{2m_e^6} \left( 1 + \frac{1}{3} \frac{\vec{p}_{e1} \cdot \vec{p}_{e2}}{E_{e1} E_{e2}} \right). \end{aligned} \quad (6.20)$$

and for the case of bosonic neutrinos we have

$$\begin{aligned}
\mathcal{M}_{0^+}^b &= |M_{GT}^{(2)}(0^+)|^2 \left[ \frac{3(E_{\nu 2} - E_{\nu 1})^2 + (E_{e 2} - E_{e 1})^2}{48m_e^2} - \frac{9(E_{\nu 2} - E_{\nu 1})^2 - (E_{e 2} - E_{e 1})^2}{144m_e^2} \frac{\vec{p}_{e 1} \cdot \vec{p}_{e 2}}{E_{e 1} E_{e 2}} \right], \\
\mathcal{M}_{2^+}^b &= |M_{GT}^{(2)}(2^+)|^2 \frac{(E_{e 1} - E_{e 2})^2}{4m_e^2} \left( 1 + \frac{1}{3} \frac{\vec{p}_{e 1} \cdot \vec{p}_{e 2}}{E_{e 1} E_{e 2}} \right).
\end{aligned} \tag{6.21}$$

The nuclear Gamow-Teller matrix elements are given by

$$M_{GT}^{(r)}(J^\pi) = \frac{(2m_e)^r}{\sqrt{s}} \sum_m \frac{\langle J_f^\pi || \sum_j \tau_j^+ \sigma_j || 1_m^+ \rangle \langle 1_m^+ || \sum_k \tau_k^+ \sigma_k || 0_i^+ \rangle}{(E_m - E_i + \Delta)^r} \tag{6.22}$$

and  $r = 1, 2, 3$ . The total decay rates for fermionic and bosonic neutrinos are expressed as

$$\begin{aligned}
\Gamma_f(0^+) &= |M_{GT}^{(1)}(0^+)|^2 \mathcal{I}_{HSD}^f(0^+), \\
\Gamma_f(2^+) &= |M_{GT}^{(3)}(2^+)|^2 \mathcal{I}_{HSD}^f(2^+)
\end{aligned} \tag{6.23}$$

and

$$\Gamma_b(J^\pi) = |M_{GT}^{(2)}(J^\pi)|^2 \mathcal{I}_{HSD}^b(J^\pi). \tag{6.24}$$

The phase space integrals are given by

$$\begin{aligned}
\mathcal{I}_{HSD}^{f,b}(J^\pi) &= \frac{2a_{2\nu}}{m_e^{11}} \int_{m_e}^{E_i - E_f - m_e} dE_{e 1} f_{J^\pi}^{f,b}(E_{e 1}, E_{e 2}, E_{\nu 1}, E_{\nu 2}) F_0(Z_f, E_{e 1}) p_1 E_{e 1} \times \\
&\int_{m_e}^{E_i - E_f - E_{e 1}} dE_{e 2} F_0(Z_f, E_{e 2}) p_2 E_{e 2} \int_0^{E_i - E_f - E_{e 1} - E_{e 2}} dE_{\nu 1} E_{\nu 2}^2 E_{\nu 1}^2.
\end{aligned} \tag{6.25}$$

The energy conservation yields

$$E_{\nu 2} = E_i - E_f - E_{e 1} - E_{e 2} - E_{\nu 1}. \tag{6.26}$$

The integrand functions are given as

$$\begin{aligned}
f_{J^\pi}^f(E_{e1}, E_{e2}, E_{\nu1}, E_{\nu2}) &= 1 & (J^\pi = 0^+), \\
&= \frac{(E_{e1} - E_{e2})^2 (E_{\nu1} - E_{\nu2})^2}{2m_e^6} & (J^\pi = 2^+), \\
f_{J^\pi}^b(E_{e1}, E_{e2}, E_{\nu1}, E_{\nu2}) &= \frac{3(E_{\nu2} - E_{\nu1})^2 + (E_{e2} - E_{e1})^2}{48m_e^2} & (J^\pi = 0^+), \\
&= \frac{(E_{e1} - E_{e2})^2}{4m_e^2} & (J^\pi = 2^+).
\end{aligned} \tag{6.27}$$

## 6.4 The two-neutrino double $\beta$ -decay with partly bosonic neutrinos

Here, we write down more general case of statistics. Let us write the mixture of fermionic and bosonic neutrino state as

$$|\nu\rangle = \hat{a}^+|0\rangle \equiv c_\delta \hat{f}^+|0\rangle + s_\delta \hat{b}^+|0\rangle = c_\delta|f\rangle + s_\delta|b\rangle. \tag{6.28}$$

Here  $|f\rangle$  and  $|b\rangle$  stand for pure fermionic and bosonic neutrino states, respectively.  $\hat{f}$  ( $\hat{f}^+$ ) and  $\hat{b}$  ( $\hat{b}^+$ ) are respectively fermionic and bosonic annihilation (creation) operators. The normalization condition of mixed neutrino state  $|\nu\rangle$  requires  $c_\delta^2 + s_\delta^2 = 1$  ( $c_\delta \equiv \cos \delta$  and  $s_\delta \equiv \sin \delta$ ). In order to derive the decay rate of the two-neutrino double  $\beta$ -decay we need to introduce the commutation/anticommutation relations with the following properties

$$\begin{aligned}
\hat{f}\hat{b} &= e^{i\phi}\hat{b}\hat{f}, & \hat{f}^+\hat{b}^+ &= e^{i\phi}\hat{b}^+\hat{f}^+, \\
\hat{f}\hat{b}^+ &= e^{-i\phi}\hat{b}^+\hat{f}, & \hat{f}^+\hat{b} &= e^{-i\phi}\hat{b}\hat{f}^+.
\end{aligned} \tag{6.29}$$

Here  $\phi$  is an arbitrary phase. The two-neutrino state we then define as

$$|\nu(k_{\nu1}), \nu(k_{\nu2})\rangle = \hat{a}_1^+ \hat{a}_2^+ |0\rangle. \tag{6.30}$$

The amplitude of the reaction  $A \rightarrow A' + 2\bar{\nu} + 2e$  can be schematically written as

$$A_{2\beta} = \int d^4x_1 d^4x_2 \langle e(p_{e1}), e(p_{e2}), \bar{\nu}(k_{\nu1}), \bar{\nu}(k_{\nu2}), A'|T [\mathcal{H}^\beta(x_1)\mathcal{H}^\beta(x_2)] |A\rangle. \tag{6.31}$$

The Hamiltonian of weak interaction is assumed to have the standard form, e.g. see eq. (5.2). With the commutation relations we find

$$A_{2\beta} = A_f [c_\delta^4 + c_\delta^2 s_\delta^2 (1 - \cos \phi)] + A_b [s_\delta^4 + c_\delta^2 s_\delta^2 (1 + \cos \phi)]. \quad (6.32)$$

$A_f$  and  $A_b$  are fermionic and bosonic parts of the amplitude, respectively. We may factorize the amplitude as

$$A_{2\beta} = \cos^2 \chi A_f + \sin^2 \chi A_b \quad (6.33)$$

by using the notation

$$\begin{aligned} \cos^2 \chi &= c_\delta^4 + c_\delta^2 s_\delta^2 (1 - \cos \phi) \\ \sin^2 \chi &= s_\delta^4 + c_\delta^2 s_\delta^2 (1 + \cos \phi). \end{aligned} \quad (6.34)$$

By performing the integration over the phase space of neutrinos interference between the fermionic  $A_f$  and bosonic  $A_b$  part of amplitude  $A_{2\beta}$  disappears. We may understand this effect by basic considerations. The wave function of identical fermions is antisymmetric with respect of interchange of two particles, while for bosons the wave function is symmetric. Assuming the impossibility to distinguish between the two identical particles the interference term consisting of symmetric and antisymmetric part turns out to be zero. The total decay rate is therefore given as

$$\Gamma_{tot} = \cos^4 \chi \Gamma_f + \sin^4 \chi \Gamma_b. \quad (6.35)$$

Here,  $\Gamma_f$  and  $\Gamma_b$  are total decay rates in cases of pure fermionic and pure bosonic neutrinos, respectively. We note that decay rates  $\Gamma_{f,b}$  are proportional to the corresponding amplitudes  $|A_{f,b}|^2$ . The specific form of the individual decay rates was given in section 6.1 under some special conditions. These are, i.e. the transitions to the  $0^+$  and  $2^+$  nuclear final states have been considered, SSD and HSD hypotheses have been taken into account. For the total decay rate of reaction we have

$$\Gamma_{tot}(J^\pi) = \cos^4 \chi \Gamma_f(J^\pi) + \sin^4 \chi \Gamma_b(J^\pi). \quad (6.36)$$

The differential decay rate normalized to unity is given as

$$P_{J^\pi} = \frac{d\Gamma_{tot}(J^\pi)}{\Gamma_{tot}(J^\pi)} = \frac{\cos^4 \chi d\omega_f(J^\pi) + \sin^4 \chi r_0(J^\pi) d\omega_b(J^\pi)}{\cos^4 \chi + \sin^4 \chi r_0(J^\pi)}, \quad (6.37)$$

with

$$d\omega_f(J^\pi) \equiv \frac{d\Gamma_f(J^\pi)}{\Gamma_f(J^\pi)}, \quad d\omega_b(J^\pi) \equiv \frac{d\Gamma_b(J^\pi)}{\Gamma_b(J^\pi)}. \quad (6.38)$$

Here, ratio  $r_0(J^\pi)$  is given in (6.12). The explicit form of the differential decay rates for pure fermionic ( $d\Gamma_f(J^\pi)$ ) and pure bosonic ( $d\Gamma_b(J^\pi)$ ) neutrinos is given by relation (6.3). In general, the normalized distributions (6.38) depend on the nuclear matrix elements. Nevertheless, with the approach of SSD hypothesis the normalized differential decay rate (6.37) is free of nuclear matrix elements [74, 88].

## 6.5 Effect of bosonic neutrinos in two-neutrino double $\beta$ -decay of $^{100}\text{Mo}$

In this section, we present the characteristics of two-neutrino double  $\beta$ -decay of  $^{100}\text{Mo}$  with the assumption of partially mixed bosonic neutrino. Subject of choice is the isotope  $^{100}\text{Mo}$  due to the high number of events collected in experiment (see [89, 91]).

The collaboration of NEMO-3 experiment has detected  $10^5$  events of  $^{100}\text{Mo}$  ( $0^+ \rightarrow 0^+$ ) decays to the ground state [89]. Measured parameters are: the sum of the electron energies, the energy of single electron and the angular distribution / angular correlation of electrons. Assumption that the double  $\beta$ -decay is governed mainly throughout the  $1^+$  intermediate nucleus ground state is known as the SSD hypothesis and give a good approximation for  $^{100}\text{Mo}$  nucleus. This fact is also confirmed by the measurements of NEMO-3 experiment [78, 79]. The advantage of SSD approach is the experimental estimation of nuclear matrix elements from the  $\log ft$  values of electron capture and single  $\beta$ -decay of intermediate nucleus ( $^{100}\text{Tc}$ ). See section 5.4 for details of obtaining these nuclear matrix elements from known  $\log ft$  values for  $^{100}\text{Tc}$ . With the use of SSD hypothesis we present herein the half-life of two-neutrino double  $\beta$ -decay of  $^{100}\text{Mo}$  for pure fermionic and pure bosonic neutrinos, respectively.

$$\begin{aligned} T_{1/2}^f(0_{g.s.}^+) &= 6.8 \times 10^{18} \text{ years} \\ T_{1/2}^b(0_{g.s.}^+) &= 8.9 \times 10^{19} \text{ years.} \end{aligned} \quad (6.39)$$

The ratio of bosonic total decay rate over fermionic one is equal to

$$r_0(0_{g.s.}^+) = 0.076. \quad (6.40)$$

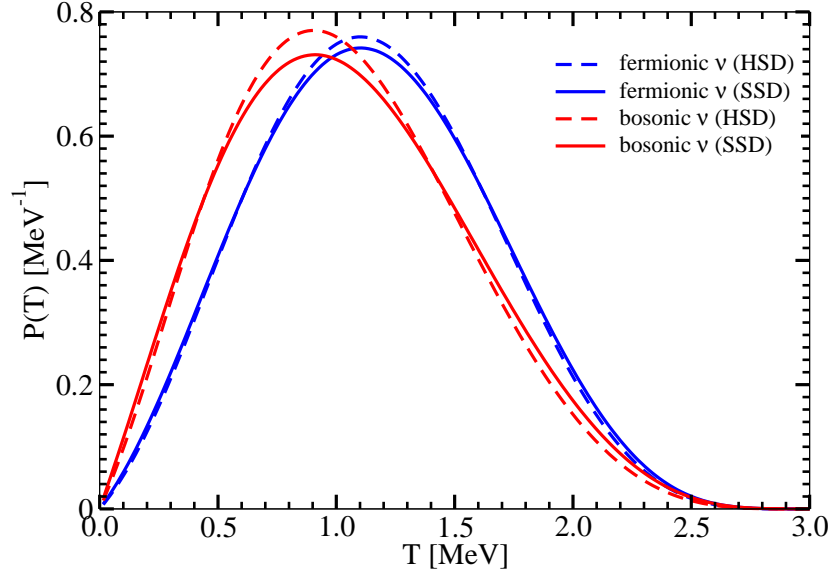


Figure 6.1: The differential decay rates normalized to unity versus the sum of the kinetic energies of the outgoing electrons  $T$  for the two-neutrino double  $\beta$ -decay of  $^{100}\text{Mo}$  to the ground state ( $0^+$ ) of final nucleus. The electron spectra are presented for the pure fermionic and pure bosonic neutrinos. The distributions have been calculated with the assumption of the SSD hypothesis and the HSD hypothesis, respectively.

This ratio gives the weight of the bosonic component of differential decay rate entering to the normalized differential decay rate (6.37). For rather small value of  $r_0$  a significant modification of distribution shall be expected when  $\sin^2 \chi$  becomes close to 1.

However, higher lying states can in principle give some not negligible contribution indeed and therefore produce a systematic error in our analysis. In order to estimate the effect of higher lying states one can assume an extreme case of HSD hypothesis. Within this assumption the main contribution to the two-neutrino double  $\beta$  decay matrix element comes from higher lying  $1^+$  states of intermediate nucleus even from the Gamow-Teller resonance region. Within this approach the energy denominator closure is introduced. It replaces the lepton energies with an average value equal to the half of the reaction energy release ( $\Delta = (E_i - E_f)/2$ ). It is worth to mention that there are different matrix elements associated with fermionic and bosonic neutrinos, see eq. (6.20) and (6.21). The advantage of the above mentioned procedure is the separation of nuclear matrix elements and phase space of outgoing leptons. Therefore, in study of normalized distributions the nuclear matrix elements can be factorized out and leave the distributions free of any nuclear model dependent assumptions. Unfortunately for the half-life or the ratio  $r_0(J^\pi)$  an appropriate nuclear model has to be taken into



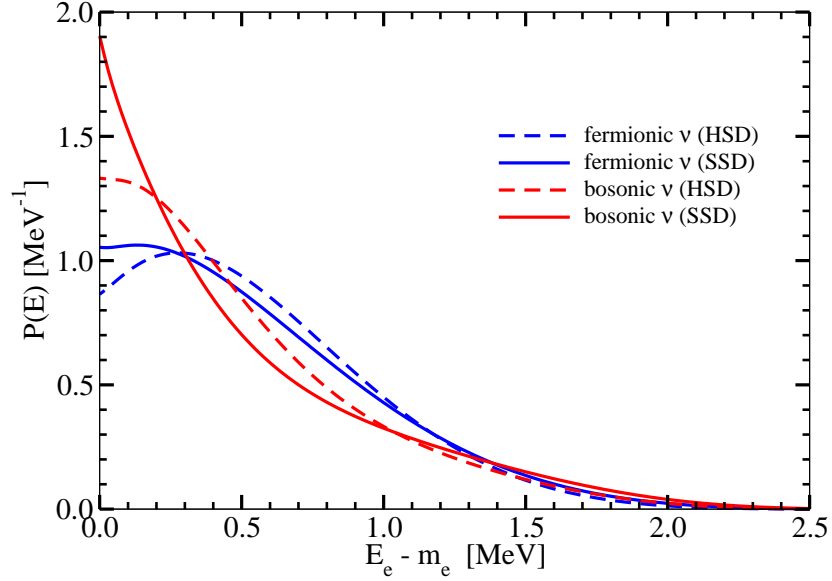


Figure 6.2: The differential decay rates normalized to unity versus the single electron kinetic energy for the two-neutrino double  $\beta$ -decay of  $^{100}\text{Mo}$  to the ground state ( $0^+$ ) of final nucleus.  $E_e$  and  $m_e$  stand for the electron energy and electron rest mass, respectively. The conventions used herein are the same as in Fig. 6.1.

account, e.g. Quasiparticle Random Phase Approximation (QRPA) or Nuclear Shell Model (NSM).

The differential decay rates versus the sum of the kinetic energies of two electrons within the SSD and HSD approaches are illustrated in Fig. 6.1. Regardless to the statistical feature of neutrinos (i.e., either fermionic or bosonic) the SSD approach yields slightly wider spectra of the sum of energies of two outgoing electrons with respect to the HSD hypothesis. However, the spectra for bosonic neutrinos are shifted to lower energies for SSD as well as for HSD approximation. The main result is the shift independence of the approach (i.e., SSD or HSD). Therefore, it can be considered as a firm effect of bosonic neutrinos.

The single electron energy spectra for bosonic and fermionic neutrinos within the SSD and HSD approximations are shown in Fig. 6.2. The electron energy spectrum becomes softer in the case of bosonic neutrino as one can see.

The spectra of the sum of energies of two outgoing electrons for the case of admixture of fermionic and bosonic neutrinos are illustrated in Fig. 6.3. The shift of spectra to the smaller energies with increasing parameter  $\sin^2 \chi$  is well understood within considerations previously mentioned. Remarkable change of the spectra is observed when  $\sin^2 \chi$  is close to unity due to the small value of  $r_0$ .

The single electron energy spectra for various values of the mixing parameter  $\sin^2 \chi$

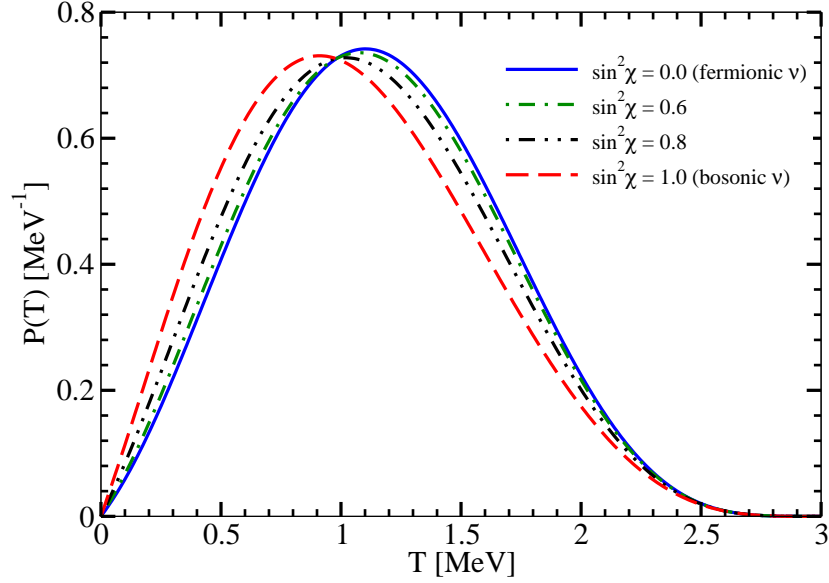


Figure 6.3: The differential decay rates normalized to the unity versus the sum of the kinetic energies of two outgoing electrons  $T$  for the two-neutrino double  $\beta$ -decay of  $^{100}\text{Mo}$  to the ground state ( $0^+$ ) of final nucleus. The results are obtained in the SSD approach. The spectra are presented for various values of mixing parameter  $\sin^2 \chi$  of bosonic component.

are illustrated in Fig. 6.4. The electron energy  $E_{kin} = 0.3$  MeV turns out to be a crucial point in the spectra. The energy distribution tends to increase with  $\sin^2 \chi$  below  $E_{kin} < 0.3$  MeV, while for the energy region  $E_{kin} = 0.3 - 1.4$  MeV it decreases.

It was already mentioned in Sec. 6.1 that the presence of bosonic part of neutrinos affects the rates of the two-neutrino double  $\beta$ -decay to the ground ( $0^+$ ) and first excited state ( $2_1^+$ ) of final nucleus in opposite way. Moreover, the ratio of decay rates to the first excited state  $2_1^+$  and to the ground state  $0^+$  does not depend on  $\log ft$  values of single  $\beta$  decay and electron capture on intermediate nuclues that are of poor accuracy eventually. Within the SSD approximation for the two-neutrino double  $\beta$  decay half-life we obtain

$$\begin{aligned}
 T_{1/2}(2_1^+) &= 1.7 \times 10^{23} \text{ years} && (\text{fermionic } \nu s) \\
 &= 2.4 \times 10^{22} \text{ years} && (\text{bosonic } \nu s).
 \end{aligned} \tag{6.41}$$

For the ratio of fermionic over bosonic half-life we get

$$r_0(2_1^+) = 7.1. \tag{6.42}$$

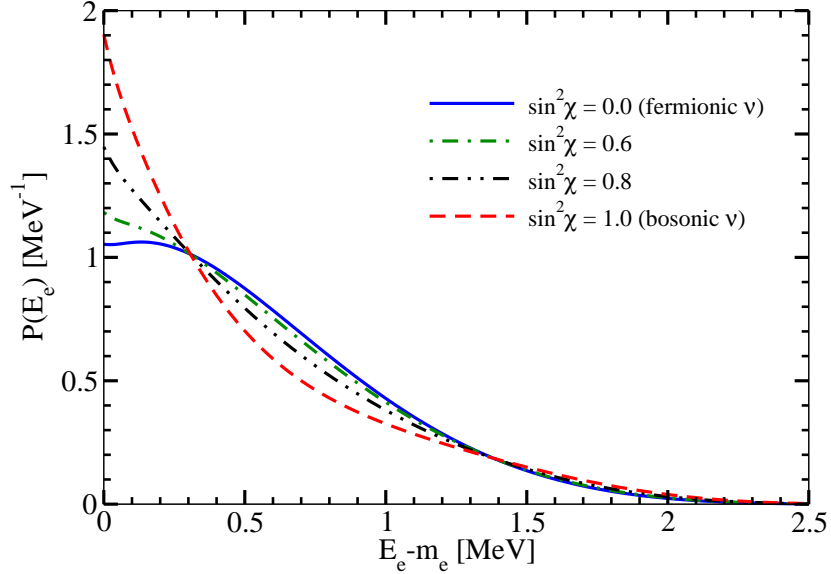


Figure 6.4: The differential decay rates normalized to unity versus the single electron kinetic energy for the two-neutrino double  $\beta$ -decay of  $^{100}\text{Mo}$  to the ground state ( $0^+$ ) of final nucleus. The results are obtained in the SSD approach. The spectra are presented for various values of mixing parameter  $\sin^2 \chi$  of bosonic component. The conventions used herein are the same as in Figs.6.2, 6.3.

The decay rate for bosonic neutrinos is larger as one can expect from the considerations mentioned in Sec. 6.1.

Recently, best known bound on value of the half-life of the two-neutrino double  $\beta$ -decay to the first excited state ( $2_1^+$ ) of final nucleus is  $T_{1/2}(2_1^+) > 1.6 \times 10^{21}$  [90] from the NEMO-3 experiment. One may expect that in near future the sensitivity of measurement will increase up to  $10^{22}$  years and thus will approach the value for the case of pure bosonic neutrinos. It is worth to mention that due to the large value of  $r_0$  even a small contribution from bosonic neutrinos can produce a remarkable distortion of the energy distributions with respect to the standard (pure fermionic neutrinos) spectra.

The electron energy distributions for the two-neutrino double  $\beta$ -decay of  $^{100}\text{Mo}$  into the  $2_1^+$  first excited state of final nucleus are illustrated in Figs. 6.5, 6.6. Here, the distortion of spectra is opposite for the decay to the  $2^+$  final state unlike the case of the decay to the  $0^+$  ground state of  $^{100}\text{Mo}$ . With increasing value of mixing parameter  $\sin^2 \chi$  the electron spectrum is shifted to higher energies. This effect is obviously related with the change of spin between initial and final nucleus. Within the transition  $0^+ \rightarrow 2_1^+$  the system of emitted leptons should carry out the spin 2. Due to the polarization of outgoing leptons (determined by  $V - A$  type of interaction) both electrons are emitted

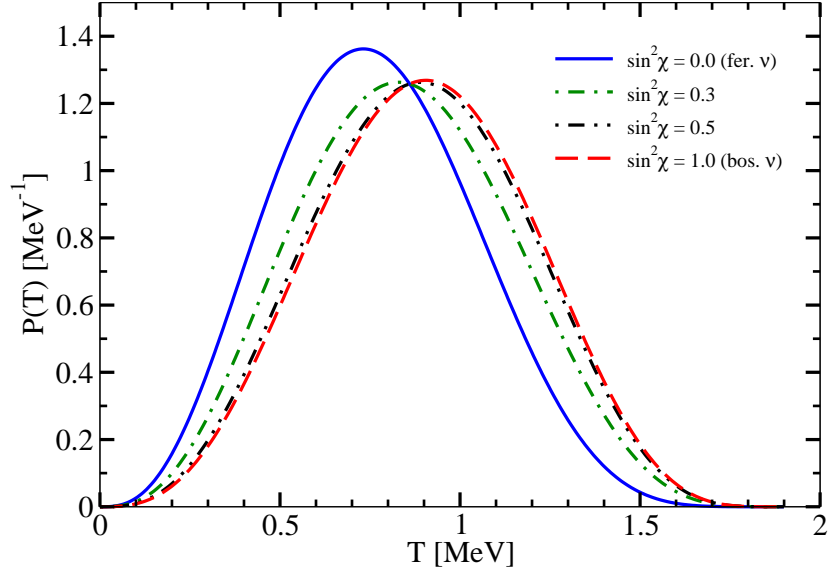


Figure 6.5: The differential decay rates normalized to the unity versus the sum of kinetic energies of two outgoing electrons  $T$  for two-neutrino double  $\beta$ -decay of  $^{100}\text{Mo}$  to the first excited state ( $2_1^+$ ) of final nucleus. The results are obtained in the SSD approach. The spectra are presented for various values of mixing parameter  $\sin^2 \chi$  of bosonic component.

preferably in the same direction and two antineutrinos in opposite direction with Pauli blocking factor. For the case of bosonic neutrinos the corresponding Pauli blocking factor vanishes and electrons might be more aligned, i.e. carry out higher energies in the end. Therefore, the spectrum is shifted to higher energies. For the transition  $0^+ \rightarrow 0^+$  the total leptonic momentum is zero, therefore possibility of electrons moving in opposite directions is more preferred. It is worth to note that even a small contribution from bosonic neutrinos cause remarkable distortion of the spectra (see Fig. 6.5) and therefore this effect can be used to gain some information on bosonic neutrinos in future experiments.

## 6.6 Restriction bounds on bosonic component of neutrinos

There are several ways how to estimate the contribution of bosonic or partly bosonic neutrinos, e.g. by use of energy spectra, total decay rates and the ratios of the total decay rates to the excited over the rates to the ground state of final nucleus. We intent to use these methods to obtain a valuable restriction on the parameter  $\sin^2 \chi$  from the existing experimental data.

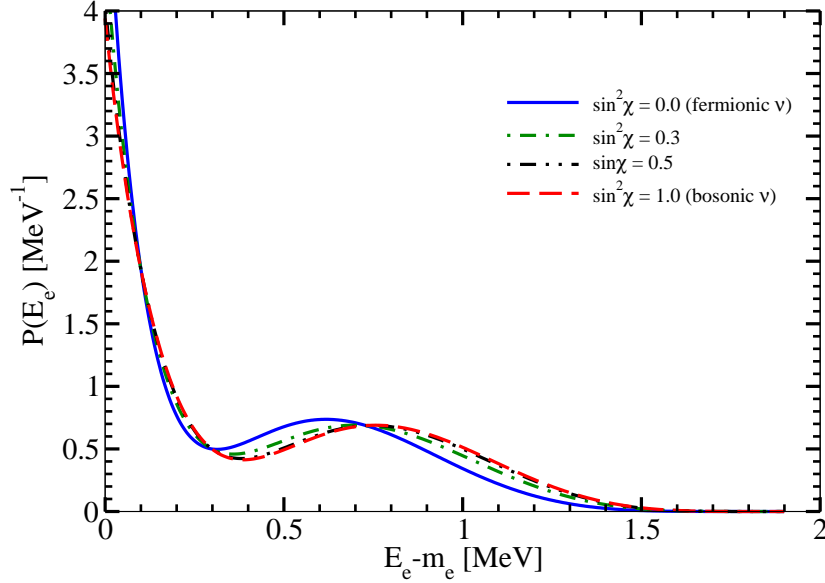


Figure 6.6: The differential decay rates normalized to the unity versus the single electron energy for the two-neutrino double  $\beta$ -decay of  $^{100}\text{Mo}$  to the first excited state ( $2_1^+$ ) of final nucleus. The results are obtained in the SSD approach. The spectra are presented for various values of mixing parameter  $\sin^2 \chi$  of bosonic component. The conventions used herein are the same as in Figs. 6.2, 6.5.

As was already mentioned for transitions  $0^+ \rightarrow 0^+$  holds  $r_0 \ll 1$ . In the case of small  $r_0$  the best bound on bosonic part of neutrinos can be obtained from the total decay rate, i.e. the half-life. A spectrum distortion due to the presence of bosonic part is rather small. On the other hand the transitions  $0^+ \rightarrow 2_1^+$  are characteristic with large values of  $r_0$ . Therefore a very strong modification of spectra are expected in this case.

In forthcoming, we present three complementary approaches of obtaining the bounds on  $\sin^2 \chi$  in more detail.

### 6.6.1 The half-life

We may obtain the restriction on  $\sin^2 \chi$  by comparing theoretically predicted and experimentally measured half-life. With the use of relation (6.36) we get

$$\sin^2 \chi = \frac{1}{1+r_0} \left[ 1 - \sqrt{\frac{T_{1/2}^f}{T_{1/2}^{exp}} - r_0 \left( 1 - \frac{T_{1/2}^f}{T_{1/2}^{exp}} \right)} \right]. \quad (6.43)$$

Here, the quantity  $r_0 = T_{1/2}^f/T_{1/2}^b$  was already introduced in (6.12).  $T_{1/2}^f$  and  $T_{1/2}^b$  are theoretically calculated half-lives for pure fermionic and pure bosonic neutrinos,

respectively.  $T_{1/2}^{exp}$  is the experimentally measured half-life. If there exist an agreement between the measured and predicted (for case of pure fermionic neutrinos) half-lives, we may introduce the upper bound on  $\sin^2 \chi$  by use of (6.43) as follows

$$\sin^2 \chi < \frac{1}{1+r_0} \left[ 1 - \sqrt{\frac{T_{1/2}^{f-min}}{T_{1/2}^{exp-max}} - r_0 \left( 1 - \frac{T_{1/2}^{f-min}}{T_{1/2}^{exp-max}} \right)} \right]. \quad (6.44)$$

$T_{1/2}^{f-min}$  is the minimal theoretically predicted value of the two-neutrino double  $\beta$ -decay half-life calculated with appropriate nuclear model (e.g. QRPA or NSM).  $T_{1/2}^{exp-max}$  is the maximal experimentally measured value of the two-neutrino double  $\beta$ -decay half-life. If  $r_0 \ll 1$  and  $r_0$  is small with respect to the relative accuracy of  $T_{1/2}^f/T_{1/2}^{exp}$ , simultaneously, then we may omit terms proportional to  $r_0$  in (6.44) and get

$$\sin^2 \chi < (1 - \sqrt{T_{1/2}^{f-min}/T_{1/2}^{exp-max}}). \quad (6.45)$$

Unfortunately, this approach requires knowledge of nuclear matrix elements, i.e. is dependent on choice of proper nuclear system description. Nevertheless, an adequate estimation of nuclear matrix elements can be obtained for some nuclei, e.g.  $^{100}Mo$  and  $^{116}Cd$  with the use of the SSD hypothesis. For the case of  $^{100}Mo$  we can take calculated value of the half-life  $T_{1/2}^f = (6.84 \pm 3.42) \times 10^{18}$  years from [88]. This half-life well agrees with the experimental value of  $T_{1/2}^{exp} = (7.11 \pm 0.54) \times 10^{18}$  years [89] obtained from the NEMO-3 experiment. We then get  $r_0(0_{g.s.}^+) = 0.086$  and for the restriction we obtain

$$\sin^2 \chi < 0.34. \quad (6.46)$$

It is worth to note that the accuracy of estimated half-life  $T_{1/2}^f$  depends crucially on the accuracy of half-life of electron capture on intermediate nucleus  $^{100}Tc$  [72]. Unfortunately, there does not exist more reliable experimental data on the half-life value for electron capture on  $^{100}Tc$ , therefore the obtained limit on  $\sin^2 \chi$  shall be reconsidered in future when more precise data will be available.

However, stronger bound can be obtained by exploring the two-neutrino double  $\beta$ -decay of  $^{116}Cd$ . The advantage is the fact that  $\log ft$  values may be achieved from beta strengths obtained with charge exchange reactions. Then for the value of half-life we obtain  $T_{1/2}^f = (2.76 \pm 0.12) \times 10^{19}$  years [92]. For the bound we get

$$\sin^2 \chi < 0.06. \quad (6.47)$$

## 6.6.2 The energy distributions

The precise measurement of differential characteristics of the two-neutrino double  $\beta$ -decay can probe more precisely bosonic or partly bosonic neutrinos. Such characteristics are measured with NEMO-3 experiment for  $^{100}\text{Mo}$ ,  $^{116}\text{Cd}$ ,  $^{150}\text{Nd}$ ,  $^{82}\text{Se}$ ,  $^{96}\text{Zr}$  and  $^{48}\text{Ca}$  isotopes.

The aim is to compare the theoretically predicted shape of spectra with the experimentally measured ones. A fit can be performed considering  $\sin^2 \chi$  as a free parameter. As was already mentioned this method is useful mostly in cases with large  $r_0$ . Therefore, it is suitable to analyze  $^{100}\text{Mo}$  decay to the ground state  $0^+ \rightarrow 0^+$ .

From the analysis of available experimental data the case of pure bosonic neutrinos ( $\sin^2 \chi = 1$ ) can be excluded [92]. By comparing the spectra (see Fig. 6.3) with the experimental data, namely the shift of maximum to higher energies, we can estimate a bound  $\sin^2 \chi < 0.6$ . It is noteworthy that there is not perfect agreement between the experimental data and theoretical spectrum.

We make a comment on single electron energy spectrum of  $^{100}\text{Mo}$  double  $\beta$ -decay also. Generally it is assumed that SSD approach is adequate in case of  $^{100}\text{Mo}$  but a small discrepancy exist between the predicted and measured spectra. However, it was pointed out that SSD is more likely realized in this case as HSD approximation [78, 79]. The spectra for partly bosonic neutrinos (see Fig.6.4) compared with data give a restriction  $\sin^2 \chi < 0.7$  [92]. We note that the theoretically predicted spectra in SSD approach are not in an ideal agreement with data. This is mostly obvious in low energy region ( $E = 0.2 - 0.4$  MeV). From our point of view a natural explanation occurs that it is an effect of partly bosonic neutrinos with parameter  $\sin^2 \chi \sim 0.5 - 0.6$ . Only with progress in data analysis of NEMO-3 experiment we may get a better bound on  $\sin^2 \chi$  hopefully in near future.

## 6.6.3 Ratios of half-lives to excited and ground state

We define the ratio of half-lives to the excited and ground state

$$r_{f,b}^*(J^\pi) \equiv \frac{T_{1/2}^{f,b}(J^\pi)}{T_{1/2}^{f,b}(0^+)} \quad (6.48)$$

for fermionic and bosonic neutrinos, separately. The advantage of introducing the ratio (6.48) is the fact that nuclear matrix elements that are for some cases known with poor accuracy are canceled in ratio with SSD (or HSD) approach. Therefore, the uncertainty of  $\log ft$  values does not have any impact on precision of the ratio (6.48).

In case of  $^{100}\text{Mo}$  transitions to  $0^+$  and  $0_1^+$  were already experimentally observed by NEMO-3 [89, 90]. So we have

$$r_{exp}^*(0_1^+) \simeq 80. \quad (6.49)$$

On the other hand the theoretically calculated values within the SSD approach are

$$\begin{aligned} r^*(0_1^+) &\simeq 61 && \text{(fermionic } \nu s) \\ &\simeq 73 && \text{(bosonic } \nu s). \end{aligned} \quad (6.50)$$

One may conclude that bosonic neutrinos fit data somehow better. Let us remark that the involved SSD approach may not be enough satisfactory. The statistics of transitions to  $0_1^+$  excited state need to be improved also.

Unlike the case of transition to  $0_1^+$  state the transition to  $2_1^+$  appears to be a better tool for study of bosonic neutrinos. For the two-neutrino double  $\beta$ -decay of  $^{100}\text{Mo}$  in the SSD approach we obtain

$$\begin{aligned} r^*(2_1^+) &\simeq 2.5 \times 10^4 && \text{(fermionic } \nu s) \\ &\simeq 2.7 \times 10^2 && \text{(bosonic } \nu s). \end{aligned} \quad (6.51)$$

These values are substantially different for fermionic and bosonic neutrinos. Unfortunately the decay to  $2_1^+$  of  $^{100}\text{Mo}$  has not been measured yet. Inserting only the limit on half-life [94] to the  $2_1^+$  excited state of  $^{100}\text{Ru}$  into (6.48) we get

$$r_{exp}^*(2_1^+) > 2.2 \times 10^2. \quad (6.52)$$

We see that this bound is too close to the value for bosonic neutrinos. Therefore, experimental evidence on the decay of  $^{100}\text{Mo}$  to  $2_1^+$  state is highly required in order to exclude pure bosonic neutrinos and to study partly bosonic neutrinos.

## Conclusions

We summarize here briefly the achieved results of analysis of partly bosonic neutrinos in the two-neutrino double  $\beta$ -decay.

Double  $\beta$ -decay is a unique process that provide a test of the Pauli exclusion principle and statistical feature of neutrinos. It is worth mentioning that statistics of neutrinos



and violation of Pauli exclusion principle is still an open question. Appearance of even small bosonic component in neutrino states can lead to a remarkable change of total decay rates as well as the energy distributions.

We defined ratio  $r_0$  of the total decay rates for bosonic to fermionic neutrinos. The nuclear systems with higher  $r_0$  are preferred due to higher sensitivity to bosonic component of neutrinos. For  $^{100}\text{Mo}$  decay to the ground state we found  $r_0(0^+) = 0.076$ . However, for  $^{100}\text{Mo}$  decay to the excited state we found rather large value  $r_0(2_1^+) = 7.1$ . We have to note that the  $^{100}\text{Mo}$  double  $\beta$ -decay to the excited state  $2_1^+$  has not been measured until now.

The introduced parameter  $\sin^2 \chi$  describes the case of mixed statistics of neutrinos, i.e. the case of partly bosonic neutrinos. The upper limit on  $\sin^2 \chi$  can be obtained by comparing theoretically predicted and experimentally measured total decay rates. However, the small accuracy of nuclear matrix elements involved in the decay rates lowers the reliability of this method. The conservative bound of  $\sin^2 \chi < 0.5$  is found for  $^{100}\text{Mo}$ , i.e. the case of pure bosonic neutrinos can be excluded. Much better restriction  $\sin^2 \chi < 0.06$  is obtained from  $^{116}\text{Cd}$  decay studies. Nevertheless, these bounds need to be verified in future with new experiments.

The transitions with large  $r_0(J^\pi)$  value are worthwhile because of higher sensitivity to spectrum distortions caused by bosonic component of neutrinos. By use of available experimental data on the transition  $0^+ \rightarrow 0^+$  for  $^{100}\text{Mo}$  a bound  $\sin^2 \chi < 0.6$  is obtained. From transition  $0^+ \rightarrow 2_1^+$  to the nuclear excited state of  $^{100}\text{Ru}$  a stronger limit can be achieved in principle due to relatively high value of  $r_0(2_1^+) \simeq 7$ . Unfortunately, more experimental results are needed for this channel. We found that the distortion of the energy spectra caused by bosonic part of neutrinos is opposite for  $0^+ \rightarrow 0^+$  and for  $0^+ \rightarrow 2_1^+$  transitions. The presence of bosonic part of neutrinos shifts the energy spectrum of outgoing electrons to low energy region for  $0^+ \rightarrow 0^+$  transition, while for the  $0^+ \rightarrow 2_1^+$  transition spectrum is shifted to higher energies.

A rather strong restriction on  $\sin^2 \chi$  might be obtained from ratios of half-lives to the excited ( $2_1^+$ ) and ground ( $0^+$ ) state of final nucleus, where the discrepancy between the bosonic and fermionic neutrino cases is quite large. However, further experimental progress in the decays to the excited states ( $2_1^+$ ) is necessary.

We note that there exist no restriction on bosonic component of neutrinos obtained from the Big Bang Nucleosynthesis. The main aim is to put a qualitative bound on the mixing parameter  $\sin^2 \chi$ . From the two-neutrino double  $\beta$ -decay we found a conservative bound  $\sin^2 \chi < 0.6$  that excludes pure bosonic neutrinos. These findings were published in Ref. [X] give in the *List of publications*.

# Summary

In this thesis the absolute scale of the neutrino masses and the statistics of neutrinos have been investigated. The focus was set on the determination of the neutrino mass from the single  $\beta$ -decays of tritium, rhenium and indium. A possible violation of the Pauli exclusion principle for neutrinos was studied in the case of the two-neutrino double  $\beta$ -decay.

## **Absolute mass scale of neutrinos in the context of the single $\beta$ -decay**

*Tritium  $\beta$ -decay (see Chapter 3)*

- By taking use of the analogy between the  ${}^3H$  and  ${}^3He$  nuclei and neutron and proton particles the super-allowed  $\beta$ -decay of tritium has been described within the Elementary Particle Treatment (EPT) of Kim and Primakoff.
- A relativistic form of the electron energy spectrum in the EPT approach has been derived. It was found that the nuclear recoil shifts the kinematical endpoint to lower value by about 3.4 eV. In addition, it is concluded that the effects of higher order terms of hadron currents are negligible.
- The relativistic Kurie function for the tritium  $\beta$ -decay has been defined and presented in a simple form suitable for the neutrino mass determination from the shape of the endpoint spectrum. A connection with the commonly used Kurie function was established.
- The role of weak interactions beyond the SM in the tritium  $\beta$ -decay near the endpoint spectrum has been studied. We showed that the effective scalar and tensor interactions cannot produce a significant effect near the endpoint and, therefore, cannot interfere with that produced by the neutrino mass.

*Rhenium and indium  $\beta$ -decay (see Chapter 4)*

- The theoretically unknown electron energy spectrum of the first unique forbidden  $\beta$ -decay of rhenium has been presented.

- By a detailed analysis it was found that the particular decay rate associated with the  $p$ -wave emission of electron dominates over the  $s$ -wave contribution to decay rate by a factor  $\sim 10^4$ .
- The Kurie function for the first unique forbidden  $\beta$ -decay of  $^{187}\text{Re}$  has been introduced. The analysis of the Kurie function for the rhenium  $\beta$ -decay showed that within a good accuracy it coincides up to a factor to the Kurie function of the super-allowed transitions.
- The electron energy spectrum of the second unique forbidden  $\beta$ -decay of  $^{115}\text{In}$  to the first nuclear excited state has been derived. It was showed that in this transition electrons are predominantly emitted in  $d$  partial waves. There is a general conclusion that the Kurie function for the unique forbidden  $\beta$ -decays with low  $Q$ -value is undistinguishable with the Kurie function of superallowed  $\beta$ -transitions.

### Statistics of neutrinos in the context of the $2\nu\beta\beta$ -decay

*A detailed description of the  $2\nu\beta\beta$ -decay (see Chapter 5)*

- A general expression for the decay-rate of the  $2\nu\beta\beta$ -decay to the ground ( $0^+$ ) and excited ( $2^+$ ) state of the final nucleus has been derived by considering in addition to electron  $s$ -waves also the emission of  $p$ -wave electrons associated with transitions through  $1^-$ -states of the intermediate nucleus.
- For  $2\nu\beta\beta$ -decay of  $^{150}\text{Nd}$  the half-life has been calculated in a phenomenological SSD approach by using the  $\log ft$  values of single  $\beta$ -transitions of the ground state of the intermediate nucleus. By performing a comparison with measured half-life it was concluded that SSD hypothesis is not realized in the case of the  $2\nu\beta\beta$ -decay of  $^{150}\text{Nd}$ .
- Normalized energy distributions of the  $2\nu\beta\beta$ -decay of  $^{150}\text{Nd}$  to the ground ( $0^+$ ) and excited ( $2^+$ ) state of the final nucleus has been presented by considering both the Single State Dominance and Higher States Dominance hypotheses.

*Statistics of neutrinos (see Chapter 6)*

- By assuming neutrinos to fulfill Bose-Einstein statistics the differential characteristics and half-life of the  $2\nu\beta\beta$ -decay have been determined. Both, transitions to the ground ( $0^+$ ) and the excited ( $2^+$ ) states of final nucleus were considered.

- Qualitative conclusion is that the pure bosonic neutrino is excluded by measured half-life of the  $2\nu\beta\beta$ -decay of  $^{100}\text{Mo}$ .
- Parameter  $\sin^2 \chi$  that describes the case of mixed statistics, i.e. partly bosonic neutrinos, has been introduced. The energy distribution dependence on the mixing parameter was studied. A conservative bound  $\sin^2 \chi < 0.6$  was obtained from data of the NEMO3 experiment.

The results and findings presented in this thesis are important for the KATRIN tritium  $\beta$ -decay experiment, which is under construction and for the planned MARE rhenium  $\beta$ -decay experiment as well as for the next-generation double  $\beta$ -decay experiments like SuperNEMO, EXO, SNO+, etc.

# Résumé

## Úvod

Neutrína zohrávali dôležitú úlohu v ranných fázach Vesmíru. V súčasnosti vieme, že iba 4% z hmoty vo Vesmíre tvorí obyčajná baryónová hmota. Zvyšných 96% hmoty Vesmíru, ktorá je nám neznáma, sa nazýva tzv. tmavá hmota. Zastúpenie neutrín v tejto komponente je stále otázkou špekulácií. Dôležité je poznamenať, že neutrína, ktoré sa oddelili od primordiálnej hmoty, tzv. reliktné neutrína, sú dodnes popri fotónoch druhými najpočetnejšími časticami. Navyše, experimenty s osciláciami neutrín [23, 24, 25] dokazujú, že existujú najmenej 2 hmotné neutrína. Aj dodnes sú nám mnohé základné vlastnosti neutrín stále neznáme.

Cieľom tejto práce je skúmanie fundamentálnych vlastností neutrín: i) absolútna škála hmotností neutrín a ii) štatistické vlastnosti neutrín.

Priame určenie absolútnej škály hmotností neutrín je možné pomocou štúdia konca spektra elektrónov emitovaných v obyčajnom  $\beta$  rozpade. Efekt nenulovej hmotností neutrín sa prejavuje deformáciou spektra pri jeho konci a posunom maximálnej energie elektrónov k nižším hodnotám.

Priame skúmanie štatistického charakteru neutrín je prevedené v rámci analýzy energetických charakteristík dvojneutrínového dvojitého  $\beta$  rozpadu.

## Štúdium hmotnosti neutrína v $\beta$ premene trícia

V súčasnosti je pozornosť k  $\beta$  spektru trícia venovaná najmä v rámci experimentu KATRIN v Karlsruhe, ktorý by mohol urobiť objav hmotnosti neutrín na úrovni  $\sim 0.35$  eV alebo dosiahnuť horný limit hmotnosti neutrín na úrovni  $\sim 0.2$  eV [31].

Z tohto hľadiska rezonuje požiadavka na precízny teoretický popis konca spektra elektrónov emitovaných v  $\beta$  premene trícia a preverenia iných vplyvov na koniec spektra než zo samotnej hmotnosti neutrín.

## Relativistické spektrum elektrónov v $\beta$ premene trícia

Relativistické spektrum elektrónov je odvodené v rámci prístupu Elementary Particle Treatment (EPT), ktorým zavádzame analógiu medzi  $\beta$  premenou trícia



a rozpadom voľného neutrónu



V rámci tohto prístupu je zahrnutý spätný ráz jadier v kinematike danej reakcie, ktorý spôsobuje, že maximálna energia elektrónov,

$$E_e^{max} = \frac{1}{2M_i} (M_i^2 + m_e^2 - (M_f + m_\nu)^2), \quad (6.55)$$

je o 3.4 eV menšia než hodnota získaná konvenčným odvodením  $E_e^{max} = (M_i - M_f - m_\nu)$ .  $M_i$  a  $M_f$  je hmotnosť  ${}^3H$  a  ${}^3He$ .  $m_e$  je hmotnosť elektrónu a  $m_\nu$  je hmotnosť neutrína. Pre spektrum elektrónov emitovaných v beta premene trícia po úpravách dostávame

$$\frac{d\Gamma}{dE_e} \simeq \frac{1}{2\pi^3} G_\beta^2 F(Z, E_e) p_e E_e (g_V^2 + 3g_A^2) \sqrt{y(y + 2m_\nu)} (y + m_\nu). \quad (6.56)$$

$p_e$  a  $E_e$  sú hybnosť a energia elektrónu. Fermiho funkcia  $F(Z, E_e)$  berie do úvahy Coulombovskú interakciu medzi emitovaným elektrónom a koncovým jadrom. Ďalej definujeme relativistický tvar Kurieho funkcie nasledovne

$$K(y) = B \left( \sqrt{y(y + 2m_\nu)} (y + m_\nu) \right)^{1/2}, \quad (6.57)$$

kde  $B = G_\beta \sqrt{g_V^2 + 3g_A^2} / \sqrt{2\pi^3}$ . Tu,  $G_\beta$  je Fermiho konštanta slabej interakcie.  $g_V$  a  $g_A$  sú konštanty renormalizácie vektorového a axiálneho toku a nezávislá premenná je  $y = E_e - E_e^{max}$ . Priebeh Kurieho funkcie (6.57) pri konci spektra je znázornený na obr. (3.3) pre rôzne hmotnosti neutrín. Môžeme vidieť, že pre nulovú hmotnosť neutrína je Kurieho funkcia lineárna, kým pre nenulovú hmotnosť je linearita narušená.

## Slabé interakcie za Štandardným Modelom v $\beta$ premene trícia

Dôsledky efektívnych skalárnych a tenzorových slabých interakcií, ktoré majú pôvod v teóriách idúcich za rámec ŠM sú študované v  $\beta$  premene trícia. Existujúce ohraničenia na hodnoty väzbových konštánt skalárnej a tenzorovej interakcie ( $g_S$  a  $g_T$  [62]) sú získané z energetického spektra koncových jadier v  $\beta$  premene, meraných na experimente WITCH na ISOLDE v CERNe. V rámci prístupu EPT je odvodené spektrum elektónov emitovaných v tríciovom  $\beta$  rozpade s prímiesami exotických interakcií v hamiltoniáne slabých interakcií nasledovne: i) štandardná  $V - A$  a skalárna ( $S$ ) interakcia. ii) štandardná  $V - A$  a tenzorová ( $T$ ) interakcia.

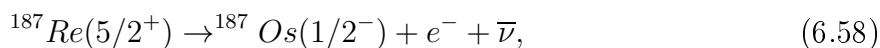
Výsledkom je aditívny člen v spektre elektrónov, ktorý pochádza z interferencie  $V - A$  a skalárnej (tenzorovej) interakcie. Numerickou analýzou pre prípad trícia prichádzame k záveru, že efekt exotických interakcií, ktorých hodnoty väzbových konštánt uvažujeme z experimentu WITCH [62] je omnoho slabší ako štandardnej  $V - A$ , a preto môže byť pri analýze konca spektra zanedbaný.

## Štúdium hmotnosti neutrína v zakázaných $\beta$ premenách rénia a india

Predmetom záujmu experimentu MARE je kalorimetrické meranie energie vyletujúcich elektrónov v réniom  $\beta$  rozpade ( $Q \sim 2.47$  keV) s presnosťou merania hmotnosti neutrína na úrovni 200 meV. Preto je dôraz kladený na precíznu znalosť teoretického priebehu spektra elektrónov vylieajúcich v réniom  $\beta$  rozpade. Nedávne merania hmotností izotopov pomocou Penningových pascí objavili, že energia reakcie v  $\beta$  rozpade  $^{115}\text{In}$  do prvého excitovaného stavu dcérskeho jadra dosahuje najnižšiu hodnotu  $Q = 155$  eV spomedzi všetkých jadrových systémov. Z tohto dôvodu je predmetom našich štúdií spektrum elektrónov emitovaných v  $\beta$  premene india.

### Teoretický popis prvej zakázanej $\beta$ premeny rénia

V prvom zakázanom  $\beta$  rozpade rénia,



je zmena spinu a parity medzi počiatočným a koncovým jadrom  $\Delta J^\pi = 2^-$ . Tá sa realizuje buď i) emitovaním elektrónu v  $s_{1/2}$  vlne a neutrína v  $p_{3/2}$  vlne, alebo

ii) emitovaním elektrónu v  $p_{3/2}$  vlně a neutrína v  $s_{1/2}$  vlně. Príspevky od vyšších parciálnych vln môžu byť zanedbané kvôli nízkej hodnote  $Q$  danej reakcie.

Energetické spektrum vyletujúcich elektrónov, ktoré doposiaľ nebolo teoreticky známe je dané nasledovne

$$N(E_e) = \frac{d\Gamma}{dE_e} = \frac{1}{2\pi^3} G_\beta^2 B R^2 p_e E_e (E_0 - E_e) \sqrt{(E_0 - E_e)^2 - m_\nu^2} \times \frac{1}{3} \left( F_1(Z, E_e) p^2 + F_0(Z, E_e) ((E_0 - E_e)^2 - m_\nu^2) \right). \quad (6.59)$$

$E_0$  je maximálna energia elektrónu v prípade nulovej hmotnosti neutrína.  $R$  je polomer jadra. Fermiho funkcie  $F_0(Z, E_e)$  a  $F_1(Z, E_e)$  berú do úvahy Coulombickú interakciu medzi koncovým jadrom a vyletujúcim elektrónom v  $s$  a  $p$  vlně. Polčas rozpadu je určený len jedným maticovým elementom

$$B = \frac{g_A^2}{6} | \langle O s_{1/2}^- | \sqrt{\frac{4\pi}{3}} \sum_n \tau_n^+ \frac{r_n}{R} \{ \sigma_1(n) \otimes Y_1(n) \}_2 | | R e_{5/2}^+ \rangle |^2, \quad (6.60)$$

ktorý je len multiplikatívnym faktorom, t.j. nemení tvar priebehu spektra. Z experimentálne známeho polčasu rozpadu ( $T_{1/2}^{exp} = 4.35 \times 10^{10} y$ ) je potom možné určiť hodnotu maticového elementu ( $B = 3.573 \times 10^{-4}$ ).  $\tau_n^+$  a  $\sigma_1(n)$  sú izospinový zvyšovací operátor a Pauliho spinový operátor  $n$ -tého nukleónu.

## Dominancia elektrónovej $p$ vlny v $\beta$ premene rénia

Rozpadová šírka  $\beta$  premeny rénia sa dá napísať ako suma dvoch príspevkov,  $\Gamma = \Gamma^{s_{1/2}} + \Gamma^{p_{3/2}}$ .  $\Gamma^{s_{1/2}}$  a  $\Gamma^{p_{3/2}}$  sú jednotlivé časti rozpadovej šírky zodpovedajúce tomu, keď sú elektróny emitované v  $s$  a  $p$  vlnách. Z numerickej analýzy týchto partikulárnych rozpadových šírok vyplýva, že  $\sim 10^4$  viac elektrónov je emitovaných v  $p$  vlně ako v  $s$  vlně. Vysvetlenie tejto dominancie elektrónovej  $p$  vlny spočíva v dvoch príčinách:

- Veľmi nízka hodnota energie danej reakcie ( $Q \sim 2.47 \text{ keV}$ ), ktorá spôsobuje, že elektrón je nerelativistický.
- Funkčná závislosť Fermiho funkcií  $F_0(Z, E_e)$  a  $F_1(Z, E_e)$  v oblasti energií pre réniový  $\beta$  rozpad.

Za účelom pochopenia dominancie elektrónovej  $p$  vlny z hľadiska kinematiky daného procesu prejdeme k limite rovinných vln emitovaných elektrónov, t.j.  $F_k(Z, E_e) \approx 1$  ( $k = 0, 1$ ). Príspevok elektrónovej  $p$  ( $s$ ) vlny je násobený kvadrátom hybnosti elektrónu



(neutrína). Hmotnosť neutrína je zanedbateľná v porovnaní s hodnotou  $Q$  a preto je maximálne dosiahnuteľná hybnosť neutrína  $\sim 2.47$  keV. Na druhej strane maximálne dosiahnuteľná hybnosť elektrónu je  $\sim 49$  keV. To znamená, že samotná kinematika procesu umocňuje vklad elektrónovej  $p$  vlny do celkovej šírky rozpadu.

Numerická analýza ukazuje, že  $F_0(Z, E_e) \ll F_1(Z, E_e)$  v oblasti energií pre réniový  $\beta$  rozpad.

## Kurieho funkcia pre prvý zakázaný $\beta$ rozpad rénia

Zanedbaním príspevku od  $s$  vlny elektrónov definujeme Kurieho funkciu v prípade prvého zakázaného  $\beta$  rozpadu rénia podobne ako pre prípad trícia:

$$K(y, m_\nu) = \mathcal{B}_{Re} \left( (y + m_\nu) \sqrt{y(y + 2m_\nu)} \right)^{1/2}, \quad (6.61)$$

kde  $\mathcal{B}_{Re} = G_\beta \sqrt{B} / \sqrt{2\pi^3} \sqrt{(R^2 p_e^2 / 3)(F_1(Z, E_e) / F_0(Z, E_e))}$  je s dobrou presnosťou konštanta. Dôvodom je nízka hodnota energie reakcie vzhľadom na pokojovú hmotnosť elektrónu.

## Druhý zakázaný $\beta$ rozpad india

Nedávne merania pomocou Penningovej pasce [64] ukázali, že druhý zakázaný  $\beta$  rozpad india do prvého excitovaného stavu dcérskeho jadra ( $^{115}\text{In}(9/2^+) \rightarrow ^{115}\text{Sn}(3/2^+) + e^- + \bar{\nu}_e$ ) je  $\beta$  prechod z doposiaľ najnižšou známou  $Q$  hodnotou reakcie  $\sim 155$  eV. Zmena medzi základným stavom jadra  $^{115}\text{In}(9/2^+)$  a prvým excitovaným stavom jadra  $^{115}\text{Sn}(3/2^+)$  je  $\Delta J^\pi = 3^+$ . Daná zmena spinu a parity je splnená ak sú elektrón a neutríno emitované vo vlnách v tomto poradí:  $d_{5/2}$  a  $s_{1/2}$ ,  $p_{3/2}$  a  $p_{3/2}$ ,  $s_{1/2}$  a  $d_{5/2}$ . Nízka hodnota energie danej reakcie a  $F_2(Z, E_e) \gg F_1(Z, E_e) \gg F_0(Z, E_e)$  spôsobujú, že dominantný vklad do rozpadovej šírky je z  $d$  vlny elektrónov. Zanedbaním  $s$  a  $p$  vlny tak definujeme Kurieho funkciu ako

$$K(y, m_\nu) = \mathcal{B}_{In} \left( (y + m_\nu) \sqrt{y(y + 2m_\nu)} \right)^{1/2}, \quad (6.62)$$

kde  $\mathcal{B}_{In} = G_\beta \sqrt{B_{In}} / (\sqrt{2\pi^3}) \sqrt{(1/9)p_e^4 F_2(Z, E_e) / F_0(Z, E_e)}$  je konštanta v dobrom priblížení. Maticový element je daný ako

$$B_{In} = \frac{g_A^2}{10} \left| \langle ^{115}\text{Sn}(3/2^+) || \sqrt{\frac{8\pi}{15}} \sum_n r_n^2 \tau_n^+ \{ \sigma_1(n) \otimes Y_2(n) \}_3 || ^{115}\text{In}(9/2^+) \rangle \right|^2. \quad (6.63)$$

Zhrnutím výsledkov dosiahnutých pre zakázané  $\beta$  rozpady rénia a india sme prišli k záveru, že pre ľubovoľný  $n$ -tý  $\beta$  rozpad s dostatočne nízkou hodnotu energie reakcie bude závislosť Kurieho funkcie totožná s tou, ktorá je pre povolené  $\beta$  prechody.

## Hypotéza dominancie jedného stavu v $2\nu\beta\beta$ rozpade

Hypotéza dominancie jedného stavu (Single State Dominance - SSD) bola navrhnutá v práci Abad, et al. [68]. SSD hypotéza postuluje pre  $2\nu\beta\beta$  aktívne jadrá, ktorých základný stav medzijadra je  $1^+$ , že maticový element  $2\nu\beta\beta$  premeny je daný maticovými elementmi dvoch  $\beta$  prechodov: i)  $\beta$  prechod spájajúci základný stav ( $0^+$ ) počiatočného jadra so základným stavom ( $1^+$ ) medzijadra a ii)  $\beta$  prechod spájajúci základný stav ( $1^+$ ) medzijadra so základným stavom ( $0^+$ ) koncového jadra. Predmetom nášho záujmu je skúmať platnosť SSD hypotézy pre  $2\nu\beta\beta$  rozpad jadra  $^{150}\text{Nd}$  s  $1^-$  základným stavom medzijadra  $^{150}\text{Sm}$ , nakoľko existencia nízko ležiacich  $1^+$  stavov jadra  $^{150}\text{Sm}$  nie je experimentálne vylúčená. To je možné pomocou diferenciálnych charakteristík, ktoré sú merané v experimente NEMO3.

V rámci odvodenia rozpadovej šírky dvojneutrínového dvojitého  $\beta$  rozpadu,  $(A, Z) \rightarrow (A, Z + 2) + 2e^- + 2\bar{\nu}$ , do  $0^+$  základného a  $2^+$  excitovaného stavu jadra sme vzali do úvahy  $s_{1/2}$  a  $p_{1/2}$  vlnu elektrónov a iba  $s_{1/2}$  vlnu neutrín. Tým môže byť tento prechod realizovaný iba cez  $0^+$ ,  $1^+$ ,  $0^-$  a  $1^-$  stavy medzijadra.

Zo známeho polčasu premeny  $\beta$  rozpadu medzijadra a hodnoty energie uvoľnenej v danej reakcii  $Q$  je možné určiť hodnotu maticového elementu tohto  $\beta$  prechodu nasledovne

$$|\langle 0^+ || \mathcal{O}(\mathcal{J}^\pi) || 1_i^\pm \rangle| = \sqrt{\frac{3D}{f_\beta(Z', E_i - E_f)T_{1/2}}}. \quad (6.64)$$

$D = (2\pi^3 \ln 2)/(G_\beta^2 m_e^5)$  je konštanta.  $f_\beta(Z', E_0)$  je integrál cez fázový priestor závislý na  $Q$  hodnote danej reakcie a  $T_{1/2}$  je polčas rozpadu. Operátory  $\mathcal{O}(\mathcal{J}^\pi)$  sú dané ako

$$\begin{aligned} \mathcal{O}(0^+) &= \sum_m \tau_m^+, & \mathcal{O}_k(1^+) &= g_A \sum_m \tau_m^+ (\vec{\sigma}_m)_k \\ \mathcal{O}(0^-) &= -g_A \left( \frac{\alpha Z'}{2} \right) \sum_m \tau_m^+ \left( \frac{\vec{x}_m \cdot \vec{\sigma}_m}{R} \right), \\ \mathcal{O}_k(1^-) &= \left( \frac{\alpha Z'}{2} \right) \sum_m \tau_m^+ \frac{1}{R} (\vec{x}_m - g_A \vec{x}_m \times \vec{\sigma}_m)_k. \end{aligned} \quad (6.65)$$

$Z'$  je protónové číslo koncového jadra a  $\alpha$  je konštanta jemnej štruktúry. Podobne pre elektrónový záchyt vieme určiť hodnotu  $\beta$  sily prechodu,  $B_{EC}^{(1\pm)} = |\langle 0_f^+ || \mathcal{O}(\mathcal{J}^\pi) || 1_i^\pm \rangle|^2$ , zo známeho polčasu

$$[T_{1/2}^{EC}(1_i^\pm \rightarrow 0_f^+)]^{-1} = \frac{m_e}{2\pi^3 \ln 2} (G_\beta m_e^2)^2 \frac{1}{2J_i + 1} B_{EC}^{(1\pm)} f_{EC-K_I, L_{II}}(Z, E_i - E_f). \quad (6.66)$$

Funckia  $f_{EC-K_I, L_{II}}(Z, E_i - E_f)$  zodpovedá integrálu cez fázový priestor. Z týchto hodnôt maticových elementov potom vieme určiť polčas  $2\nu\beta\beta$  rozpadu ako

$$\begin{aligned} \left(T_{1/2}^{2\nu-SSD}(0_f^+)\right)^{-1} &= \frac{m_e (G_\beta m_e^2)^4}{8\pi^7 \ln 2} I^{2\nu-SSD}(0_f^+) \\ &\quad \times |\langle 0_f^+ || \mathcal{O}(1^-) || 1^- \rangle|^2 |\langle 1^- || \mathcal{O}(1^-) || 0_i^+ \rangle|^2. \end{aligned} \quad (6.67)$$

$I^{2\nu-SSD}(0_f^+)$  je integrál cez fázový priestor emitovaných leptónov. Pre jadro  $^{150}\text{Nd}$  je hodnota polčasu  $2\nu\beta\beta$  rozpadu za predpokladu realizácie SSD hypotézy  $T_{1/2}^{2\nu-SSD}(0^+) = 4.02 \times 10^{24}r$ , pričom experimentálna hodnota je  $T_{1/2}^{2\nu-exp}(0^+) = 8.2 \times 10^{18}r$ . Z ich porovnania je očividné, že hypotéza SSD sa nerealizuje pre prípad  $2\nu\beta\beta$  rozpadu  $^{150}\text{Nd}$ .

V práci [74] bola vyslovená hypotéza dominancie vyšších stavov ( Higher States Dominance - HSD ), ktorá predpokladá, že dominantný vklad do maticového elementu pochádza z vyššie ležiacich  $1^+$  stavov.

Platnosť oboch hypotéz (SSD i HSD) je možné verifikovať pomocou spektra energie jedného elektrónu normalizovaného celkovou rozpadovou šírkou,

$$\mathcal{P}_{J_f^+}^{2\nu-N}(E_{e1}) = \frac{1}{\Gamma_{J_f^+}^{2\nu-N}} \frac{d\Gamma_{J_f^+}^{2\nu-N}}{dE_{e1}} \quad (N = SSD, HSD). \quad (6.68)$$

Výhodou tohto prístupu je, že v prípade SSD hypotézy je spektrum nezávislé na maticových elementov. V prípade hypotézy HSD zavedením aproximácie energetických menovateľov ( $E_{ei} + E_{\nu j} \approx (E_i - E_f)/2$ ,  $i, j = 1, 2$ ) sa stane normalizované spektrum nezávislé od jadrových maticových elementov. Pre prípad  $2\nu\beta\beta$  rozpadu jadra  $^{150}\text{Nd}$  za predpokladu SSD a HSD hypotéz je spektrum jedného elektrónu normalizované na jednotku znázornené na obr. (5.5).

# Štatistické vlastnosti neutrín v rámci dvojneutrínového dvojitého $\beta$ rozpadu

Predpoklad možného narušenia Pauliho vylučovacieho princípu bol už diskutovaný vo viacerých článkoch [80], no zatiaľ žiaden konzistentný mechanizmus nebol navrhnutý. Je možné, že vďaka unikátnym vlastnostiam neutrín (neutralita, veľmi nízka škála hmotností) je narušenie Pauliho princípu silnejšie v neutrínovom sektore ako v sektoroch ostatných častíc. Možnosť bozónových neutrín bola už študovaná v rámci astrofyzikálnych a kozmologických procesov [84, 85]. Dvojneutrínový dvojitý  $\beta$  rozpad je unikátny proces z toho hľadiska, že sa ho zúčastňujú dve neutrína. Skúmaním charakteristík  $2\nu\beta\beta$  rozpadu tak možno priamo študovať štatistické vlastnosti neutrín.

## Bozónové neutrína v $2\nu\beta\beta$ premene

Pre kreačné operátory neutrín zavedieme komutačné vzťahy ( $d^\dagger(k_{\nu 1})d^\dagger(k_{\nu 2}) = d^\dagger(k_{\nu 2})d^\dagger(k_{\nu 1})$ ), kým pre elektróny predpokladáme štandardné antikomutačné vzťahy ako pre fermióny.

Ukazuje sa, že zmena znamienka v komutačných vzťahoch sa prejaví do znamienka výrazov

$$\begin{aligned} K_m^{f,b} &= \frac{1}{E_m - E_i + E_{e1} + E_{\nu 1}} \pm \frac{1}{E_m - E_i + E_{e2} + E_{\nu 2}} \\ L_m^{f,b} &= \frac{1}{E_m - E_i + E_{e1} + E_{\nu 2}} \pm \frac{1}{E_m - E_i + E_{e2} + E_{\nu 1}}. \end{aligned} \quad (6.69)$$

Kombinácie  $\mathcal{K}_m^{f,b} + \mathcal{L}_m^{f,b}$  a  $\mathcal{K}_m^{f,b} - \mathcal{L}_m^{f,b}$  vstupujú do rozpadovej šírky  $2\nu\beta\beta$  premeny do základného  $0^+$  stavu koncového jadra. Pri  $2\nu\beta\beta$  premene do excitovaného  $2^+$  stavu vstupuje iba kombinácia  $\mathcal{K}_m^{f,b} - \mathcal{L}_m^{f,b}$  do rozpadovej šírky. Pre analýzu bozónového neutrína je vhodné zaviesť pomer rozpadových šírok pre bozónové a fermiónové neutrína  $r_0(J^\pi) \equiv \Gamma_b(J^\pi)/\Gamma_f(J^\pi)$  do základného ( $0^+$ ) a vzbudeného ( $2^+$ ) stavu koncového jadra.

Výhodou v rámci hypotézy SSD je to, že v danom pomere  $r_0$  sa maticové elementy  $\beta$  rozpadu a elektrónového záchytu medzijadra vykrátia. Preto je vhodné obrátiť pozornosť na jadro  $^{100}\text{Mo}$ , u ktorého je realizácia SSD hypotézy už potvrdená [94]. Pre  $2\nu\beta\beta$  rozpad  $^{100}\text{Mo}$  do základného  $0^+$  stavu dostávame

$$\begin{aligned} T_f^{1/2}(0_{g.s.}^+) &= 6.8 \times 10^{18} \text{ r} \\ T_b^{1/2}(0_{g.s.}^+) &= 8.9 \times 10^{19} \text{ r}. \end{aligned} \quad (6.70)$$

Tak máme  $r_0(0_{g.s.}^+) = 0.076$ . Pre prípad  $2\nu\beta\beta$  rozpad  $^{100}\text{Mo}$  do vzbudeného  $2^+$  stavu dostávame

$$\begin{aligned}
T_f^{1/2}(2_1^+) &= 1.7 \times 10^{23} \text{ r} \\
T_b^{1/2}(2_1^+) &= 2.4 \times 10^{22} \text{ r}.
\end{aligned}
\tag{6.71}$$

Dostaneme tak  $r_0(2_1^+) = 7.1$ . Rozdiel medzi fermiónovými a bozónovými neutrínami je najviac evidentný pri rozpade do  $2_1^+$  excitovaného stavu koncového jadra.

## 6.2 Prípado čiasočne bozónových neutrín v rámci $2\nu\beta\beta$ rozpadu

Pre prípad čiasočne bozónových neutrín píšeme neutrínový stav ako kombináciu fermiónového a bozónového neutrína  $|\nu\rangle = \cos\delta|f\rangle + \sin\delta|b\rangle$ . Amplitúda  $2\nu\beta\beta$  rozpadu,  $A_{2\beta} = \cos^2\chi A_f + \sin^2\chi A_b$ , je daná ako lineárna kombinácia amplitúdy  $2\nu\beta\beta$  rozpadu daná pre čiaso fermiónové a bozónové neutrína. Parameter  $\sin^2\chi$  vyjadruje veľkosť bozónovej komponenty neutrín. Rozpadová šírka je potom daná  $\Gamma_{tot} = \cos^4\chi\Gamma_f + \sin^4\chi\Gamma_b$ . Nie je tu interferencie medzi fermiónovou a bozónovou časťou. Dôvodom je fakt, že pri zámene dvoch nerozlíšiteľných častíc fermióny dávajú znamienko mínus, kým bozóny znamienko plus v danej amplitúde. Nakoľko však integrujeme cez fázoový priestor, každý antisymetrický člen voči zámene  $\nu_1 \leftrightarrow \nu_2$  vymizne. Preto nie je interferencia medzi fermiónovou a bozónovou časťou amplitúdy. Pre celkovú rozpadovú šírku  $2\nu\beta\beta$  premeny do základného aj vzbudeného stavu dostávame  $\Gamma_{tot}(J^\pi) = \cos^4\chi\Gamma_f(J^\pi) + \sin^4\chi\Gamma_b(J^\pi)$ .

Normalizovaná diferencálna rozpadová šírka je daná ako

$$P_{J^\pi} = \frac{d\Gamma_{tot}(J^\pi)}{\Gamma_{tot}(J^\pi)} = \frac{\cos^4\chi d\omega_f(J^\pi) + \sin^4\chi r_0(J^\pi)d\omega_b(J^\pi)}{\cos^4\chi + \sin^4\chi r_0(J^\pi)},
\tag{6.72}$$

kde  $d\omega_f(J^\pi) \equiv d\Gamma_f(J^\pi)/\Gamma_f(J^\pi)$  a  $d\omega_b(J^\pi) \equiv d\Gamma_b(J^\pi)/\Gamma_b(J^\pi)$ . Vidíme, že pomer  $r_0(J^\pi)$  váhuje bozónovú komponentu neutrín v diferencálnej rozpadovej šírke. To znamená, že pre veľké  $r_0$  stačí aj malá komponenta bozónových neutrín na to, aby sa prejavila v spektre.

Na obrázkoch (6.1,6.2) sú ilustrované sumárne energetické spektrum dvoch vyletujúcich elektrónov a energetické spektrum jedného vyletujúceho elektrónu za predpokladu realizácie hypotéz SSD i HSD pre čiaso fermiónové a čiaso bozónové neutrína do základného stavu ( $0^+$ ) koncového jadra. Ďalej, na obrázkoch (6.6,6.5) sú ilustrované sumárne energetické spektrum dvoch vyletujúcich elektrónov a energetické spektrum jedného vyletujúceho elektrónu za predpokladu realizácie SSD hypotézy do excitovaného stavu ( $2_1^+$ ) koncového jadra pre prípad čiasočne bozónových neutrín.

Efekt bozónového neutrína je slabo závislý na voľbe danej hypotézy (SSD/HSD) a prejavuje sa v spektre elektrónov tým, že maximum sa posúva k nižším hodnotám.

## Ohraničenia na bozónovú komponentu neutrín

Existujú tri rôzne spôsoby akými môžeme získať ohraničenie na bozónovú komponentu neutrín ( $\sin^2 \chi$ ). Prvý spôsob je porovnanie teoreticky určeného polčasu rozpadu s experimentálne nameraným. Horné ohraničenie je

$$\sin^2 \chi < (1 - \sqrt{T_{1/2}^{f-min} / T_{1/2}^{exp-max}}). \quad (6.73)$$

$T_{1/2}^{f-min}$  je minimálna teoreticky určená hranica pre polčas a  $T_{1/2}^{exp-max}$  je maximálna hodnota, ktorá je experimentálne nameraná. Toto ohraničenie platí za predpokladu  $r_0 \ll 1$ , čo je však veľmi dobre splnené pre prechody  $0^+ \rightarrow 0^+$ . Nevýhoda je potreba výpočtu jadrových maticových elementov.

Pre prípad  $^{100}Mo$  a  $^{116}Cd$  je možné určiť polčasy zo známych *logft* hodnôt v rámci hypotézy SSD. Získané ohraničenia sú  $\sin^2 \chi < 0.34$  ( $^{100}Mo$ ) a  $\sin^2 \chi < 0.06$  ( $^{116}Cd$ ).

Ďalšou možnosťou je zaviesť  $\sin^2 \chi$  ako fitovací parameter, t.j. určiť jeho hodnotu pomocou dostupných dát zo spektier energie jedného elektrónu a sumárnej energie oboch elektrónov. Táto metóda je vhodná pre veľké  $r_0$ . Z dostupných dát (NEMO3) plynie ohraničenie  $\sin^2 \chi < 0.7$  [92], t.j. prípad čisto bozónového neutrína je vylúčený.

Tretia možnosť je definovať pomer polčasov rozpadov do excitovaného a základného stavu

$$r_{f,b}^*(J^\pi) \equiv \frac{T_{1/2}^{f,b}(J^\pi)}{T_{1/2}^{f,b}(0^+)} \quad (6.74)$$

separátne pre fermiónové a bozónové neutrína. Za predpokladu SSD hypotézy pre  $^{100}Mo$  máme

$$\begin{aligned} r_f^*(0_1^+) &\simeq 61 \\ r_b^*(0_1^+) &\simeq 73. \end{aligned} \quad (6.75)$$

Prechod do  $0_1^+$  bol nameraný experimentom NEMO 3 [89, 90] a teda  $r_{exp}^*(0_1^+) \simeq 80$ . Na prvý pohľad sa zdá, že bozónové neutrína lepšie vyhovujú experimentálnym dátam. Rozdiel môže byť zapríčinený samotným predpokladom SSD hypotézy.

Prechod do  $2_1^+$  stavu sa javí byť vhodnejším nástrojom na štúdium bozónových neutrín. Za predpokladu SSD hypotézy pre  $^{100}Mo$  máme

$$\begin{aligned} r_f^*(2_1^+) &\simeq 2.5 \times 10^4 \\ r_b^*(2_1^+) &\simeq 2.7 \times 10^2. \end{aligned} \quad (6.76)$$

Pre  $2\nu\beta\beta$  rozpad jadra  $^{100}\text{Mo}$  do  $2_1^+$  stavu existuje iba dolné ohraničenie na polčas rozpadu [94], s ktorým dostaneme  $r_{exp}^*(2_1^+) > 2.2 \times 10^2$ . Súčasná experimentálna hodnota je teda blízko prahu vylúčenia čisto bozónových neutrín. Progres v meraní  $2\nu\beta\beta$  rozpadu jadra  $^{100}\text{Mo}$  do  $2_1^+$  stavu koncového jadra by umožnil urobiť závery aj pre prípad čiastočne bozónového neutrína.

## Záver

V danej práci boli diskutované fundamentálne vlastnosti neutrín. Menovite absolútna škála hmotností neutrín a narušenie Pauliho vylučovacieho princípu pre neutrína v kontexte obyčajného a dvojitého  $\beta$  rozpadu. Originálne výsledky, ktoré boli prezentované v danej práci zazneli na viacerých medzinárodných konferenciách a workshopoch a taktiež boli opublikované v zahraničných karentovaných žurnáloch. Dané výsledky a zistenia sú dôležité pre tríciový experiment KATRIN, ktorý je vo fáze spúšťania a pre plánovaný experiment merajúci réniový  $\beta$  rozpad MARE, ako aj pre pripravované experimenty merajúce dvojité  $\beta$  rozpad ako napr. SuperNEMO, EXO, SNO+ a pod.

# Appendix A

## Phase space integrals evaluation within the relativistic treatment of tritium $\beta$ -decay

We present here details of calculation of the phase space integrals necessary for the electron energy spectrum in tritium  $\beta$ -decay. We recall the integrals that need to be calculated.

$$\begin{aligned}\mathcal{K} &= \int \frac{d^3 p_f}{E_f} \frac{d^3 p_\nu}{E_\nu} \delta^{(4)}(Q - P_f - P_\nu) \\ (\mathcal{L}_\nu)^\rho &= \int \frac{d^3 p_f}{E_f} \frac{d^3 p_\nu}{E_\nu} \delta^{(4)}(Q - P_f - P_\nu) (P_\nu)^\rho \\ (\mathcal{N}_{\nu f})^{\rho\sigma} &= \int \frac{d^3 p_f}{E_f} \frac{d^3 p_\nu}{E_\nu} \delta^{(4)}(Q - P_f - P_\nu) (P_\nu)^\rho (P_f)^\sigma, \end{aligned} \quad (\text{A.1})$$

with  $Q = P_i - P_e$ . The notation is the same as in sec. 3.2.

### Integration of $\mathcal{K}$

The integral is indeed a scalar function of the four-momentum  $Q$ . Most apparent scalar consisting of four-momentum  $Q$  is  $Q^2$ . Then the Lorentz invariance of  $Q^2$  allow us to perform the calculation in a particular frame, where  $Q = (Q_0, \mathbf{0})$ , i.e., the rest frame associated with the center of mass of the system containing the final nucleus and the antineutrino.



$$\begin{aligned}
\mathcal{K} &= \int \int \frac{d^3 p_f}{E_f} \frac{d^3 p_\nu}{E_\nu} \delta^{(4)}(Q - P_f - P_\nu) \\
&= \int dE_f d\Omega_f \frac{1}{E_\nu} \delta(Q_0 - E_f - E_\nu) p_f
\end{aligned} \tag{A.2}$$

Here, for the energy of neutrino we have  $E_\nu = \sqrt{m_\nu^2 + E_f^2 - M_f^2}$ . We shall take the advantage of the expression

$$\delta(f(x)) = \frac{\delta(x - x_0)}{|f'(x_0)|}. \tag{A.3}$$

For the sake of simplicity here we assume that function  $f(x)$  has only one zero-point, i.e. the  $x_0$ , what is for the case of tritium  $\beta$ -decay true so far. Then we have

$$\left| \frac{\partial(Q_0 - E_\nu - E_f)}{\partial E_f} \right| = \left| \frac{-E_f}{E_\nu} - 1 \right| = \frac{Q_0}{E_\nu}. \tag{A.4}$$

The argument of the delta function is zero for

$$E_f^0 = (Q_0^2 + M_f^2 - m_\nu^2)/(2Q_0). \tag{A.5}$$

For the  $\mathcal{K}$  integral we get

$$\begin{aligned}
\mathcal{K} &= 4\pi \int dE_f \frac{\sqrt{E_f^2 - M_f^2}}{E_\nu} \frac{E_\nu}{Q_0} \delta(E_f - E_f^0) \\
&= 2\pi \frac{\sqrt{[Q_0^2 - (M_f + m_\nu)^2][Q_0^2 - (M_f - m_\nu)^2]}}{Q_0^2}
\end{aligned} \tag{A.6}$$

Taking the advantage of Lorentz invariance of the  $\mathcal{K}$  integral we may replace  $Q_0^2$  with  $Q^2$  and get the integral in general form

$$\mathcal{K} = 2\pi \frac{\sqrt{[Q^2 - (M_f + m_\nu)^2][Q^2 - (M_f - m_\nu)^2]}}{Q^2}. \tag{A.7}$$

We notice that in the laboratory frame, which is the subject of choice for almost all cases,  $Q^2 = M_i^2 + m_e^2 - 2E_e M_i$ .

## Integration of $\mathcal{L}_\nu^\rho$

We consider the integral

$$(\mathcal{L}_\nu)^\rho = \int \frac{d^3 p_f}{E_f} \frac{d^3 p_\nu}{E_\nu} \delta^{(4)}(Q - P_f - P_\nu) (P_\nu)^\rho \quad (\text{A.8})$$

as a vector function of the four-momentum  $Q$  that may be written in a general way as

$$\mathcal{L}_\nu^\rho = B Q^\rho, \quad (\text{A.9})$$

where the function  $B = B(Q^2)$  might be the scalar function of the  $Q$  at most. By multiplying  $(\mathcal{L}_\nu)^\rho$  with  $Q_\rho$  we get

$$B Q^2 = \int \frac{d^3 p_f}{E_f} \frac{d^3 p_\nu}{E_\nu} (P_\nu \cdot Q) \delta^{(4)}(Q - P_f - P_\nu). \quad (\text{A.10})$$

The scalar product  $(P_f \cdot Q)$  we evaluate using the four-momentum conservation law.

$$\begin{aligned} P_f^2 &= (Q - P_\nu)^2 \\ M_f^2 &= Q^2 - 2(P_\nu \cdot Q) + m_\nu^2 \\ (P_\nu \cdot Q) &= \frac{1}{2}[Q^2 + m_\nu^2 - M_f^2]. \end{aligned} \quad (\text{A.11})$$

Then we have

$$\begin{aligned} B Q^2 &= \frac{1}{2}[Q^2 + m_\nu^2 - M_f^2] \int \frac{d^3 p_f}{E_f} \frac{d^3 p_\nu}{E_\nu} \delta^{(4)}(Q - P_f - P_\nu) \\ &= \frac{1}{2}[Q^2 + m_\nu^2 - M_f^2] \mathcal{K}. \end{aligned} \quad (\text{A.12})$$

Eventually, we have

$$\begin{aligned} (\mathcal{L}_\nu)^\rho &= \frac{(Q \cdot P_f)}{Q^2} \mathcal{K} Q^\rho \\ &= \frac{(Q^2 + m_\nu^2 - M_f^2)}{2Q^2} \mathcal{K} Q^\rho. \end{aligned} \quad (\text{A.13})$$

## Integration of $\mathcal{N}_{\nu f}^{\rho\sigma}$

The integral

$$(\mathcal{N}_{\nu f})^{\rho\sigma} = \int \frac{d^3 p_f}{E_f} \frac{d^3 p_\nu}{E_\nu} \delta^{(4)}(Q - P_f - P_\nu) (P_\nu)^\rho (P_f)^\sigma \quad (\text{A.14})$$

takes the form of the second rank tensor. We may express the integral with the use of  $Q$  vector as follows

$$(\mathcal{N}_{\nu f})^{\rho\sigma} = C g^{\rho\sigma} + D Q^\rho Q^\sigma, \quad (\text{A.15})$$

where  $C = C(Q^2)$  and  $D = D(Q^2)$  are scalar functions of  $Q^2$  at most. By multiplying  $\mathcal{N}^{\rho\sigma}$  with the metric tensor  $g_{\rho\sigma}$  we get

$$4C + DQ^2 = (P_\nu \cdot P_f) \mathcal{K}. \quad (\text{A.16})$$

By multiplying  $\mathcal{N}^{\rho\sigma}$  with  $Q_\rho Q_\sigma$  we find

$$CQ^2 + DQ^2Q^2 = (Q \cdot P_\nu) (Q \cdot P_f) \mathcal{K}. \quad (\text{A.17})$$

By solving the set of these two equations we find

$$\begin{aligned} C &= \frac{1}{3} \left( (P_\nu \cdot P_f) - \frac{(Q \cdot P_\nu) (Q \cdot P_f)}{Q^2} \right) \mathcal{K} \\ D &= -\frac{1}{3Q^2} \left( (P_\nu \cdot P_f) - 4 \frac{(Q \cdot P_\nu) (Q \cdot P_f)}{Q^2} \right) \mathcal{K} \end{aligned} \quad (\text{A.18})$$

The integral  $(\mathcal{N}_{\nu f})^{\rho\sigma}$  then takes the form

$$\begin{aligned} (\mathcal{N}_{\nu f})^{\rho\sigma} &= \frac{1}{3} \left( (P_\nu \cdot P_f) - \frac{(Q \cdot P_\nu) (Q \cdot P_f)}{Q^2} \right) \mathcal{K} g^{\rho\sigma} \\ &\quad - \frac{1}{3} \left( (P_\nu \cdot P_f) - 4 \frac{(Q \cdot P_\nu) (Q \cdot P_f)}{Q^2} \right) \mathcal{K} \frac{Q^\rho Q^\sigma}{Q^2}. \end{aligned} \quad (\text{A.19})$$

## Scalar products of four-momenta

Eventually, we need to evaluate the scalar products of four-momenta of particles involved in the tritium  $\beta$ -decay. They are given as follows:

$$\begin{aligned}
 Q^2 &= M_i^2 + m_e^2 - 2M_i E_e \equiv (m_{12})^2 \\
 Q^2 &= (P_i - P_e)^2 = M_i^2 + m_e^2 - 2(P_e \cdot P_i) \\
 P_{ei} &= (P_e \cdot P_i) = \frac{1}{2}[M_i^2 + m_e^2 - Q^2] = M_i E_e
 \end{aligned} \tag{A.20}$$

$$\begin{aligned}
 Q^2 &= M_i^2 + m_e^2 - 2M_i E_e \\
 &= 2(E_e^{max} - E_e)M_i + M_i^2 + m_e^2 - 2M_i E_e^{max} \\
 &= 2yM_i + (M_f + m_\nu)^2
 \end{aligned} \tag{A.21}$$

$$\begin{aligned}
 Q^2 &= (P_f + P_\nu)^2 = M_f^2 + m_\nu^2 + 2(P_f \cdot P_\nu) \\
 P_{\nu f} &= (P_f \cdot P_\nu) = \frac{1}{2}[Q^2 - M_f^2 - m_\nu^2] = M_i \left( y + \frac{m_\nu M_f}{M_i} \right)
 \end{aligned} \tag{A.22}$$

$$\begin{aligned}
 P_{Qi} &= (Q \cdot P_i) = (P_i \cdot P_i) - (P_e \cdot P_i) = M_i^2 - \frac{1}{2}[M_i^2 + m_e^2 - Q^2] \\
 &= \frac{1}{2}[Q^2 + M_i^2 - m_e^2] = M_i(M_i - E_e).
 \end{aligned} \tag{A.23}$$

$$\begin{aligned}
 P_{Qe} &= (Q \cdot P_e) = (P_i \cdot P_e) - (P_e \cdot P_e) = \frac{1}{2}[M_i^2 + m_e^2 - Q^2] - m_e^2 \\
 &= \frac{1}{2}[M_i^2 - m_e^2 - Q^2] = M_i E_e - m_e^2
 \end{aligned} \tag{A.24}$$

$$\begin{aligned}
 P_{Q\nu} &= (Q \cdot P_\nu) = (P_f \cdot P_\nu) + (P_\nu \cdot P_\nu) = \frac{1}{2}[Q^2 - M_f^2 - m_\nu^2] + m_\nu^2 \\
 &= \frac{1}{2}[Q^2 - M_f^2 + m_\nu^2] = M_i \left( y + \frac{m_\nu(M_f + m_\nu)}{M_i} \right)
 \end{aligned} \tag{A.25}$$

$$\begin{aligned}
 P_{Qf} &= (Q \cdot P_f) = (P_f \cdot P_f) + (P_\nu \cdot P_f) = M_f^2 + \frac{1}{2}[Q^2 - M_f^2 - m_\nu^2] \\
 &= \frac{1}{2}[Q^2 + M_f^2 - m_\nu^2] = M_i \left( y + \frac{M_f(M_f + m_\nu)}{M_i} \right)
 \end{aligned} \tag{A.26}$$

$$\begin{aligned}
(P_e \cdot \mathcal{L}_\nu) &= \frac{(Q^2 + m_\nu^2 - M_f^2)}{2Q^2} (Q \cdot P_e) \mathcal{K} \\
&= \frac{M_i(M_i E_e - m_e^2)}{(m_{12})^2} \left( y + \frac{m_\nu(M_f + m_\nu)}{M_i} \right) \mathcal{K}
\end{aligned} \tag{A.27}$$

$$\begin{aligned}
P_e^\rho P_i^\sigma (\mathcal{N}_{\nu f})_{\rho\sigma} &= \frac{1}{3} \left( (P_\nu \cdot P_f) - \frac{(Q \cdot P_\nu)(Q \cdot P_f)}{Q^2} \right) \mathcal{K} (P_e \cdot P_i) \\
&\quad - \frac{1}{3} \left( (P_\nu \cdot P_f) - 4 \frac{(Q \cdot P_\nu)(Q \cdot P_f)}{Q^2} \right) \mathcal{K} \frac{(Q \cdot P_e)(Q \cdot P_i)}{Q^2}.
\end{aligned} \tag{A.28}$$

We simplify with result

$$\begin{aligned}
P_e^\rho P_i^\sigma (\mathcal{N}_{\nu f})_{\rho\sigma} &= \frac{\mathcal{K}}{3Q^2Q^2} \left( (P_\nu \cdot P_f) Q^2 - (Q \cdot P_\nu)(Q \cdot P_f) \right) \left( (P_e \cdot P_i) Q^2 - (Q \cdot P_e)(Q \cdot P_i) \right) \\
&\quad + \frac{\mathcal{K}}{Q^2Q^2} (Q \cdot P_e)(Q \cdot P_i)(Q \cdot P_\nu)(Q \cdot P_f) \\
&= \frac{\mathcal{K}}{3(m_{12}^2)^2} M_i^2 (m_e^2 - E_e^2) M_i^2 y \left( y + \frac{m_\nu M_f}{M_i} \right) \\
&\quad + \frac{\mathcal{K}}{(m_{12}^2)^2} (M_i E_e - m_e^2) (M_i^2 - M_i E_e) M_i \left( y + \frac{m_\nu(M_f + m_\nu)}{M_i} \right) \\
&\quad \times (y M_i + M_f(M_f + m_\nu))
\end{aligned} \tag{A.29}$$

# Appendix B

## Distorted relativistic electron wave function with Coulomb field

The creation of electron and antineutrino takes place simultaneously in the bulk of the nucleus in the nuclear  $\beta$ -decay. Unlike the antineutrino, the electron carries an electric charge. It is worth to mention that the Coulombic interaction between the electron and the final nucleus is not negligible in the  $\beta$ -decay. The electron wave function is distorted in presence of the electromagnetic field of the final nucleus and the overlap of the electron wave function with the bulk of the nucleus is enhanced.

For the emphasis of nuclear  $\beta$ -decay description, it is very convenient to expand the electron wave function into the terms of partial waves. A few terms are presented explicitly.

The electron wave function is expanded into spherical waves

$$\Psi(E, \vec{r}) = \Psi_S(E, \vec{r}) + \Psi_P(E, \vec{r}) + \Psi_D(E, \vec{r}) + \dots \quad (\text{B.1})$$

in similarity with atomic physics notation of  $S$ ,  $P$  and  $D$  being the electron wave functions with orbital angular momentum  $l = 0$ ,  $l = 1$  and  $l = 2$ , respectively.

We recall that a free spin 1/2 particle is described by the Dirac equation

$$(-i\gamma^\mu \partial_\mu + m)\Psi(p, r) = 0, \quad (\text{B.2})$$

where the solutions are given as

$$\Psi_s(p, r) = u_s(p)e^{ipr}, \quad u_s(p) = \sqrt{\frac{E+m}{2E}} \begin{pmatrix} \chi_s \\ \frac{\vec{p} \cdot \vec{\sigma}}{E+m} \chi_s \end{pmatrix}. \quad (\text{B.3})$$

Here,  $u_s(p)$  denotes the Dirac spinor with four-momentum  $p$  and spin projection  $s$ . However, in order to describe the real situation we have to take into account the Coulomb interaction between the emitted electron and final nucleus.

$$(-i\gamma^\mu\partial_\mu + m + e\gamma^\mu A_\mu)\Psi(p, r) = 0. \quad (\text{B.4})$$

The electromagnetic four-potential takes the form  $A_\mu = (V(\vec{r}), \vec{0})$  in the frame associated with the final nucleus with  $V(\vec{r})$  being the Coulomb potential of final nucleus. For the purpose of our calculations presented in this thesis we assume the electric charge distribution inside the nucleus to be of the homogenous form

$$V(r) = \begin{cases} -(\frac{\alpha Z}{2R})(3 - (\frac{r}{R})^2) & r < R \\ -\frac{\alpha Z}{r} & r \geq R \end{cases} \quad (\text{B.5})$$

$R$  stands for the nuclear radius  $R = 1.1A^{1/3} fm$  and  $\alpha = 1/137$  is the fine structure constant. We adopt here the approach from [95] to find solutions of the equation (B.4) in a form

$$\Psi_s(p, r) = \sum_{\kappa, \mu} a_{\kappa\mu}(\hat{p}, s)\Psi_{\kappa\mu}(p, r). \quad (\text{B.6})$$

Here,  $\kappa$  denotes the principal quantum number of the total angular momentum of electron that consists from the orbital angular momentum  $l$  and spin  $s(= 1/2)$  and  $\mu$  is the  $z$ -th component of this total angular momentum.  $\kappa$  is defined as

$$\kappa = \begin{cases} l & j = l - 1/2 \\ -l - 1 & j = l + 1/2 \end{cases} \quad (\text{B.7})$$

We see that  $\kappa$  takes either positive or negative integers. In the notation familiar to the atomic physics we have  $\kappa = -1, 1, -2, 2, \dots(s_{1/2}, p_{1/2}, p_{3/2}, d_{3/2}, \dots)$ .

Partial wave functions are defined as

$$\Psi_{\kappa\mu}(p, r) = \begin{pmatrix} \tilde{g}_\kappa(E, r)\chi_{\kappa\mu}(\hat{r}) \\ i\tilde{f}_\kappa(E, r)\chi_{-\kappa\mu}(\hat{r}) \end{pmatrix}. \quad (\text{B.8})$$

The weight factor  $a_{\kappa\mu}(\hat{p}, s)$  in (B.6) describes the electron with certain four-momentum  $\hat{p}$  and polarization  $s$ . We mention that for the limit case  $r \rightarrow \infty$  for the weight factor holds

$$a_{\kappa\mu}(\hat{p}, s) = 4\pi i^{l_\kappa} C(l_\kappa, \frac{1}{2}, j_\kappa; \mu - s, s) Y_{l_\kappa}^{\mu-s}(\hat{p}). \quad (\text{B.9})$$

The angular part of the electron wave function is expressed as

$$\chi_{\kappa\mu}(\hat{r}) = \sum_{\sigma=\pm 1/2} C(l_\kappa, \frac{1}{2}, j_\kappa; \mu - \sigma, \sigma) Y_{l_\kappa}^{\mu-\sigma}(\hat{r}) \chi_\sigma. \quad (\text{B.10})$$

Here,  $\chi_\sigma$  is the two-component Pauli spinor with polarization  $\sigma$  and  $Y_{l_\kappa}^{\mu-\sigma}$  are the spherical harmonics.

Modified radial functions are given by

$$\begin{pmatrix} \tilde{g}_\kappa(E, r) \\ \tilde{f}_\kappa(E, r) \end{pmatrix} = e^{-i\Delta_\kappa^C} \begin{pmatrix} g_\kappa(E, r) \\ f_\kappa(E, r) \end{pmatrix}. \quad (\text{B.11})$$

The overall phase shift  $e^{-i\Delta_\kappa^C}$  is introduced for the sake of the fulfilling the boundary condition at  $r \rightarrow \infty$  and in our calculations can be omitted ( $e^{-i\Delta_\kappa^C} = 1$ ). The subject of our interest is the radial wave functions near the origin, therefore we may express them in terms of power series

$$\begin{aligned} \begin{pmatrix} g_\kappa(E, r) \\ f_\kappa(E, r) \end{pmatrix} &= A_\kappa \begin{pmatrix} g_\kappa^{(i)}(E, r) \\ f_\kappa^{(i)}(E, r) \end{pmatrix} = \\ &= A_\kappa \frac{(pr)^{k-1}}{(2k-1)!!} \sum_{l=0}^{\infty} \begin{pmatrix} b_{\kappa,l} \\ a_{\kappa,l} \end{pmatrix} \left(\frac{r}{R}\right)^l. \end{aligned} \quad (\text{B.12})$$

Here, the coefficients  $a_{\kappa,l}, b_{\kappa,l}$  are the same as in [95]. The constants of normalization are evaluated from the continuity condition at  $r = R$  and are estimated up to terms of  $(\alpha Z)^2$  as

$$\tilde{A}_{\pm k} \cong \sqrt{\frac{E \pm m}{2E}} \sqrt{F_{k-1}(Z, E)}, \quad (\text{B.13})$$

where  $k = 1, 2, \dots$  and the Fermi functions  $F_{k-1}(Z, E)$  are given by

$$F_{k-1}(Z, E) = \left[ \frac{\Gamma(2k+1)}{\Gamma(k)\Gamma(2\gamma_k+1)} \right]^2 (2pR)^{2(\gamma_k-k)} |\Gamma(\gamma_k + iy)|^2 e^{\pi y}. \quad (\text{B.14})$$

Here,  $\gamma_k = \sqrt{k^2 - (\alpha Z)^2}$  and  $y = \alpha Z E / p$ .

For the purpose of our calculations we shall rewrite the expansion (B.1) as



$$\Psi(E, \vec{r}) = \Psi_{s_{1/2}}(E, \vec{r}) + \Psi_{p_{1/2}}(E, \vec{r}) + \Psi_{p_{3/2}}(E, \vec{r}) + \dots \quad (\text{B.15})$$

It is worth to note that particular terms of expansion correspond to the situation when spin  $s(= 1/2)$  is parallel or antiparallel with respect to the orbital angular momentum  $l$ . This turns out to be an advantage in the derivation of the decay rate of forbidden  $\beta$ -decays when the change of spin and parity between the initial and final nuclei has to be carried out by leptons. The fact, whether the individual term from the expansion (B.15) contribute to the decay rate or not, is easily seen from the selection rules for the change of angular momentum and parity in  $\beta$ -decay.

For the purpose of our calculation it is sufficient to have an explicit form of the electron wave function expanded up to the  $d_{5/2}$ -wave of electrons. From [95] we have

$$\Psi_S = \begin{pmatrix} \tilde{g}_{-1}\chi_s \\ \vec{\sigma}\cdot\hat{p} \tilde{f}_1\chi_s \end{pmatrix}, \quad (\text{B.16})$$

$$\Psi_P = i \begin{pmatrix} (\tilde{g}_1(\vec{\sigma}\cdot\hat{r})(\vec{\sigma}\cdot\hat{p}) + \tilde{g}_{-2}[3(\hat{r}\cdot\hat{p}) - (\vec{\sigma}\cdot\hat{r})(\vec{\sigma}\cdot\hat{p})])\chi_s \\ (-\tilde{f}_{-1}(\vec{\sigma}\cdot\hat{r}) + \tilde{f}_2[3(\hat{r}\cdot\hat{p})(\vec{\sigma}\cdot\hat{p}) - (\vec{\sigma}\cdot\hat{r})])\chi_s \end{pmatrix}, \quad (\text{B.17})$$

$$\begin{aligned} \Psi_D = & - \begin{pmatrix} g_{+2} & [+3(\hat{p}\cdot\hat{r})(\vec{\sigma}\cdot\hat{r})(\vec{\sigma}\cdot\hat{p}) - 1] \chi_s \\ f_{-2} & [-3(\hat{p}\cdot\hat{r})(\vec{\sigma}\cdot\hat{r}) + (\vec{\sigma}\cdot\hat{p})] \chi_s \end{pmatrix} \\ & + \begin{pmatrix} g_{-3} & [-\frac{15}{2}(\hat{p}\cdot\hat{r})^2 + 3(\hat{p}\cdot\hat{r})(\vec{\sigma}\cdot\hat{r})(\vec{\sigma}\cdot\hat{p}) - 1] \chi_s \\ f_{+3} & [-\frac{15}{2}(\hat{p}\cdot\hat{r})^2(\vec{\sigma}\cdot\hat{p}) + 3(\hat{p}\cdot\hat{r})(\vec{\sigma}\cdot\hat{r}) - (\vec{\sigma}\cdot\hat{p})] \chi_s \end{pmatrix}. \end{aligned} \quad (\text{B.18})$$

In order to have more convenient form of the electron wave function, i.e. expressed in terms of the Dirac spinors, it is necessary to do some algebra. After calculation for the electron wave functions we get

$$\begin{aligned} \Psi_{s_{1/2}} &= \begin{pmatrix} \tilde{g}_{-1}\chi_s \\ \vec{\sigma}\cdot\hat{p} \tilde{f}_1\chi_s \end{pmatrix} \\ &= \sqrt{F_0(Z, E)} u_s(p), \end{aligned} \quad (\text{B.19})$$

$$\begin{aligned} \Psi_{p_{1/2}} &= i \begin{pmatrix} \tilde{g}_1(\vec{\sigma}\cdot\hat{r})(\vec{\sigma}\cdot\hat{p})\chi_s \\ -\tilde{f}_{-1}(\vec{\sigma}\cdot\hat{r})\chi_s \end{pmatrix} \\ &= i \frac{\alpha Z}{2} \frac{r}{R} \sqrt{F_0(Z, E)} \gamma_0 \vec{\gamma}\cdot\hat{r} u_s(p), \end{aligned} \quad (\text{B.20})$$

$$\begin{aligned}
\Psi_{p3/2} &= i \begin{pmatrix} \tilde{g}_{-2}[3(\hat{r}\cdot\hat{p}) - (\vec{\sigma}\cdot\hat{r})(\vec{\sigma}\cdot\hat{p})]\chi_s \\ \tilde{f}_2[3(\hat{r}\cdot\hat{p})(\vec{\sigma}\cdot\hat{p}) - (\vec{\sigma}\cdot\hat{r})]\chi_s \end{pmatrix} \\
&= i\sqrt{F_1(Z, E)} \left( \vec{r}\cdot\vec{p} + \frac{1}{3}(\vec{\gamma}\cdot\vec{r})(\vec{\gamma}\cdot\vec{p}) \right) u_s(p),
\end{aligned} \tag{B.21}$$

$$\begin{aligned}
\Psi_{d3/2} &= - \begin{pmatrix} g_{+2} [ +3(\hat{p}\cdot\hat{r})(\vec{\sigma}\cdot\hat{r})(\vec{\sigma}\cdot\hat{p}) - 1 ] \chi_s \\ f_{-2} [ -3(\hat{p}\cdot\hat{r})(\vec{\sigma}\cdot\hat{r}) + (\vec{\sigma}\cdot\hat{p}) ] \chi_s \end{pmatrix} \\
&= \frac{1}{5}\sqrt{F_1} \left[ (\vec{p}\cdot\vec{r})(\vec{\gamma}\cdot\vec{r})(\vec{\gamma}\cdot\vec{p}) - (\vec{p}\cdot\vec{r}) \frac{3}{2}\alpha Z\gamma^0 \left( \vec{\gamma}\cdot\frac{\vec{r}}{R} \right) \right. \\
&\quad \left. + \frac{(pr)^2}{3} + \frac{1}{3} \frac{r^2}{R} \frac{3}{2}\alpha Z\gamma^0 (\vec{\gamma}\cdot\vec{p}) \right] u_s(p),
\end{aligned} \tag{B.22}$$

$$\begin{aligned}
\Psi_{d5/2} &= \begin{pmatrix} g_{-3} \left[ -\frac{15}{2}(\hat{p}\cdot\hat{r})^2 + 3(\hat{p}\cdot\hat{r})(\vec{\sigma}\cdot\hat{r})(\vec{\sigma}\cdot\hat{p}) - 1 \right] \chi_s \\ f_{+3} \left[ -\frac{15}{2}(\hat{p}\cdot\hat{r})^2(\vec{\sigma}\cdot\hat{p}) + 3(\hat{p}\cdot\hat{r})(\vec{\sigma}\cdot\hat{r}) - (\vec{\sigma}\cdot\hat{p}) \right] \chi_s \end{pmatrix} \\
&= -\sqrt{F_2} \left[ \frac{(\vec{p}\cdot\vec{r})^2}{2} + \frac{(pr)^2}{15} + \frac{1}{5}(\vec{p}\cdot\vec{r})(\vec{\gamma}\cdot\vec{r})(\vec{\gamma}\cdot\vec{p}) \right] u_s(p).
\end{aligned} \tag{B.23}$$

# Appendix C

## Fierz transformation

The Fierz transformation is presented here. The aim of the Fierz transformation is to recouple the electron and neutrino wave functions together in order to make the calculation of traces easier and more transparent. We assume the expression to be in following form,

$$\bar{\Psi}(p_{e1}, \vec{x}) \gamma_\mu (1 - \gamma_5) \Phi^c(k_{\nu1}, \vec{x}) \cdot \bar{\Psi}(p_{e2}, \vec{y}) \gamma_\nu (1 - \gamma_5) \Phi^c(k_{\nu2}, \vec{y}). \quad (\text{C.1})$$

Here, the following term,

$$\bar{\Psi}(p_{e1}, \vec{x}) \gamma_\mu (1 - \gamma_5) \Phi^c(k_{\nu1}, \vec{x}) \cdot \bar{\Phi}(k_{\nu2}, \vec{y}) \gamma_\nu (1 + \gamma_5) \Psi^c(p_{e2}, \vec{y}), \quad (\text{C.2})$$

is expressed in scalar components in the form,

$$(\bar{\Psi}(p_{e1}, \vec{x}))_{\rho'} (\gamma_\mu (1 - \gamma_5))_{\rho' \rho} (\Phi^c(k_{\nu1}, \vec{x}))_\rho \cdot (\bar{\Phi}(k_{\nu2}, \vec{y}))_{\sigma'} (\gamma_\nu (1 + \gamma_5))_{\sigma' \sigma} (\Psi^c(p_{e2}, \vec{y}))_\sigma. \quad (\text{C.3})$$

For the sake of simplicity we establish the matrix notation

$$\begin{aligned} A_{\rho' \rho} &= (\gamma_\mu (1 - \gamma_5))_{\rho' \rho} \\ B_{\sigma' \sigma} &= (\gamma_\nu (1 + \gamma_5))_{\sigma' \sigma}. \end{aligned} \quad (\text{C.4})$$

Here, we expand the matrices  $A, B$  into the complete set of unitary matrices  $O^i$ .

$$A_{\rho' \rho} B_{\sigma' \sigma} = \sum_{i,j} a_{ij} O_{\rho' \sigma}^i O_{\sigma' \rho}^j \quad (\text{C.5})$$

Multiplying the equation by  $O_{\sigma\rho}^i O_{\rho\sigma'}^j$ , we obtain for the coefficients  $a_{ij}$  the following,

$$a_{ij} = \frac{Tr A O^j B O^i}{Tr(O^i)^2(O^j)^2}. \quad (C.6)$$

For the special case of our interest, i.e.  $A = \gamma_\mu(1 - \gamma_5)$  and  $B = \gamma_\nu(1 + \gamma_5)$ , the non-zero contribution give only the terms:

$$\begin{array}{ccc} a_{ij} & O_{\rho'\sigma}^i & O_{\sigma'\rho}^j \\ 1/2 & (1 + \gamma_5) & \gamma_\nu \gamma_\mu (1 - \gamma_5) \\ 1/8 & \sigma_{\alpha\beta} (1 + \gamma_5) & \gamma_\nu \sigma_{\alpha\beta} \gamma_\mu (1 - \gamma_5) \end{array} \quad (C.7)$$

Summing these results we finally obtain the necessary relation as follows,

$$\begin{aligned} & \bar{\Psi}(p_{e1}, \vec{x}) \gamma_\mu (1 - \gamma_5) \Phi^c(k_{\nu1}, \vec{x}) \bar{\Psi}(p_{e2}, \vec{y}) \gamma_\nu (1 - \gamma_5) \Phi^c(k_{\nu2}, \vec{y}) = \\ & = \frac{1}{2} \bar{\Psi}(p_{e1}, \vec{x}) (1 + \gamma_5) \Psi^c(p_{e2}, \vec{y}) \bar{\Phi}(k_{\nu2}, \vec{y}) \gamma_\nu \gamma_\mu (1 - \gamma_5) \Phi^c(k_{\nu1}, \vec{x}) \\ & + \frac{1}{8} \bar{\Psi}(p_{e1}, \vec{x}) \sigma_{\alpha\beta} (1 + \gamma_5) \Psi^c(p_{e2}, \vec{y}) \bar{\Phi}(k_{\nu2}, \vec{y}) \gamma_\nu \sigma_{\alpha\beta} \gamma_\mu (1 - \gamma_5) \Phi^c(k_{\nu1}, \vec{x}) \\ & = -\frac{1}{2} \bar{\Psi}(p_{e1}, \vec{x}) (1 + \gamma_5) \Psi^c(p_{e2}, \vec{y}) \bar{\Phi}(k_{\nu1}, \vec{y}) \gamma_\nu \gamma_\mu (1 - \gamma_5) \Phi^c(k_{\nu2}, \vec{x}) \\ & + \frac{1}{8} \bar{\Psi}(p_{e1}, \vec{x}) \sigma_{\alpha\beta} (1 + \gamma_5) \Psi^c(p_{e2}, \vec{y}) \bar{\Phi}(k_{\nu1}, \vec{y}) \gamma_\nu \sigma_{\alpha\beta} \gamma_\mu (1 - \gamma_5) \Phi^c(k_{\nu2}, \vec{x}) \end{aligned} \quad (C.8)$$

This recoupling make it easy to evaluate the traces in the calculation of the non-polarized double  $\beta$ -decay half-life presented in Chapter 5.

# List of publications

- I. R. Dvornický, and F. Šimkovic (2012)  
Second unique forbidden  $\beta$ -decay of  $^{115}\text{In}$  and neutrino mass:  
Workshop on Calculation of Double-Beta-Decay Matrix Elements (MEDEX'11):  
American Institute of Physics Conference Proceedings, Vol. 1417, p. 33-36.
- II. R. Dvornický, K. Muto, F. Šimkovic, and A. Fässler (2011)  
Absolute mass of neutrinos and the first unique forbidden  $\beta$ -decay of  $^{187}\text{Re}$ :  
Physical Review C, Vol. 83, No. 4, Art. No. 045502
- III. R. Dvornický, F. Šimkovic, and K. Muto (2010)  
The absolute mass of neutrino and the first unique forbidden  $\beta$ -decay of  $^{187}\text{Re}$ :  
Particle Physics at the Year of Astronomy: Proceedings of the Fourteenth Lomonosov  
Conference on Elementary Particle Physics, Singapore: World Scientific Publish-  
ing, p. 166-169
- IV. R. Dvornický (2010)  
Tritium and rhenium beta decay as a way for neutrino mass estimation: Proceed-  
ings of Študentská vedecká konferencia FMFI UK, Bratislava 2010:  
Zborník príspevkov, Bratislava: Fakulta Matematiky, Fyziky a Informatiky UK,  
2010, p. 279
- V. R. Dvornický, F. Šimkovic, and A. Fässler (2010)  
Beyond the standard model interactions in  $\beta$ -decay of tritium:  
Progress in Particle and Nuclear Physics, Vol. 64, No. 2, p. 303-305
- VI. K. Muto, R. Dvornický, and F. Šimkovic (2010)  
Nuclear structure aspects of single and double beta decays for neutrino mass:  
Progress in Particle and Nuclear Physics, Vol. 64, No. 2, p. 228-231
- VII. R. Dvornický, and F. Šimkovic (2009)  
Measuring mass of neutrinos with  $\beta$ -decays of tritium and rhenium:  
Workshop on Calculation of Double-Beta-Decay Matrix Elements (MEDEX'09):  
American Institute of Physics Conference Proceedings, Vol. 1180, p. 125-129

- VIII. F. Šimkovic, R. Dvornický, and A. Fässler (2008)  
Exact relativistic tritium  $\beta$ -decay endpoint spectrum in a hadron model:  
Physical Review C, Vol. 77, No. 5, Art. No. 055502
- IX. S.V. Semenov, F. Šimkovic, R. Dvornický, and V.A. Bednyakov (2008)  
Calculation of  $2\nu 2\beta$ -transition intensities in  $^{48}\text{Ca}$ :  
Proceedings of the 2-nd International Conference: Current Problems in Nuclear  
Physics and Atomic Energy, Kyiv: Institute for Nuclear Research of National  
Academy of Sciences of Ukraine, p. 422-424
- X. A.S. Barabash, A.D. Dolgov, R. Dvornický, F. Šimkovic, and A.Yu. Smirnov  
(2007):  
Statistics of neutrinos and the double beta decay:  
Nuclear Physics B, Vol. 783, No. 1-2, p. 90-111
- XI. R. Dvornický, F. Šimkovic, and A. Fässler (2007)  
Nuclear and particle physics aspects of the  $2\nu\beta\beta$ -decay of  $^{150}\text{Nd}$ :  
Workshop on Calculation of Double-Beta-Decay Matrix Elements (MEDEX'07):  
American Institute of Physics Conference Proceedings, Vol. 942, p. 28-32
- XII. S. Semenov, F. Šimkovic, A.Yu. Gaponov, and R. Dvornický (2007)  
Contribution of the excited  $1+$  states to the  $^{116}\text{Cd}$   $2\nu 2\beta$ -transition amplitude:  
Proceedings of the International Conference: Current Problems in Nuclear Physics  
and Atomic Energy, Part II, Kyiv: Institute for Nuclear Research of National  
Academy of Sciences of Ukraine, p. 473-478

## Cited by

- S.N. Gninenko, A.Yu. Ignatiev, and V.A. Matveev, Int.J.Mod.Phys. A **26**, 4367 (2011).
- Werner Rodejohann, Int.J.Mod.Phys. E **20**, 1833 (2011).
- W. Tornow, Nucl. Phys. A **844**, 57 (2010).
- Benjamin Monreal, and Joseph A. Formaggio, Phys.Rev. D **80**, 051301 (2009).

# Bibliography

- [1] P.J.E. Peebles, Phys. Rev. Lett. **16**, 410 (1966).
- [2] G. Steigman, D.N. Schramm, J.E. Gunn, Phys. Rev. Lett. **B66**, 202 (1977).
- [3] E. Fermi, Z. Phys. **88**, 161 (1934).
- [4] G. Hanna and B. Pontecorvo, Phys. Rev. **75**, 983 (1949).
- [5] M. Göppert-Mayer, Phys. Rev. **48**, 512 (1935).
- [6] S. R. Elliott, A. A. Hahn, and M. Moe, Phys. Rev. Lett., **59**, 2020 (1987).
- [7] V. I. Tretyak and Yu. G. Zdesenko, At. Dat. Nucl. Dat. Tabl., **80**, 83 (2002).
- [8] F.T. Avignone, S.R. Elliott, and J.Engel, Rev. Mod. Phys., **80**, 481 (2008).
- [9] E. Majorana, Nuovo Cim. **14**, 171 (1937).
- [10] W. Furry, Phys. Rev. **56**, 1184 (1939).
- [11] J. Schechter and J. W. F. Valle, Phys. Rev. D, **25**, 2591 (1982).
- [12] T.D. Lee, C.N. Yang, Phys. Rev. **104**, 254 (1956).
- [13] R.P. Feynman, M. Gell-Mann, Phys. Rev. **109**, 193 (1958).
- [14] E.C.G. Sudarshan, R.E. Marshak, Phys. Rev. **109**, 1860 (1958).
- [15] S. Weinberg, Phys. Rev. Lett. **19**, 1264 (1967).
- [16] F.J. Hasert *et al.*, Phys. Lett. B **46**, 121 (1973);  
F.J. Hasert *et al.*, Phys. Lett. B **46**, 138 (1973);  
F.J. Hasert *et al.*, Nucl. Phys. B **73**, 1 (1974).
- [17] B. Adeva *et al.*, Phys. Lett. B **231**, 509 (1989);  
D. Decamp *et al.*, Phys. Lett. B **231**, 519 (1989);  
M.Z. Arkway *et al.*, Phys. Lett. B **231**, 530 (1989);  
P.A. Aarnio *et al.*, Phys. Lett. B **321**, 539 (1989).

- [18] B. Pontecorvo, Sov. Phys. JETP **6**, 429 (1957);  
B. Pontecorvo, Sov. Phys. JETP **7**, 172 (1958).
- [19] Z. Maki, M. Nakagawa, S. Sakata, Prog. Theor. Phys. **28**, 870 (1962).
- [20] B. Pontecorvo, Sov. Phys. JETP **26**, 984 (1968).
- [21] V. Gribov and B. Pontecorvo, Phys. Lett. B **28**, 493 (1969).
- [22] S.M. Bilenky, B. Pontecorvo, Phys. Lett. B **61**, 248 (1976),  
S.M. Bilenky, B. Pontecorvo, Sov. J. Nucl. Phys. **24**, 316 (1976);  
S.M. Bilenky, B. Pontecorvo, Nuovo Cim. Lett. **17**, 569 (1976).
- [23] A. Gando et al. (KamLAND Collaboration), Phys. Rev. D, **83**, 052002 (2011).
- [24] K. Abe et al. (T2K Collaboration). Phys. Rev. Lett., **107**, 041801 (2011).
- [25] H.D. Kerret (Double Chooz Collaboration), LowNu11, November 9-12, 2011, Seoul National University, Seoul, Korea.
- [26] T. Schwetz, M. Tórtola, and J.W.F. Valle. New J. Phys., **10**, 113011 (2008).
- [27] A. Habig et al. (MINOS Collaboration), Mod. Phys. Lett. A, **25**, 1219 (2010).
- [28] K. N. Abazajian et al., Astropart. Phys., **35**, 177 (2011).
- [29] J.D. Vergados. Phys. Rep., **133**, 1 (1986).
- [30] S. Pascoli, S.T. Petcov, and T. Schwetz., Nuc. Phys. B, **734**, 24 (2006).
- [31] A. Osipowicz et al., hep-ex/0109033;  
L. Bornschein *et al.*, Nucl. Phys. A **752**, 14 (2005).
- [32] E. Andreotti *et al.*, Nucl. Instrum. Meth. A **572**, 208 (2007);  
M. Sisti *et al.*, Nucl. Phys. B **168**, 48 (2007).
- [33] S.M. Bilenky, A. Faessler, W. Potzel, and F. Šimkovic, Eur. Phys. J., **71**, 1754 (2011).
- [34] P.D. Serpico, Phys. Rev. Lett, **98**, 171301 (2007).
- [35] S.A. Thomas, F.B. Abdalla, and O. Lahav, Phys. Rev. Lett, **105**, 031301 (2010).
- [36] A.S. Barabash, AIP Conf. Proc., **1417**, 5 (2011).
- [37] F. Šimkovic, A. Faessler, H. Müther, V. Rodin, and M. Stauf, Phys. Rev. C, **79**, 055501 (2009).



- [38] Dong-Liang Fang, A. Faessler, V. Rodin, and F. Šimkovic, Phys. Rev. C, **82**, 051301 (2010).
- [39] L. Baudis et al., Phys. Rev. Lett. **83**, 41 (1999).
- [40] R. Arnold et al. (NEMO3 Collaboration), Phys. Rev. Lett. **95**, 182302 (2005).  
V.I. Tretyak and the NEMO 3 collaboration, AIP Conf. Proc. **1417**, 125 (2011).
- [41] C. Arnaboldi et al. (CUORICCINO Collaboration), Phys. Lett. B, **584**, 260 (2004).
- [42] A. Gando et al. (KamLAND-Zen Collaboration), arXiv:1201.4664 [hep-ex].
- [43] H.L. Harney H. V. Klapdor-Kleingrothaus, A. Dietz and I. V. Krivosheina, Mod. Phys. Lett. A, **16**, 2409 (2001).  
H. V. Klapdor-Kleingrothaus and I.V. Krivosheina, Mod. Phys. Lett. A, **21**, 1547 (2006).
- [44] I. Abt et al. (GERDA Collaboration), arXiv:0404039[hep-ex],  
S. Schoenert (GERDA Collaboration), J. Phys. Conf. Ser., **203**, 012014 (2010).
- [45] F. Alessandria et al. (CUORE Collaboration), arXiv:1109.0494 [nucl-ex].
- [46] N. Ackerman et al. (EXO Collaboration), Phys. Rev. Lett., **107**, 212501 (2011).  
R. Gornea (EXO Collaboration), J. Phys. Conf. Ser., **136**, 012039 (2010).
- [47] R. Arnold et al. (SuperNEMO Collaboration), Eur. Phys. J, **70**, 927 (2010).
- [48] Ch. Kraus (SNO+ Collaboration), Prog. Part. Nucl. Phys., **64**, 273 (2010).
- [49] Ch. Kraus et al., Eur. Phys. J. C **40**, 447 (2005).
- [50] V.M. Lobashev, Nucl. Phys. A **719**, 153 (2003).
- [51] E.W. Otten, C. Weinheimer, Rept. Prog. Phys. **71**, 086201 (2008).
- [52] N. Doss, J. Tennyson, A. Saenz, S. Jonsell, Phys. Rev. C **73**, 025502 (2006).
- [53] S. Gardner, V. Bernard, and Ulf-G. Meißner, Phys. Lett. B **598**, 188 (2004).
- [54] J.M. Carmona and J.L. Cortés, Phys. Lett. B **494**, 75 (2000).
- [55] G.J. Stephenson, Jr., T. Goldman, and B.H.J. McKellar, Phys. Rev. D **62**, 093013.
- [56] C.E. Wu, W.W. Repko, Phys. Rev. C **27**, 1754 (1983).

- [57] S.S. Masood, S. Nasri, J. Schechter, M.A. Tórtola, J.W.F. Valle, and C. Weinheimer, Phys. Rev. C **76**, 045501 (2007).
- [58] C.W. Kim and H. Primakoff, Phys. Rev. 139, B 1447 (1965); 140, B 566 (1965); C.W. Kim, Phys. Rev. 146, 691 (1966).
- [59] N.J. Stone, Oxford University preprint, <http://ie.lbl.gov/toi.html>
- [60] B. Budick, J. Chen, and H. Lin, Phys. Rev. Lett. **67**, 2630 (1991).
- [61] J.J. Simpson, Phys. Rev. C **35**, 752 (1987).
- [62] N. Severijns et al., Rev. Mod. Phys. **78** (2006) 991.
- [63] P. Herczeg, Prog. Part. Nucl. Phys. **46** (2001) 413.
- [64] B.J. Mount, M. Redshaw and E.G. Myers, Phys. Rev. Lett. **103**, 122502 (2009); J.S.E. Wieslander et al., Phys. Rev. Lett. **103**, 122501 (2009).
- [65] Particle Data Group, W.M. Yao et al., J. Phys. G **33**, 1 (2006).
- [66] C. Arnaboldi et al., Phys. Rev. Lett. **96**, 042503 (2006).
- [67] Konopinski, The theory of beta radioactivity, Oxford at clarendon press.
- [68] J. Abad, A. Morales, R. Nunez-Lagos, and A. Pacheco, Ann. Fis. A, **80**, 9 (1984).
- [69] W.C. Haxton, and G.J. Stephenson, Jr., Prog. Part. Nucl. Phys., **12** (1984) No. 409.
- [70] V.I. Tretyak, and Yu.G. Zdesenko, At. Dat. Nucl. Dat. Tabl., **80**, 83 (2002).
- [71] Commins, E.: Weak interactions. McGraw-Hill, 1973
- [72] A. Garcia, et al., Phys. Rev. C, **47**, 2910 (1993).
- [73] S.V. Semenov, F. Šimkovic, V.V. Khrushev, and P. Domin, Phys. Atom. Nucl., **63**, 1196 (2000);  
S.V. Semenov, F. Šimkovic, and P. Domin, Part. Nucl. Lett., **109**, 26 (2001).
- [74] F. Šimkovic, P. Domin, and S.V. Semenov, J. Phys. G, **27**, 2233 (2001).
- [75] Barabash, A.S.: Phys. Rev. C **81**, 035501 (2010).
- [76] H. Ejiri, and H. Toki, J. Phys. Soc. Jpn., **65**, 7 (1996).
- [77] Akimune, H. et al.: Phys. Lett. B, ed. 394, vol. 1997, no. 23

- [78] R. Arnold et al. JETP Lett. **80** (2004) 377.
- [79] The NEMO Collaboration (Yu. Shitov et al.) Phys. At. Nucl. **69** (2006) 2090.
- [80] A.Yu. Ignatiev, V.A. Kuzmin, Yad. Fiz. **46** (1987) 786 [Sov. J. Nucl. Phys. **46** (1987) 786]; JETP Lett. **47** (1988) 4;  
 L.B. Okun, Pis'ma ZhETF, **46** (1987) 420 [JETP Lett. **46** (1987) 529]; Yad. Fiz. **47** (1988) 1192;  
 O.W. Greenberg, R.N. Mohapatra, Phys. Rev. Lett. **59** (1987) 2507
- [81] L.B. Okun, Uspekhi Fiz. Nauk **158** (1989) 293 [Sov. Phys. Usp. **32** (1989) 543],  
 L.B. Okun, Comments Nucl. Part. Phys., **19** (1989) 99.
- [82] M. Goldhaber, G. Scharff-Goldhaber, Phys. Rev. **73** (1948) 1472;  
 E. Fishbach, T. Kirsten and O. Shaeffer, Phys. Rev. Lett. **20** (1968) 1012;  
 F. Reines, H.W. Sobel, Phys. Rev. Lett. **32** (1974) 954;  
 R.D. Amado, H. Primakoff, Phys. Rev. C **22** (1980) 1338;  
 K. Deilamian, J. D. Gillaspay and D. Kelleher, Phys. Rev. Lett. **74** (1995) 4787;  
 A.S. Barabash et al., JETP Lett. **68** (1998) 112;  
 S. Bartalucci et al., Phys. Lett. B **641** (2006) 18.
- [83] R. Bernabei et al., Phys. Lett. B **408** (1997) 439;  
 E. Baron, R.N. Mohapatra, V.L. Teplitz, Phys. Rev. D **59** (1999) 036003;  
 R. Arnold et al., Eur. Phys. J. A **6** (1999) 361
- [84] L. Cucurull, J.A. Grifols, R. Toldra, Astropart. Phys. **4**, (1996) 391.
- [85] A.D. Dolgov, A.Yu. Smirnov, Phys. Lett. B **621** (2005) 1.
- [86] H.S. Green, Phys. Rev. **90** (1953) 270;  
 O.W. Greenberg, Phys. Rev. Lett. **13** (1964) 598;  
 O.W. Greenberg, A.M.L. Messiah, Phys. Rev. **138** (1965) B1155.
- [87] A.Yu. Ignatiev, V.A. Kuzmin, hep-ph/0510209.
- [88] P. Domin, S. Kovalenko, F. Šimkovic, S.V. Semenov, Nucl. Phys. A **753** (2005) 337.
- [89] The NEMO Collaboration (R. Arnold et al.) Phys. Rev. Lett. **95** (2005) 182302.
- [90] R. Arnold et al., Nucl. Phys. A **781** (2007) 209.

- [91] H.V. Klapdor-Kleingrothaus, *et al*, Eur. Phys. J. A **12** (2001) 147;  
H.V. Klapdor-Kleingrothaus, A. Dietz, I.V. Krivosheina, O. Chkvorets, Nucl. Instrum. Meth. A **522** (2004) 371.
- [92] A.S. Barabash, A.D. Dolgov, R. Dvornicky, F. Simkovic, A.Yu. Smirnov, Nucl. Phys. B **783** (2007) 90.
- [93] S. Choubey, K. Kar, Phys. Lett. B **634** (2006) 14.
- [94] A.S. Barabash, AIP Conf.Proc. **942** (2007) 8.  
A.S. Barabash et al., Phys. Lett. B **345** (1995) 408.
- [95] M. Doi, T. Kotani and E. Takasugi, Prog. Theor. Phys. (Supp.) **83**, 1 (1985).